The role of the cancer kinome in the healthy and injured heart: focus on Flt3 and Plk2

Inauguraldissertation

zur

Erlangung der Würde eines Doktors der Philosophie vorgelegt der

Philosophisch-Naturwissenschaftlichen Fakultät

der Universität Basel

von

Daria Monogiou Belik

aus

Griechenland

Basel, April 2022

Genehmigt von der Philosophisch-Naturwissenschaftlichen Fakultät der Universität Basel auf Antrag von

Dissertationsleiterin: Prof. Dr. med. Gabriela Kuster Pfister

Koreferent: Prof. Dr. Christoph Handschin

Fakultätsverantwortlicher: Prof. Dr. Primo Leo Schär

Basel, 21st of April 2020

Prof. Dr. Martin Spiess

Dekan der Philosophisch-Naturwissenschaftlichen Fakultät

«…πρὸς ἐμαυτὸν δ᾽ οὖν ἀπιὼν ἐλογιζόμην ὅτι τούτου μὲν τοῦ ἀνθρώπου ἐγὼ σοφώτερός εἰμι· κινδυνεύει μὲν γὰρ ἡμῶν οὐδέτερος οὐδὲν καλὸν κἀγαθὸν εἰδέναι, ἀλλ᾽ οὗτος μὲν οἴεταί τι εἰδέναι οὐκ εἰδώς, ἐγὼ δέ, ὥσπερ οὖν οὐκ οἶδα, οὐδὲ οἴομαι· ἔοικα γοῦν τούτου γε σμικρῷ τινι αὐτῷ τούτῳ σοφώτερος εἶναι, ὅτι ἃ μὴ οἶδα οὐδὲ οἴομαι εἰδέναι.»

ΠΛΑΤΩΝ, Ἀπολογία Σωκράτους, 21d

Translation: «…so as I was leaving, I used to say to myself that I am wiser than this person; because I am afraid neither of us knows almost anything worthwhile, however he thinks he knows something without knowing it and I do not know nor do I think I know. So it seems to me that I am a little wiser than him, that is to say only, that at least I do not think I know what I do not know.»

PLATO, Apology of Socrates, 21d

Table of Contents

Acknowledgements

This thesis was written during the COVID-19 world pandemic outbreak in early 2020. A situation that made the whole writing process a bit stressful and definitely “adventuresome”. It is undeniably a one-in-a-life-time experience to remember...

First of all, I would like to express my gratitude to my supervisor, Prof. Dr. med Gabriela Kuster, for giving me the opportunity to conduct an exciting and impactful research project in her laboratory and for all the knowledge that I acquired throughout. I would also like to express my gratitude to the members of Myocardial Research laboratory: Vera, Lifen, Giacomo, Michika, who helped me on daily basis to cope with the challenges that a PhD project brings about. My PhD Committee members, Prof. Dr. Primo Schär and Prof. Dr. Christoph Handschin, for their wise inputs and suggestions during conduction of this project. Colleagues from ZLF who shared their knowledge (and reagents) with me.

Next, I would like to sincerely thank my friends all around the world for supporting and encouraging me in their own ways throughout these years. Friends from Greece who have been by my side on my personal and scientific path already for many years prior to my PhD adventures. Friends who I made after moving to Basel, who became indispensable part of my life and with whom I shared so many unforgettable experiences and moments. In particular, friends from Russian br/lunch for incredibly interesting and sophisticated discussions about science, literature, art, sports, traveling and more. My Russian language skills are better than ever now. Catalan and Franco-Italian mafias for all those personal heartwarming moments that made me laugh and cry (at the same time sometimes). Friends outside my scientific world whom I met under unusual and unexpected circumstances, who brighten up my life, without

trying to understand what kind of research I do. My Crossfit community for making me stronger not only physically, but also mentally, especially while writing this thesis.

Thank you all for inspiring me to be a better person!

Finally, I would like to express my endless gratitude to my family in Greece and Russia. To my parents who always supported my choices, believed in me more than I believed in myself and never had any doubt that I would succeed in any of my endeavors. I am truly happy that I can make them proud having completed my PhD research and having written this dissertation.

Спасибо вам. Я вас очень люблю. Σας ευχαριστώ. Σας αγαπώ πολύ.

Summary

In this work we investigated the effects of the Fms-like tyrosine kinase 3 (Flt3) targeting inhibitor quizartinib in the infarcted mouse heart. Flt3 is a transmembrane receptor tyrosine kinase (TK) that is involved in the regulation of normal hematopoiesis. Activating mutations of Flt3 account for 30% of all cases of acute myeloid leukemia (AML). Therefore, Flt3-targeting inhibition through pharmacological means can be applied for AML treatment. However, due to the homology among kinase receptors in both malignant and healthy cells, those treatments may lack specificity and interfere with other signaling pathways that are also important for cardiac homeostasis and function, leading to cardiotoxicity.

Our laboratory previously identified that Flt3-signaling has a cytoprotective role during ischemic cardiac injury, such as myocardial infarction (MI). Given that Flt3 is a target for cancer therapy and plays an important cytoprotective role during MI, we investigated the effects of pharmacological inhibition of Flt3 in the heart upon MI. Specifically, we studied the role of quizartinib, a second-generation Flt3 inhibitor with high selectivity and an efficient single agent in clinical trials in patients with AML.

We showed that quizartinib, administered to five week old male mice for three weeks prior to induction of MI, did not affect cardiac dimensions or function after one week post-MI in comparison to vehicle. However, apoptotic cell death was significantly enhanced in both the infarct border zone and the remote myocardium of quizartinib-treated vs. vehicle-treated mice. No significant differences were observed in cardiomyocyte size or fibrotic area. A three week post-MI analysis showed cardiac dilation and decline in cardiac function to be more persistent in quizartinib-treated infarcted mice vs. quizartinib-treated sham mice than in vehicle-treated infarcted mice vs. their corresponding sham. Immunohistochemical assays showed no

differences in apoptosis or fibrosis after three weeks between quizartinib and vehicle-treated mice. Comparable studies in Flt3-receptor deficient mice, which did not present differences in cardiac function and remodeling upon quizartinib administration, suggested that these effects are related to the inhibition of Flt3 and that the drug appears to have on-target toxicity. *In vitro* experiments showed that quizartinib decreased cell viability and increased apoptosis in H9c2 cells in a dose dependent manner. In addition, quizartinib at both high (20μM) and low concentrations (5μM) augmented H_2O_2-induced cell death and apoptosis beyond additive degree. In conclusion, this work showed that short-term pharmacological inhibition of Flt3 decreases cell viability and potentiates hypoxic cardiomyocyte death *in vitro* and *in vivo*.

Due to more frequent and widespread use of TK targeting cancer therapies, there is an increasing need to more thoroughly investigate and comprehend the role of the targeted TK in heart function, in order to foresee any potential adverse effect or toxicity. In this study we explored cardiac structure and function upon ischemic injury in combination with a potent TK targeting cancer treatment. Patients with underlying cardiac disease are often excluded from clinical trials, hence safety of such therapies in these patients is unknown. The findings of our study raise concerns regarding potential cardiotoxicity of quizartinib (or Flt3-targeting in general) in patients with underlying ischemic heart disease.

List of abbreviations

AML: acute myeloid leukemia
ALL: acute lymphoblastic leukemia
ATP: adenosine triphosphate
BM: bone marrow
BNP: B-type natriuretic peptide
BrdU: 5-bromo-2`- desoxyuridine
BSA: bovine serum albumin
CCND: cyclin D
CDK: cyclin-dependent kinase
CFU-GM: colony forming unit granulocyte macrophage
CHF: congestive heart failure
CI: confidence interval
CMML: chronic myelomonocytic leukemia
CSF-1: colony-stimulating factor 1
CR: complete response
DABCO: 1,4-Diazabicyclo[2.2.2]-octane
DAPI: 4',6-diamidino-2-phenylindole
DC: dendritic cells
DMEM: Dulbecco`s Modified Eagle`s Medium
DSB: double-strand breaks
ECG: echocardiogram
ECM: extracellular matrix
EGFR: epidermal growth factor receptor
EF: ejection fraction
EtOH: ethanol
FBS: fetal bovine serum
FGF: fibroblast growth factor
FITC: fluorescein isothiocyanate
FLK-2: fetal liver kinase-2
Flt3: Fms-like tyrosine kinase 3
Flt3L: Fms-like tyrosine kinase 3 ligand
GAPDH: glyceraldehyde 3-phosphate dehydrogenase
GIST: gastrointestinal stromal tumor
HBSS: Hank's buffered salt solution
HF: heart failure
Hoechst: bisBenzimide H33342 trihydrochloride
HR: hazard ratio
HSCT: hematopoietic stem cells transplantation
IC50: half maximal inhibitory concentration
IL: interleukin
JM: juxtamembrane
KCL: potassium chloride
Kdr: kinase insert domain receptor
KI: kinase inhibitor
KO: knock out
LAD: left anterior descending
LS: longitudinal strain
LV: left ventricular

LVEF: left ventricular ejection fraction
LVID: left ventricular internal dimension
LVAW: left ventricle anterior wall
LVPW: left ventricle posterior wall
MDS: myelodysplasia
MI: myocardial infarction
MODS: multiorgan dysfunction syndrome
MRI: magnetic resonance imaging
MTD: maximum tolerated dose
MTT: 3-(4,5-dimethylthiazol-2-yl)-2,5-diphenyltetrazolium bromide
NF-kB: nuclear factor-kappa B
NRVM: neonatal rat ventricular myocytes
ON: overnight
ORR: overall response rate
OS: overall survival
PBD: polo box domain
PBS: phosphate buffered saline
PCR: polymerase chain reaction
PDGF: platelet derived growth factor receptor
PFA: parafolmaldehyde
PI: propidium iodide
PIA: plasma inhibitory activity
PI3K: phosphoinositol-3-kinase
RIPA: radioimmunoprecipitation assay
PKC: protein kinase C
Plk2: polo-like kinase
PR: partial response
ROS: reactive oxygen species
RR: relative risk
RT: room temperature
RTK: receptor tyrosine kinase
RT-PCR: reverse pranscription PCR
s.c.: subcutaneous
STK-1: human stem cell kinase-1
TBS: tris-buffered saline
TKD: tyrosine kinase domain
TKI: tyrosine kinase inhibitor
TNF: tissue necrosis factor
TUNEL: Terminal deoxynucleotidyl transferase dUTP nick end labeling
VEGF: vascular endothelial growth factor
VEGFR: vascular endothelial growth factor receptor
WGA: wheat germ agglutinin
WT: wild type

Chapter 1: Role of Fms-like tyrosine kinase 3-targeting inhibitor quizartinib in the infarcted heart

Introduction

1. Cardiac complications in cancer survivors over time: field of cardio-oncology

Over the last decades there have been remarkable improvements and achievements in the development of antitumor agents that successfully increase the survival rates of the cancer patients. Cancer therapy-induced cardiotoxicity is one of the leading adverse effects of many oncologic regimens, requiring for the appropriate prophylactic measures and thorough monitoring. This prompted the quest for a broader range of options in the management of cancer patients. Collaboration between oncologists and cardiologists is essential in order to tackle these critical issues. Cardio-oncology is a new multidisciplinary specialty that aims to provide screening, monitoring and suitable therapy to the patients with heart disease during or after cancer treatment [1].

1.1 Incidents of cardiotoxicity

The cardiotoxicity associated with anti-cancer treatment was initially observed in 1967 when two pediatric patients treated with daunomycin at St. Jude Children's Research Hospital in Tennessee, USA, developed acute heart failure and eventually died [2]. Another cardiotoxic incident happened in the 1970s in adult patients who received adriamycin and developed heart failure [3].

Over the last years, the 5-year survival rates of the cancer patients have significantly increased. For instance, the breast cancer survival rate increased by 16% (75% to 91%) from 1975 to 2010 and survival of non-Hodgkin lymphoma improved from 42% to 71% during the same period of time [4]. Because cardiotoxicity may occur later in life, it is therefore crucial to have life-long follow-up of these patients.

The Childhood Cancer Survivor Study conducted by Armstrong and colleagues, included cancer patients of age younger than 21 who were monitored for approximately 24.5 years after diagnosis together with 4301 of their healthy siblings. This study showed that cancer survivors had significantly higher risks of a severe, disabling, life-threatening or fatal health condition, which were increasing proportionally to age above 35 years [5]. Interestingly, besides the risk of developing another malignancy, the most frequently affected organ was the heart with a hazard ratio (HR) of 7.9 [95% CI 5.4-11.6] for the overall risk of any cardiovascular involvement. Heart failure [HR 11.4, 95% CI 4.7-27.3], stroke [HR 7.0, 95% CI 3.3-14.8] and myocardial infarction [HR 5.0, 95% CI 3.0-8.3] were the most common complications, emphasizing the prevalence of cardiotoxic side effects among cancer survivors (**figure 1**).

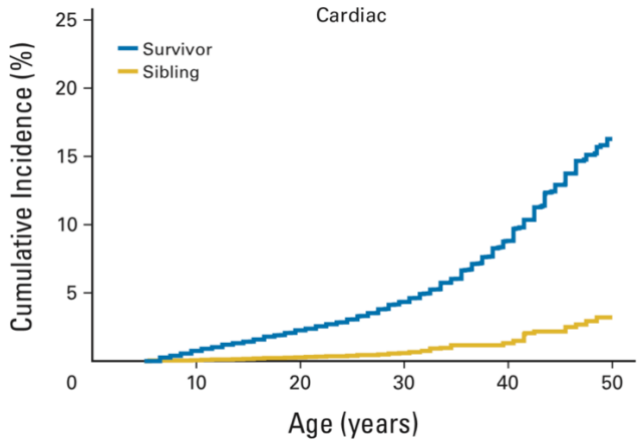

Figure 1. Cumulative incidence of grade 3 to 5 cardiac events over time in childhood cancer survivors [5]

Another study conducted by Mertens and colleagues came to the conclusion that incidents of cardiovascular events are the major nonmalignant cause of death among survivors of childhood cancers, responsible for a 7-fold higher risk of death among such patients when compared with their age-matched peers. The underlying cause is thought to be late effects of cardiotoxic cancer therapy [6]. As far as adult cancer patients are concerned, identification of the incidence of cardiovascular (CV) diseases that can be attributed to anti-cancer regiments is complicated by already pre-existing cardiovascular disease. In the breast cancer survivors group the overall incidence of cardiotoxicity is 33% after treatment with breast cancer therapies, therefore making CV diseases the main factor of mortality [7]. The various types of CV complications, caused by anti-cancer treatment include myocardial dysfunction, heart failure (HF), coronary artery disease, valvular heart disease, arrhythmias, thromboembolic disease, peripheral vascular disease, hypertension, stroke and pulmonary hypertension [8].

Overall, cardiotoxicity is reported to be the second leading cause of long-term morbidity and mortality among cancer survivors [9], with secondary malignancies cited as the primary cause of death [10].

1.2 Diagnosis

Cardiac dysfunction triggered by cardiotoxic anti-cancer drugs can appear as early as during the initiation of treatment or as late as years or even decades after its completion. Moreover, patients with essentially reduced ejection fractions have a poor prognosis [11]. Thus, proper methods for punctual diagnosis and management of potential cardiotoxicity and cardiac complications are required.

Since the 1970s endomyocardial biopsy with assessment of histologic grade according to the Billingham scoring system has been used as the main method to evaluate and diagnose the cardiotoxicity occurring after treatment with anthracycline chemotherapy, such as doxorubicin, daunorubicin, epirubicin or idarubicin [12, 13]. However, due to its invasive nature and high complication rate, this method has been gradually replaced by non-invasive cardiac imaging that gives the possibility to screen and monitor cancer patients during the treatment. The up-to-date clinical methods for cardiac imaging include nuclear imaging, echocardiography and magnetic resonance imaging (MRI), among which two-dimensional (2-D) and three-dimensional (3-D) echocardiography are the most frequently applied techniques [14, 15]. Such techniques are mainly based on the assessment of left ventricular (LV) ejection fraction (EF), the reduction of which has been directly associated with higher mortality rates [16]. Clinical studies showed that a drop of LVEF by more than 10 percentage points from baseline to less than 50% is an indication of cardiotoxicity [17, 18].

Despite being the most conventional parameter of systolic function, LVEF occasionally has low diagnostic sensitivity and provides low predictive potential for detection of subclinical myocardial injury [11]. When LVEF reduction in cancer patients is detected, they have already undergone irreversible myocyte damage [19]. As a result, earlier markers and parameters to identify cardiac deterioration stemming from anti-cancer drug toxicity are required. For example, echocardiographic myocardial strain analysis using 2-D speckle tracking imaging started being used for detection of subclinical cardiac complications. Global longitudinal strain (GLS) is a valuable early marker to monitor systolic function and predict any further decline in LVEF [20]. Reduction in GLS by 15% during cancer treatment is an indication of potential risk of cardiotoxicity [20]. However, there are some current limitations of the method that include time-consuming data analysis as well as variability in echocardiography machines and

software packages that may produce variability in strain results, therefore complicating the data comparison [21]. In addition to imaging, serum markers such as troponin I or T, and B-type natriuretic peptide (BNP), a cardiac neurohormone secreted from cardiac ventricles when the wall tension is enhanced, can be used as potential biomarkers for monitoring cardiotoxicity [22]. However, there is not currently sufficient data to confirm their prognostic potential for chemotherapy-induced cardiomyopathy.

2. Tyrosine kinases in health and disease

The response to extracellular and intracellular stimuli is crucial for all complex living organisms. Many members of the cell surface receptor tyrosine kinase (RTK) family have been characterized as important regulators of essential cellular processes, such as proliferation, differentiation, survival, cell migration and cell cycle control [23, 24]. Tyrosine kinases are enzymes that catalyze transfer of a phosphate residue from adenosine triphosphate (ATP) to tyrosine residues in appropriate substrates. Phosphorylation can affect the activity, subcellular location and stability of the phosphorylated substrate protein (**figure 2**). To date, 58 RTKs have been identified in humans [25], and they all share a similar molecular architecture. The structure of RTKs, their mechanism of action and key factors of the intracellular signal transduction pathways that they activate, are evolutionally conserved from the nematode Caenorhabditis elegans to humans and therefore are tightly regulated. Consequently, genetic changes or abnormalities that modify RTK activity, cellular distribution, regulation or expression can lead to a variety of diseases. Mutations that result in aberrant activation of their signalling pathways have been associated with the development of cancers, diabetes, inflammation, bone disorders and arteriosclerosis [26]. Thus, a detailed investigation of RTK physiology is of high importance in order to understand and therefore prevent progression of potential diseases and also, to develop drugs that can control RTK abnormal activity.

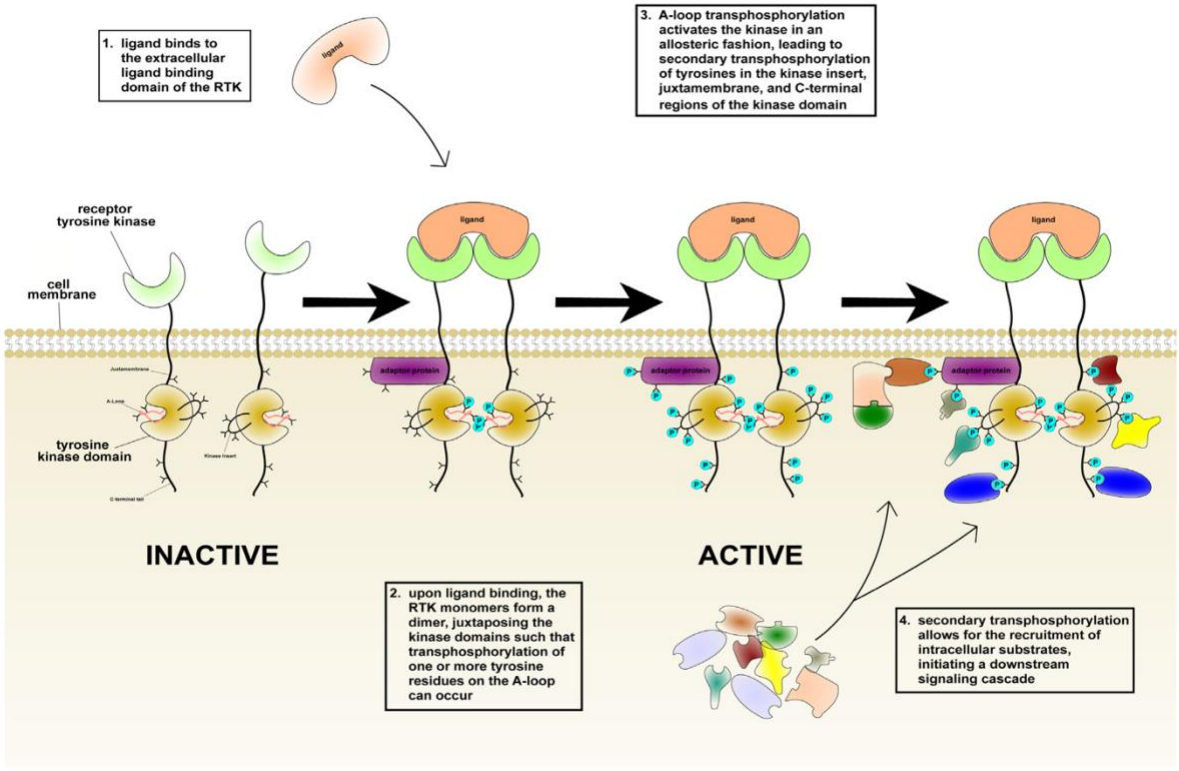

Figure 2. Activation of tyrosine kinase receptors [27]

2.1 The role of fms-like tyrosine kinase 3 (Flt3) in hematopoiesis

Flt3 (Fms-like tyrosine kinase 3), also known as FLK-2 (fetal liver kinase-2) and STK-1 (human stem cell kinase-1 [28]) is a member of the class III receptor tyrosine kinase family (RTKIII) playing a significant role in normal hematopoietic cell survival and proliferation [29]. The Flt3 gene is located on chromosome 13q12 [30] and carries strong structural similarities with the other members of the RTKIII receptor families. It has been identified that RTKIII family members, such as Flt3, FMS, platelet-derived growth factor receptor (PDGFR) and KIT, are comprised of five immunoglobulin-like (Ig-like) domains in the extracellular region, a juxtamembrane (JM) domain, a tyrosine kinase (TK) domain divided by a kinase insert (KI) domain and a C-terminal domain in the intracellular region (**figure 3**) [31, 32].

Figure 3. The domain structure of Flt3 [33]

The murine Flt3 gene was cloned from fetal liver and placenta cells in 1991 by two independent groups and it encodes a 1000- amino acid protein (**figure 3**) [34, 35]. Human Flt3 was cloned from a pre-B cell library and from a CD34-positive hematopoietic stem cell-enriched library and it encodes a 993–amino acid protein [28, 36]. Flt3 is predominantly expressed in the brain, the placenta, immature hematopoietic cells and the gonads [37, 38].

Flt3 is a trans-membrane receptor. Under physiological conditions, the monomeric receptor remains inactive until the extracellular domain interacts with its own ligand. Flt3 ligand (FL or Flt3LG or Flt3L) is a member of a small family of hematopoietic growth factors, which also includes the colony-stimulating factor 1 (CSF-1) and the stem cell factor (SCF, also known as KIT ligand) [39]. This family of growth factors is expressed as membrane bound precursors that undergo proteolytical cleavage in order to release the soluble ligand. Both proteolytical processing of the membrane-bound ligand and alternative splicing contribute to the production of soluble ligand [40]. FL binding leads to receptor dimerization and therefore, activation of the kinase domain with resultant autophosphorylation. The ligand binds to Flt3 with a constitutive high affinity (Kd), which has been estimated to be between 200 and to 500 pM using human myeloid leukemia cell [41]. Autophosphorylation triggers the initiation of biochemical signaling pathways that promote and regulate cell growth, proliferation and apoptosis inhibition. Ras-GAP, PLC-β, PI3-kinase, STAT5 and MAP kinase are all significant cytoplasmic signaling molecules that are associated with Flt3 activation (**figure 4**).

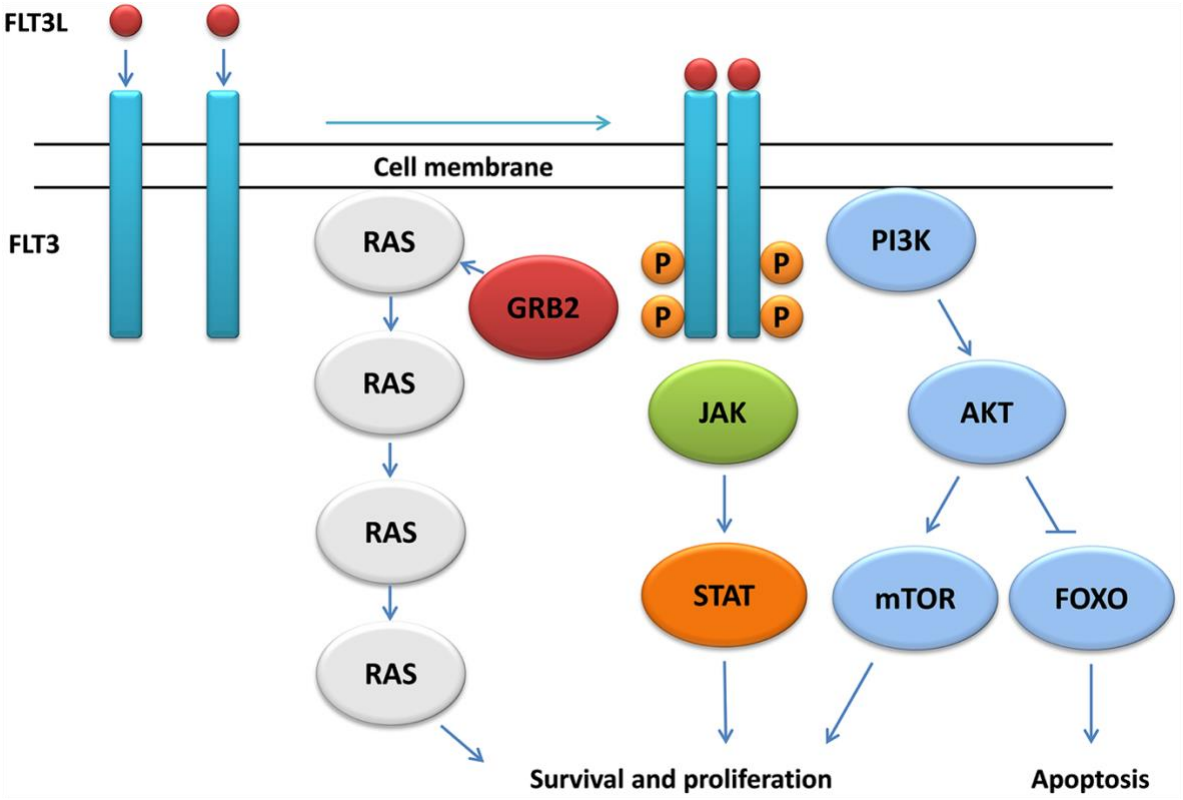

Figure 4. Flt3 signaling pathway [33]

Flt3 expression patterns have been studied on the cellular level and predominantly in a variety of human and murine cell lines of myeloid and B-lymphoid lineage. Signals induced by ligand-triggered activation of Flt3 primarily influence early hematopoietic development, whereas mature murine myeloid, erythroid, mast, macrophage and megakaryocyte cell lines do not express Flt3 [42]. In particular, Flt3 has been found to be expressed in a small number of quiescent hematopoietic progenitor cells, while its expression decreases upon differentiation [43]. It is expressed during myeloid cell and B cell commitment reaching the highest levels in pre-B cells and colony forming unit granulocyte macrophage (CFU-GM) progenitors. After final differentiation of those cells, Flt3 expression decreases and is only maintained in a subpopulation of monocytes. Moreover, a large number of CD34-positive cells expresses Flt3 in bone marrow and cord blood cells [44] and a smaller fraction of CD34-negative cells that are destined to become dendritic cells (DC) [45]. Despite Flt3 expression being absent in most

of the mature cells, Flt3 and its ligand dynamically modulate DC homeostasis and development [46, 47]. Additionally, Flt3 and FL are involved in DC mediated natural killer cell activation [48]. Consequently, Flt3 seems to be implicated at the interface of innate and acquired immunity (**figure 5**) [49, 50].

Interestingly, Flt3 knock out mice undergo normal development and appear healthy as adults. They also carry unaltered numbers of myeloid progenitor cells and CFUs, however they have significant hematopoietic stem cell deficiencies, in particular defects in B-lymphoid progenitors. Pro-B and pre-B cells appear to be smaller and B-lymphoid progenitor cells are fewer in number in comparison to wild type animals. Moreover, bone marrow cells derived from Flt3 knock out animals show defective repopulation capacity after transplantation into irradiated hosts [51]. Overall, inhibition of Flt3 signaling is not lethal despite its important role in many developmental steps of blood cell formation.

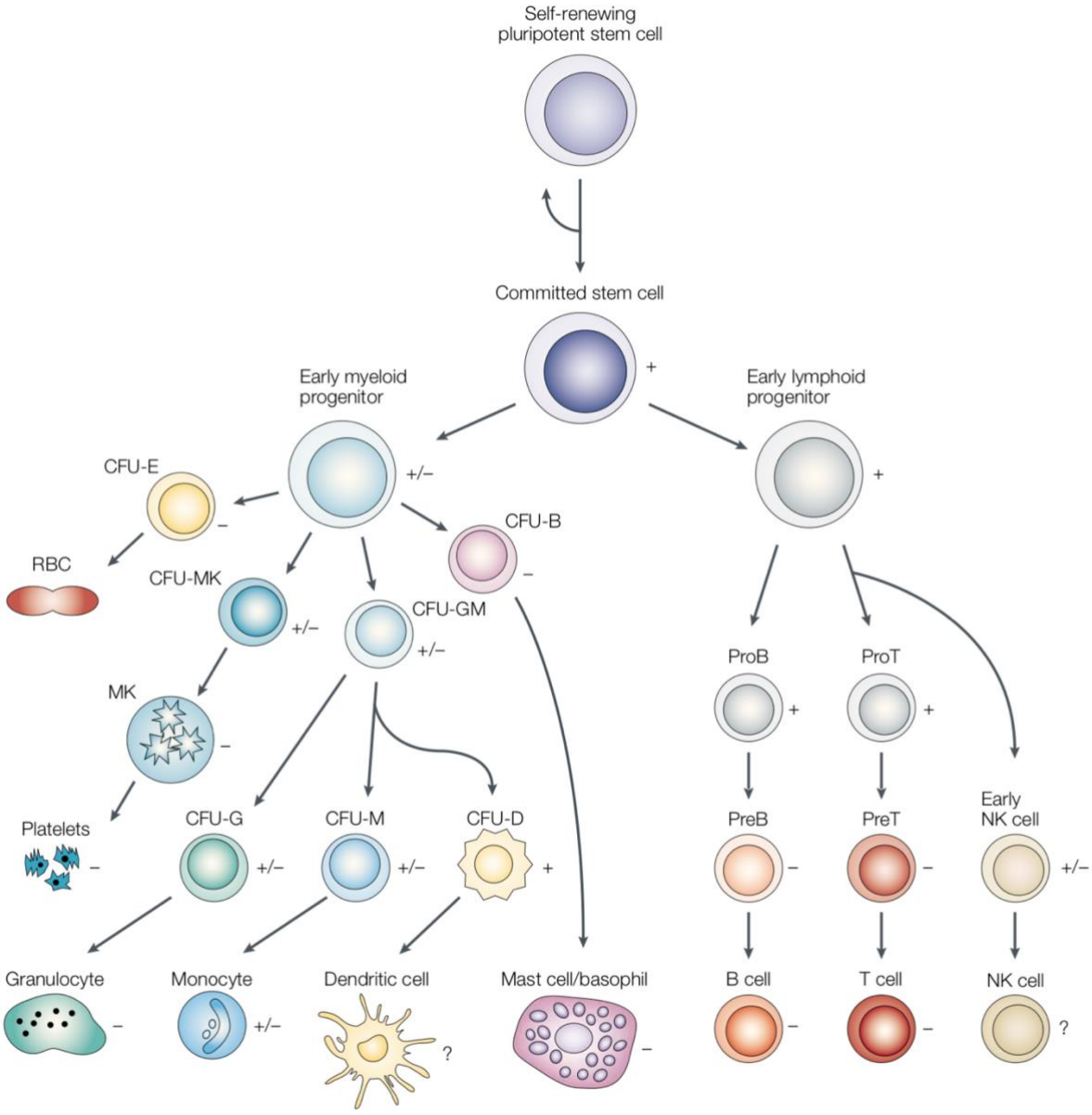

Figure 5. Expression of Flt3 in normal hematopoiesis. Maturation and differentiation of cells during normal hematopoiesis and indication about how expression of Flt3 is linked to this process (shown as +, −, +/− or ? (unknown)) [29]

2.2 Flt3 mutations in hematopoietic malignancies

Aberrant activation and expression of Flt3 is commonly identified in hematopoietic malignancies. In most cases it occurs due to activating mutation in Flt3 gene [52]. Flt3 mutations are prevalent in patients with Acute Myeloid Leukaemia (AML), in whom its expression is upregulated in 70% to 100% of cases [53]. Moreover, 5–10% of patients with Myelodysplasia (MDS) and 1–3% of Acute Lymphoblastic Leukemia (ALL) patients carry mutations in the Flt3 gene. Such mutations are also occasionally found in 20% of pediatric leukemias and are associated with poor prognosis [54]. However, some leukemias are also characterized by a higher than normal expression level of wild type Flt3 [55]. Cases of wild type Flt3 overexpression in hematopoietic malignancies were reported. For instance, expression of Flt3 on leukemic blasts was identified in 18 of 22 AML and 3 of 5 ALL cases by Rosnet *et al* [56]. Carow and colleagues noticed that Flt3 mRNA expression is amplified in 33 of 33 B-lineage ALL, 11 of 12 AML and 3 of 11 T-cell ALL cases in comparison to Flt3 mRNA expression normal bone marrow. On the protein level they did not detect Flt3 expression in normal bone marrow, however they saw Flt3 protein in 14 of 14 B-cell ALL, 36 of 41 AML and 1 of 4 T-cell ALL cases [57]. These experiments suggest that Flt3 expression may be implicated in the proliferation or survival of leukemic blasts. Flt3 is also highly expressed in leukemia and lymphoma cell lines, including pre-B, myeloid and monocytic cell lines [58, 59].

Two types of mutations have been attributed to the deregulation of the Flt3 receptor and identified to be involved in the development of AML: internal tandem duplications of the juxtamembrane region, called Flt3-ITD, and point mutations in the tyrosine kinase domains, Flt3-TKD (**figure 6**) [55]. ITD mutations in AML patients were first described in 1996 by Nakao *et al* [60]. The ITD mutations introduce an in-frame duplication of a part of the juxtamembrane region [61]. The duplications may vary in length from 3 to ≥ 400 base pairs,

but the reading frame and a head to tail orientation are always preserved. ITDs trigger ligand-independent dimerization leading to constitutive Flt3 autophosphorylation and therefore, activation and cytokine-independent proliferation of hematopoietic cells. It has been suggested that Flt3-ITD induces STAT5 phosphorylation and subsequent DNA binding [62], also activating the Ras/MEK/Erk and PI3K signalling pathways. MAP kinase and STAT5 were found to be constitutively phosphorylated and activated in all clinically isolated AML blasts with Flt3-ITD [63]. STAT5 incites its target genes such as cyclin D1, c-myc and the anti-apoptotic gene p21, which are involved in cell growth [64, 65] and which would normally not be expressed upon binding of FL to its wild-type receptor, thus indicating the effect of Flt3-ITD in the aberrant cell growth of leukemia cells [63]. Another outcome of the aberrant STAT5 signaling is the production of increased reactive oxygen species (ROS) that leads to frequent DNA double-strand breaks (DSBs), repair errors and therefore, resulting in genomic instability [66]. Sallmyr and colleagues suggested a possible mechanism for ROS generation showing a direct association of RAC1-GTP, an essential component of ROS producing NADPH oxidases, binding to STAT5. Inhibition of STAT5 led to diminished production of ROS. They concluded that the aggressiveness of the disease and the poor prognosis of AML patients with Flt3-ITD mutations might occur as a result of increased genomic instability created by elevated endogenous ROS, increased DNA damage and decreased end-joining fidelity. Additionally, Scheijen *et al.* proposed another potential mechanism by which Flt3-ITD might promote survival and proliferation of AML cells. Flt3-ITD is capable of phosphorylating and subsequently suppressing the Forkhead family of transcription factors member FOXO3a, an important pro-apoptotic regulator [67].

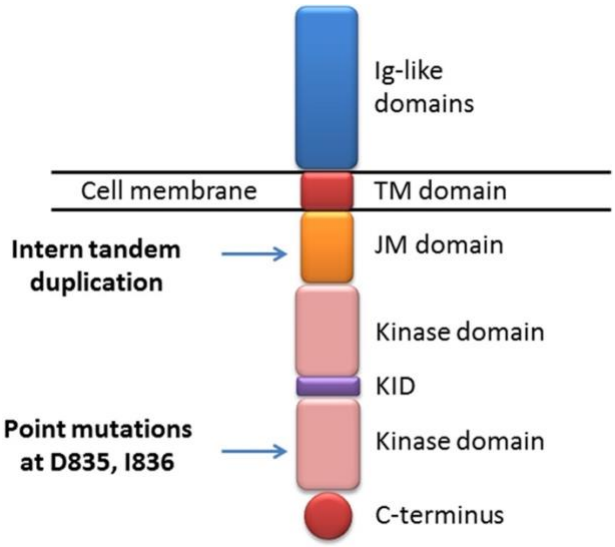

Figure 6. Locations of activating mutations of Flt3 [33]

Flt3-ITDs are present in 30–40% of AMLs, 5–10% of cases of MDS and in a few incidents of ALL (1–3%) [29]. ITD mutation is also an independent prognostic marker of poor clinical outcome in AML patients with a risk of relapse [68].

Point mutations in the tyrosine kinase domain of Flt3 are the second most common type of Flt3 mutations found in AML (**figure 6**). In particular, the D835 mutation (aspartic acid at position 835) is located in the activation loop of Flt3 and promotes ligand independent autophosphorylation and uncontrollable cell proliferation [69, 70]. Under normal conditions when Flt3 ligand does not bind to the receptor, the activation loop of the wild type Flt3 kinase domain maintains a closed autoinhibitory conformation, therefore blocking access to the peptide substrate and ATP binding sites [71]. TKD mutations trigger the opening of the activation loop and subsequently, transition to an active state even without Flt3 ligand binding.

Choudhary *et al.* [72] showed that Flt3-ITD and Flt3-TKD mutations exhibit differences in their signaling mechanisms that could have important implications for their transforming

capacity in the development of leukemia, despite the ligand-independent receptor activation that both induce. In myeloid progenitor cells, each mutated receptor activates different downstream signaling pathways. For example, the expression of Flt3-ITD led to constitutive and strong activation of STAT5 in IL-3–dependent murine myeloid cell line 32Dcl3. In contrast, STAT5 was only marginally activated by Flt3-D835Y in the absence or presence of FL. One additional study in which DNA microarrays were used to identify and compare the gene expression profiles related to Flt3-ITD and Flt3-TKD and the outcome in childhood AML conducted by Lacayo and colleagues, showed that there is also heterogeneity in the genetic program that these two types of mutations induce [73]. Moreover, Grundler and colleagues [74] used a murine bone marrow transplantation model to show that Flt3-ITD and TKD mutants cause different types of disease. Flt3-TKD develops a malignancy with longer latency and distinct hematologic manifestations in comparison to Flt3-ITD. It drives an oligoclonal lymphoid disease, whereas Flt3-ITD contributes to the development of an oligoclonal myeloproliferative disorder. Such differences are attributed to the differential induction of the STAT5 pathway, which is induced by Flt3-ITD, but not by Flt3-TKD in this particular murine bone marrow transplantation model. In another study, Muller and colleagues [75] demonstrated that contrary to Flt3-ITD, STAT5 deletion in Flt3-TKD mice does not have a crucial impact on disease onset and progression, suggesting that STAT5 in Flt3-TKD-induced signalling does not exert essential functions. Intriguingly though, the immunophenotype of Flt3-TKD mice is notably similar to that of Flt3-ITD mice where STAT5 was deleted, suggesting that STAT5 phosphorylation and activation in Flt3-ITD cells is an important target that induces the differences in the immunophenotypes of Flt3-TKD and Flt3-ITD. Moreover, STAT5 elimination alone is not sufficient to hinder the disease onset in Flt3-ITD and Flt3-TKD mice [75]. Muller and colleagues in the same study also showed that Flt3-ITD results in a different activation of downstream signalling pathways depending on the hematopoietic cell type. Flt3-

ITD activates STAT5 in myeloid but not in lymphoid progenitor cells. When Flt3-ITD is expressed in a myeloid progenitor cell, STAT5 target gene activation leads to subsequently increased proliferation and cell survival. In case of STAT5 deletion, minor proliferative signals can be transmitted in both myeloid and lymphoid progenitor cells leading to lymphoid expansion. Such signal transduction pathway might be identical to Flt3-TKD signalling, as the resulting disease phenotype is highly similar [75].

Furthermore, *in vivo* implications of the two mutations were investigated in a knock-in model. Flt3-TKD mice survived longer and manifested myeloproliferative neoplasms that are less aggressive than Flt3-ITD animals. They also did not demonstrate hematopoietic stem cell deficiency as was observed in Flt3-ITD animals. Overall, the Flt3-TKD mice exhibit less aggressive hematopoietic disease in comparison to the Flt3-ITD mice. The Flt3-TKD mice are characterized by prolonged survival, less severe myeloproliferation, no significant blockage in B-cell differentiation and a broader spectrum of disease. Similar to the Flt3-ITD mutation, the Flt3-TKD mutation per se is insufficient to promote leukemia in the absence of cooperative mutational factors [76].

2.3 Flt3 in the heart

Flt3 receptor and its ligand have been identified in whole heart homogenates. Ayach and colleagues [77] sought to investigate the mechanistic contributions of c-kit+ bone marrow-derived hematopoietic stem/progenitor cells in the maintenance and repair of damaged myocardium after myocardial infarction (MI), using c-kit-deficient mice. They saw that Flt3 ligand expression was significantly greater after MI in both the c-kit-deficient mice and c-kit-deficient mice that received bone marrow transplantation. This level of Flt3 ligand demonstrates a previously unreported level of increase in cardiac Flt3 ligand expression after

MI, which is, in turn, much more exaggerated in c-kit-deficient mice, suggesting a potential synergetic compensatory mechanism by Flt3 ligand in c-kit-deficient mice.

Tian and colleagues [78] investigated the effect of Flt3 receptor and Flt3 ligand in organs of mice with multiorgan dysfunction syndrome (MODS), which commonly occurs subsequent to severe burns, trauma or major surgical stress. They observed that Flt3 ligand administration in the dose of 5μg/kg once daily for 7 days improved the immune status and alleviated the heart damage in mice with late-phase MODS, as pathological changes in the form of myocardial interstitial edema with vasodilatation and hyperemia appeared less severe in the Flt3 ligand treated mice in comparison to control animals.

Moreover, Pfister and colleagues [79] demonstrated that Flt3 ligand exerts cytoprotective effects in the injured heart when administered exogenously at therapeutic concentrations. They found that Flt3 receptor is present in cardiomyocytes and upregulated after undergoing oxidative stress, results consistent with those described in Ayach`s experiments showing increase in Flt3 expression in the post-myocardial infarction mouse heart. Such upregulation implies a specific role of Flt3 and its ligand in the ischemically injured heart. Moreover, they showed that Flt3 activation stimulated by the exogenous ligand, decreased cardiomyocyte apoptosis *in vitro* and in the infarct border zone *in vivo* and improved post-MI function and remodelling by reducing the infarct size. The investigators also provided evidence of activation of Akt-dependent pro-survival signaling when cardiomyocytes exposed to oxidative stress were treated with Flt3 ligand, as it was also shown for Flt3 expressing leukaemia cells [80].

3. Flt3 Inhibitors

Since the discovery of the important complications and high frequency of Flt3-ITD mutations in patients with AML in 1996 [60], many small molecules for the therapeutic targeting of aberrant Flt3 signalling have been developed with the goal of decreasing relapse rate and improving survival of the patients. Patients with Flt3-ITD develop resistance to conventional chemotherapy and thus, are classified into a high-risk category, according to the 2017 European LeukemiaNET (ELN) genetic risk stratification. Besides the chemotherapy some AML patients that are at the high risk of relapse undergo hematopoietic stem cell transplantation (HSCT). However, the overall survival rate is only 30-40% [81]. In order to alleviate such outcomes, there is a number of Flt3 inhibitors that have been investigated in clinical trials. In general, tyrosine kinase inhibitors (TKIs) are small molecules that inhibit the enzymatic activity of tyrosine kinases and block downstream signaling activation [82].

First generation Flt3 inhibitors were not designed specifically for the Flt3 receptor, but they were nonspecific inhibitors with additional activity against receptor targets such as c-Kit, PDGFR and vascular endothelial growth factor receptor (VEGFR). Only when the role of Flt3 in the development of AML was established, drug screening was initiated to find small molecules among TKIs originally generated for other oncogenic targets, that are selective for Flt3 [83]. Thus, second generation Flt3 inhibitors were developed to be more potent and selective for the receptor in order to improve their performance and tolerability in the patients with AML. Flt3 inhibitors are further classified according to the mechanism of their interaction with the receptor. All Flt3 inhibitors prevent ATP from binding to the tyrosine kinase domain, consequently blocking phosphorylation and activation of the Flt3 receptor [70], [84]. However, type I inhibitors (lestaurtinib, midostaurin, crenolanib, gilteritinib) attach to the receptor in both

in its active and inactive forms, whereas type II inhibitors (sorafenib, quizartinib, ponatinib) interact with a hydrophobic region of Flt3 that is only accessible in the inactive form.

The following table shows examples of Flt3 inhibitors and their targets.

Table 1. FLT3 inhibitors

Agent	Tyrosine kinase targets	Indications	Adverse effects	Reference
First-generation				
Sorafenib phase III, FDA approved	**RAF-1, MEK, BRAF VEGF, c-KIT, PDGFR, ERK, Flt3**	Renal cell carcinoma, Hepatocellular carcinoma, AML	**hypertension, cardiac ischemia,** arterial thromboembolic events, hemorrhage, nausea, anorexia, fatigue, diarrhea	**[85]**
Sunitinib phase III, FDA approved	**PDGFR, VEGFR-1/2, KIT, Flt3**	Renal cell carcinoma, Gastrointestinal stromal tumor, pancreatic neuroendocrine tumor, AML	haemorrhage, **hypertension**, adrenal dysfunction, hypothyroidism, fatigue, nausea, diarrhea, anorexia, **cardiomyopathy, congestive heart failure, decreased ejection fraction**	**[86], [87]**
Midostaurin phase III, FDA approved	**PKC, VEGR, PDGFR, CDK1, c-Src, c-Syk, c-Fgr, c-KIT, Flt3**	Advanced systemic mastocytosis, myelodysplastic syndrome, AML	nausea, vomiting, when in combination with other drugs: neutropenia, thrombocytopenia, leukocytosis **decreased ejection fraction**	**[88]**
Lestaurtinib phase III	**tropomyosin receptor kinases, neurotrophin receptors, JAK2, Flt3**	Myelofibrosis, AML	anemia, leukopenia, thrombocytopenia, diarrhea, nausea, anorexia, gastritis, sepsis, multiorgan failure, **myocardial infarction**	**[89], [90]**
Tandunitib phase II	**PDGFR, c-KIT, Flt3**	Glioblastoma, metastatic renal cell carcinoma, AML	diarrhea, edema nausea, lymphopenia, leukopenia, fatigue, prolonged QTc, proteinuria, thrombocytopenia, hypophosphatemia, anemia, neutropenia, **hypertension**, muscle weakness, hypophosphatemia	**[91]**
Second-generation				
Quizartinib phase III Approved in Japan	**c-KIT, PDGFR, CSF1R, Flt3**	AML	QT prolongation, myelosuppression, nausea, vomiting, diarrhea, pyrexia, fatigue, febrile neutropenia, nausea	**[92]**
Crenolanib phase III	**PDGFRα/β, KIT, Flt3-WT, Flt3-ITD, Flt3-TKD, Flt3-D835**	systemic mastocytosis AML	nausea, vomiting, diarrhea, infections, rash	**[92]**
Gilteritinib phase III, FDA approved	**AXL, Flt3**	AML	elevated liver enzymes, diarrhea, pyrexia, febrile neutropenia, **hypertension**, thrombocytopenia, pneumonia	**[93]**
Ponatinib phase II	**BCR/ABL, RET, c-KIT, TIE2, VEGFR, PDGFR, FGFR, EPH, SRC, Flt3**	Chronic myelogenous leukemia	rash, abdominal pain, fatigue, **hypertension**, headache, myelosuppression, nausea, pyrexia, diarrhea	**[92]**
Others				
Cabozantinib phase II	**VEGFR-1/2/3, Kit, MET, AXL, KIT, RET, Flt3**	Hepatocellular carcinoma,	thrombocytopenia, neutropenia,	**[94]**

		non-small-cell lung carcinoma, ovarian carcinoma	anemia, **palpitations, sinus bradycardia, ventricular arrhythmia**	
G-749 preclinical phase	**Flt3-ITD, D835Y, ITD/F691 L, ITD/N676D**			**[95]**
SEL24-B489 Preclinical phase	**PIM, Flt3-ITD**			**[95]**

Specific examples of approved first-generation Flt3 inhibitors

- **Sorafenib**

Sorafenib is an oral multikinase inhibitor of RAF-1, VEGF, c-KIT, PDGFR, ERK and Flt3. It has been approved against renal cell and hepatocellular carcinomas; however, it has a potent anti-leukemic effect in Flt3-mutated AML patients and is able to inhibit Flt3-ITD activity by 100% with an IC50 of 69.3 ng/ml [96]. One of the suggested mechanisms of its effective action is that sorafenib triggers Flt3-ITD leukemic cells to secrete IL-15, prolonging the survival time of the patients [97]. Moreover, CD3+ cell invasion in the epidermis, low blast numbers, high levels of CD8+ lymphocytes in the bone marrow and high expression of COL4A3, TLR9, FGF1 and IL-12 genes have been noticed in the patients who received sorafenib [98]. It reduces Smac mimetic-induced necroptosis in apoptosis-resistant leukemic cells [99]. It has also the potential to inhibit Src kinase-mediated STAT3 phosphorylation and to limit the expression of apoptotic regulatory factors, such as Mcl-1 and Bcl-2 [100].

Combination of sorafenib with standard chemotherapy, such as decitabine, has been applied to treat Flt3-ITD AML. Initially, in preclinical study the drugs showed synergistic anti-tumor effects in cell lines isolated from patients with Flt3-ITD-mutated AML. In a clinical study where 6 patients were involved, 5 of them had positive responses. The median survival time of the patients was 155 days and the drugs were well tolerated [101]. In another study combination of 5-azacytidine and sorafenib was administered to a pregnant patient with Flt3-ITD AML.

After 1 cycle of the treatment the number of bone marrow blasts was significantly reduced and Flt3-ITD was not detectable. The patient did not receive transfusion and her neutrophil count was physiological after 4 cycles of therapy. The child was born healthy [102]. Sorafenib has been also tested in patients with Flt3 mutated AML older than 60 years in a phase II trial. It was added to induction, consolidation and maintenance therapies. Thirty nine out of 54 patients that were enrolled were Flt3-ITD positive. The 1-year overall survival (OS) in Flt3-ITD patients was 62% [103].

Sorafenib has also been used in patients who underwent HSCT. Sorafenib was administered to 17 patients with Flt3-ITD-positive AML in combination with allogenic HSCT. Among those patients 10 initiated the sorafenib intake after transplantation. Fourteen of the patients achieved complete response (CR), however 5 patients eventually progressed. There were signs of toxicity in 5 patients, but they remained in molecular remission when the dosage was modified. Combination of sorafenib with allogenic HSCT allowed lower relapse rate and longer leukemia-free survival in patients with Flt3-ITD mutated AML [104]. In another study 27 pediatric patients with Flt3-ITD-positive AML received sorafenib as a maintenance agent after HSCT. Molecular remission was achieved in 25 patients and the 1-year OS was 92% [105]. A long term follow-up (median 7.5 years) of 29 patients with relapsed Flt3-ITD AML after allogenic HSCT and sorafenib treatment showed survival of 6 patients with 5 patients achieving sustained complete remission and 4 patients in treatment-free remission for a median of 4.4 years [106].

- **Sunitinib**

Sunitinib (SU11248) is a small-molecule Flt3 inhibitor with selectivity for PDGFR, VEGFR1/2, KIT and Flt3 [107]. It has both direct anti-tumor and anti-angiogenic properties. It has been approved for treating renal cell carcinoma, gastrointestinal stromal tumor and AML. Sunitinib has been shown to reduce STAT5 phosphorylation in patients with Flt3-ITD [108]. It can also be used in combination with cytarabine or daunorubicin showing synergic effects in inhibiting proliferation and survival of primary myeloblasts expressing Flt3-ITD, Flt3-D835V or Flt3 wild type (WT) [109]. Moreover, the drug leads to arrest in the G1 phase of the cell cycle, decreases anti-apoptotic factor expression and enhances pro-apoptotic factor expression [110]. Sunitinib is used in combination with standard chemotherapy. Twenty-two patients over 60 years with Flt3-ITD AML were recruited for a phase I/II clinical study and received sunitinib with intensive chemotherapy [111]. Thirteen patients, including 8 patients with Flt3-ITD mutation, achieved complete remission (CR)/complete remission with incomplete blood count recovery (CRi). The median overall survival of 17 patients was 1.6 years, relapse-free 1 year and event-free 0.4 year. In another phase I trial 15 patients with refractory AML received sunitinib and those with Flt3 mutations presented morphologic or partial responses. When treated with 50mg of the drug patients did not experience dose-limiting toxicity. The grade 2 adverse effects were fatigue, edema and ulcerations [112].

- **Midostaurin**

Midostaurin (CGP41251, PKC412) is a semi-synthetic derivative of staurosporine, the original “pan-kinase” inhibitor, derived from the bacterium Streptomyces staurosporeus. Midostaurin has a broad spectrum of kinase activity, including protein kinase C (PKC), Flt3, VEGR,

PDGFR, CDK1, c-Src, c-Syk, c-Fgr, and c-KIT [113-115]. It was initially developed to treat solid tumors, however its Flt3 inhibitory activity was discovered in a drug screen of apoptosis-inducing compounds in cells expressing Flt3-ITD [83]. Midostaurin was subsequently investigated for its potential anti-leukemic effect. It was approved by the US FDA in 2017 for the treatment of Flt3-mutated AML [46]. It has also been approved for newly diagnosed patients with Flt3-mutated AML and advanced systemic mastocytosis. The results of phase I, in which patients with refractory or relapsed AML were administered midostaurin with bortezomib only or combined with mitoxantrone, etoposide and cytarabine showed an overall response rate (ORR) of 82.5% [116]. In another study a variety of midostaurin doses, all-trans retinoic acid and CLAG chemotherapy (cladribine combined with high doses of arabinoside cytosine, mitoxantrone and G-CSF) were applied to treat AML and 22% of all patients achieved CR and 11% achieved CRi [117]. Interestingly, when midostaurin was combined with a standard chemotherapy and administered to newly diagnosed patients with AML, its efficacy was increased [118]. The CR rate of patients who received midostaurin at 50 mg twice a day was 80% and in particular, of patients with mutated Flt3 92% and of patients with Flt3-WT 74%. However, the 1-year and 2-year OS of patients with Flt3-mutated AML were similar to those of patients with Flt3 WT. Moreover, midostaurin used in combination with a standard chemotherapy managed to prolong the OS in patients with Flt3-mutated AML without any significant increase in severe side effects [119].

Specific example of approved second-generation Flt3 inhibitors

- **Gilteritinib**

Gilteritinib (ASP2215) is a combined Flt3 and AXL inhibitor. It has been shown to reduce the phosphorylation levels of Flt3 and its downstream targets both *in vitro* and *in vivo* without

noticeable severe toxicity [120]. It also decreased the capacity of Flt3-ITD leukaemia cells to form colonies [121]. In a clinical trial it was well tolerated in 252 relapsed AML patients. The ORR was 40% in Flt3-mutated patients at doses higher than 80 mg/day. More than 5% of the patients experienced serious side effects such as fever, disease progression, neutropenia, sepsis, acute renal failure, pneumonia, pyrexia, bacteremia and respiratory failure [122]. In another open-label, phase I study, the drug was also shown to be well tolerated in Japanese patients with relapsed AML. The ORR in patients with mutated Flt3 was 80% and with Flt3 WT 36.4%. The observed side effects included thrombocytopenia and increased creatine phosphokinase. Phase II suggested a recommended dose of 120mg/day and a maximum tolerated dose (MTD) of 200mg/day [93]. A phase III clinical trial comparing gilteritinib with a salvage chemotherapy regimen in relapsed Flt3-mutated AML patients showed that gilteritinib provides significantly longer survival and there is a higher percentage of patients with remission than under salvage chemotherapy [123]. It was FDA approved in November 2018.

4. Quizartinib

Quizartinib (also known as AC220) is a second-generation Flt3 receptor tyrosine kinase inhibitor and the first drug specifically designed to selectively inhibit Flt3 [82]. It has from 10 to 50 times stronger *in vivo* potency than first-generation inhibitors [124-126]. Despite also having a minor activity against KIT, PDGFR and CSF1R, it is highly selective for the Flt3 receptor already at nanomolar concentrations [127].

The molecular formula of quizartinib is N-(5-(1,1-Dimethylethyl)isoxazol-3-yl)-N'-(4-(7-(2-(morpholin-4-yl)ethoxy)imidazo(2,1-b)benzothiazol-2-yl)phenyl)urea (**figure 7**) and it was produced by Ambit Biosciences. Daiichi-Sankyo Company Limited is currently responsible for its clinical investigations [128].

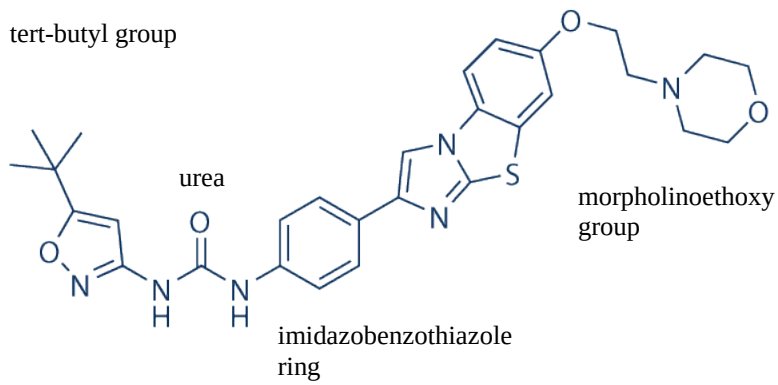

Figure 7. Quizartinib chemical structure [129]

Quizartinib was detected through a systematic screening process from a scaffold focused library of compounds against a panel of 402 kinases, which represent 80% of human kinases. In this important study conducted by Zarrinkar and colleagues, human leukaemia cell lines MV4-11, carrying homozygous Flt3-ITD mutation, and RS4-11, carrying wild type Flt3, were used to identify the ability of these compounds to inhibit Flt3 in the cellular environment [124]. Quizartinib turned out to be the strongest in inhibiting Flt3 autophosphorylation both in the Flt3-ITD and wild type cell lines. They also examined the cellular selectivity of the agent by measuring the cellular proliferation of A375 cells that carry BRAF mutation without any Flt3 dependency. Quizartinib had no effect on the growth of the A375 cells, whereas midostaurin, sorafenib and lestaurtinib inhibited the growth of A375 cells, confirming quizartinib selectivity against Flt3. Moreover, Zarrinkar and colleagues proceeded to study the quizartinib efficacy against Flt3 receptor *in vivo* by using a tumor xenograft model in which leukemic human MV4-11 cells were inserted subcutaneously to generate the disease. For this experiment, they administered 10 mg/kg of quizartinib and sunitinib to the animals once a day orally for 28 days and observed the size of the tumor for additional 60 days after treatment termination. The results showed that quizartinib leads to rapid and complete regression of tumor without its

reappearance during the 60 days after the treatment period. In contrast, sunitinib despite also resulting in tumor size reduction, has less rapid effects in comparison to quizartinib. There was also tumor regrowth resumed immediately upon discontinuation of treatment in all but one of the animals during the 60 days post treatment observation period. One more experiment in a mouse model, in which leukemic MV4-11 cells were injected into bone marrow-ablated animals done by the same researchers, showed that quizartinib prolongs survival in a dose dependent fashion. Moreover, they isolated primary AML blasts from the peripheral blood of a 55-year-old man with relapsed and refractory AML and observed that quizartinib inhibited autophophorylation at an IC50 of 2nM and cell proliferation and survival at an IC50 of 0.3nM [124]. Its efficacy prevails the results achieved with other Flt3 inhibitors, such as lestaurtinib (CEP701), sorafenib, sunitinib, NVP-AST487 in primary leukemia cells [130-132].

Quizartinib along with other second-generation inhibitors, such as crenolanib and gilteritinib, have been shown to hinder the proliferation of MV4-11 cells harbouring Flt3-ITD mutation at nanomolar concentrations (quizartinib 0.56 nM, crenolanib 1.3 nM, and gilteritinib 0.92 nM) [124, 133]. Type I inhibitors, such as gilteritinib and crenolanib, are capable of inhibiting the activity of the Flt3-TKD mutated Flt3, whereas type II inhibitors, such as quizartinib, ponatinib and sorafenib, are not. Mori and colleagues showed that quizartinib has weaker potential to inhibit Flt3 receptor with D835Y and ITD/D835Y mutations in comparison to ITD mutation alone [120]. Moreover, crenolanib has also been demonstrated to have inhibitory activity against Flt3-ITD/D835Y mutations in sorafenib-resistant MOLM-13 cells and in Ba/F3 cells harboring Flt3-ITD and secondary KD mutations *in vivo* and *in vitro*. The same study showed crenolanib to inhibit drug-resistant AML primary blasts with Flt3-ITD and D835H/Y mutations [133]. Such difference in activity between the type I and type II inhibitors is attributed to the interaction between the Flt3 inhibitor and the ATP-binding site of the Flt3 intracellular TKD

[134]. Gilteritinib and crenolanib bind to the ATP binding site of the receptor also when in its active conformation, whereas quizartinib and other type II receptors bind to the hydrophobic region neighboring to the ATP-binding site that is only accessible when the receptor is in its inactive conformation. This explains that due to Flt3-TKD mutations converting the receptor into its active form, quizartinib becomes ineffective to inhibit TKD mutated Flt3 [135, 136].

The pharmacokinetic profile of quizartinib shows that the drug has high absorption properties reaching a maximum plasma level of 3.8 μM (2100 ng/mL) in mice within 2h of dosing. A single dose of 10mg/kg results in peak plasma concentration that is more than 30-fold higher than the IC50 required for Flt3-ITD inhibition and it is sufficient for sustained Flt3-ITD inhibition in mice for over 24h [124].

Pratz and colleagues compared six Flt3 inhibitors (lestaurtinib, midostaurin, sorafanib, sunitinib, KW-2449 and quizartinib) in an *in vitro* study and identified quizartinib as the most potent, especially in human plasma [126]. Interestingly, the majority of small molecule kinase inhibitors are highly hydrophobic and protein bound and a low nanomolar IC50 in culture medium does not necessarily have the same potency in plasma. However, quizartinib has been measured with a plasma inhibitory activity (PIA) assay to be at minimum 25 times more potent against Flt3 in plasma [137]. Moreover, Gunawardane and colleagues [138] showed that quizartinib can prolong the inhibition of Flt3 signalling due to its slow binding kinetics, leading to induction of apoptosis, reductions in tumor volume and pharmacodynamic endpoints. It can be used to inhibit signalling in cells with Flt3-ITD or in wild type cells. However, the apoptosis can be achieved only in cells with constitutive Flt3 activation, irrespective of ITD or wild type. Even a transient brief exposure is sufficient to induce durable inhibition of Flt3 and its

signalling pathways, as well as to have a lasting effect on cell viability in Flt3-dependent cells *in vitro* and *in vivo*.

Despite the fact that sustained Flt3 inhibition induces apoptosis in the Flt3-ITD AML blasts in suspension culture [126, 139], Flt3-ITD blasts undergo terminal myeloid differentiation when stimulated with marrow derived cytokines [140, 141]. In an *in vitro* co-culture of primary Flt3-ITD blasts with human bone marrow stroma, Flt3 inhibition induces cell cycle arrest and gradual terminal myeloid differentiation rather than apoptosis. Such an effect has been observed in patients administered quizartinib [142] and the potential reason is a persistent activation of MAPK signalling mediated by stromal derived cytokines [143]. Therefore, relapsed Flt3-ITD AML patients treated with quizartinib, show a quick apoptosis of peripheral blasts and over time terminal myeloid differentiation of bone marrow blasts. This can lead to an efflux of peripheral blood neutrophils, when the differentiated myeloid cells leave the bone marrow. However, due to neutrophils derived from Flt3-ITD blasts, some leukemic clones remained in the bone marrow, leading to the generation of resistant clones [142]. The difficulty in eliminating resistant leukemic clones is consistent with results based on genome sequencing studies which showed that Flt3-ITD mutations occur as cooperating events in the development of AML. AML cells acquire additional mutations at relapse that might contribute to chemotherapy resistance [144].

4.1 Clinical trials for quizartinib

Monotherapy

In the first human Phase I clinical study quizatinib was administered as monotherapy once a day in escalating doses from 12 to 450mg in 76 patients with relapse or refractory AML irrespective of Flt3-ITD status. The median age of patients was 60 years. Two patients were administered 300mg quizartinib reaching the grade 3 QTc prolongation as the dose-limiting toxicity. Significant clinical responses were observed from doses of 18mg and higher. Median survival of patients was 14 weeks. Ten out of 18 with Flt3-ITD responded to quizartinib [145].

Efficacy and safety of quizartinib monotherapy were assessed in the phase II trial and involved two cohorts of patients of age 60 years and older in the first cohort and of patients of age 18 and older in the second. Patients carried Flt3-ITD and Flt3 WT. Female patients in both cohorts received 90 mg/day of the drug, whereas male patients received up to 135 mg/day. Treatment was in 28-day cycles. Flt3-ITD patients of the first cohort had median OS of 25.3 weeks, whereas Flt3 WT patients- 19.0 weeks. Flt3-ITD patients of the second cohort had median OS of 23.1 weeks, whereas Flt3 WT patients- 25.6 weeks. Adverse effects were noticed in both cohorts and included myelosuppression and QTc prolongation that was alleviated with dose modifications [146].

In another study, patients older than 70 years with relapsed or/and refractory AML had a clear benefit with quizartinib which is important, as they have more limited treatment options due to age [147].

Lower doses of quizartinib were also investigated in a randomized, open-label, phase IIb study, where 76 patients with relapsed/refractory Flt3-ITD mutated AML received 30 and 60mg of

quizartinib. The rate of grade 2 and higher QTc prolongation was more pronounced in the group that received 60mg of drug (17% vs 11%), whereas grade 3 QTc was 5% in the group treated with 30mg and 3% in that treated with 60mg. OS was better for the high than the low dose (60 vs 30 mg: 27.3 vs 20.9 weeks). Sixty one percent of patients treated with 30mg of the drug had to increase the dose due to lack or loss of response, whereas only 14% of those receiving 60mg needed an increase. These results show that quizartinib is effective at low doses with 60mg being the most clinically acceptable [148].

Taken together, quizartinib emerged as the most effective single agent among Flt3-targeted therapies in patients with relapsed/refractory Flt3-ITD AML. Its high efficacy and decent safety profile are encouraging to continue clinical trials for further evaluation of the drug in the treatment of leukemia.

Combination with other therapies

Although quizartinib shows promising effects as a monotherapy, duration of response is limited. Other inhibitors were not as powerful as single agents, but showed more potency when combined with chemotherapy [149, 150]. Therefore, a number of studies have been conducted to evaluate the effect of quizartinib when combined with other therapies.

Quizartinib was administered in combination with cytarabine and daunorubicin in newly diagnosed AML patients, unselected for Flt3 mutation in a phase I open-label, sequential group dose-escalation trial. The drug was initiated on day 4 of chemotherapy and tested at 3 dose levels (60mg/daily for 7 days, 60mg/daily for 14 days and 40 mg/daily for 14 days) on 19 patients (median age of 43.8 years). The ORR was 84%. The maximum tolerated dose (MTD) was 40 mg/daily for 14 days. Three patients underwent dose-limiting toxicity in form of

pericardial effusion, febrile neutropenia, decreased platelet count, QTc prolongation and pericarditis. This study showed that quizartinib can be efficiently administered alongside the standard chemotherapy to the patients with AML [151].

Another study examined the combination of quizartinib with azacitidine or low dose cytarabine (LDAC). A dose of 20mg of cytarabine was administered twice/daily for 10 days or dose of azacytidine of 75mg/m^2 for 7 days in the phase I trial. In the following phase II 60mg of quizartinib was administered daily in combination of azacytidine and LDAC. ORR was 67% and patients survived up to 14.8 months. The side effects included electrolyte abnormalities, elevated bilirubin and QTc prolongation [152].

The latest global phase III, open-label randomized trial QuANTUM-R enrolled patients with Flt3-ITD mutated relapsed/refractory AML. Patients received either single agent quizartinib in dose of 60mg orally or salvage chemotherapy: fludarabine, cytarabine, filgrastim, idarubicin (FLAG-IDA), mitoxantrone, etoposide, cytarabine (MEC) or low-dose cytarabine. The OS of the patients who received quizartinib was longer than those who received the chemotherapy (6.2 vs 4.7 months, respectively). Patients treated with quizartinib had reduction in the risk of death in comparison to those treated with chemotherapy and also, less adverse effects with the exception of QT prolongation. This is the first trial showing that quizartinib has survival advantage as a single agent over salvage chemotherapy in Flt3 mutated relapsed/ refractory AML [153].

Given the poor outcome of patients with Flt3-ITD AML when treated with chemotherapy, these patients are often recommended allogeneic HSCT. However, despite the initial benefit there is still a high risk of relapse. This led to suggestion of quizartinib administration as maintenance

therapy after allogeneic HSCT. Phase I and II studies identified 60mg/daily as the highest dose for daily administration in relapsed/refractory AML and showed that quizartinib can be applied safely in the post allogeneic HSCT [154, 155].

Table 2. Clinical trials of quizartinib in myeloid malignancies [128]

Study	Phase	Status	Findings	Reference/ Identifier
Phase I study of quizartinib administered daily to patients with relapsed/ refractory AML irrespective of Flt3-ITD status	I	**Completed**	Total 76 patients were enrolled. ORR was 30%. In Flt3-ITD+ patients, ORR was 53% versus 14% in Flt3-ITD – patients. Quizartinib, single agent was overall well tolerated. MTD was 200 mg daily; prolonged QTc was the DLT.	NCT00462761 **[156]**
Quizartinib, an Flt3 inhibitor, as monotherapy in patients with relapsed/ refractpory AML: an open-label, multicenter, single arm, phase II trial	II (cohort 1) (patients > 60 years) II (cohort 2) (patients >18 years)	**Completed** **Completed**	157 patients were enrolled. Single agent quizartinib showed activity and was well tolerated amongst older patients; CRc was 56% in Flt3-ITD+ patients. 176 patients were enrolled. Single agent quizartinib was safe and effective amongst the younger relapsed/refractory AML. The CRc was 46% in the Flt3-ITD+ patients. 35% patients successfully bridged to HSCT.	NCT00989261 **[157]**
Phase IIb study of two dosing regimens of quizartinib monotherapy in Flt3-ITD-mutated, relapsed or refractory AML	IIb	**Completed**	Quizartinib was effective and less toxic at lower doses. CRc rates (47%) between the 30 and 60 mg dose levels were comparable to higher doses of quizartinib. Median OS, CRc duration and HSCT rates were higher in the 60 mg arm than the 30 mg arm.	NCT01565668 **[155]**
Phase I study of quizartinib in combination with induction and consolidation chemotherapy in patients with newly diagnosed AML	I	**Completed**	19 patients with newly diagnosed AML were enrolled. Quizartinib at 40 mg daily for 14 d starting day 4 of standard chemotherapy was the MTD. ORR was 84%. In Flt3-ITD + patients the CRc was 67%.	NCT01390337 **[151]**
The combination of quizartinib with azacitidine or low dose cytarabine is highly active in patients with Flt3-ITD mutated myeloid leukemia: interim report of phase I/II trial	I/II	**Recruiting**	To date, 52 patients have been enrolled (aza=38; LDAC=14). ORR was 67–77% in aza arm and 23% in LDAC arm. 11 patients proceeded to HSCT.	**[152]**
Results of a phase I study of quizartinib as maintenance therapy in subjects with AML in remission following allogeneic hematopoietic stem cell transplant	I	**Completed**	13 patients with Flt3-ITD mutated AML in remission following HSCT were enrolled. 77% patients received maintenance for >1 year; 38% patients completed maintenance for 2 years. Only 1 patient relapsed.	NCT01468467 **[154]**
QuANTUM–R: phase III study of quizartinib monotherapy versus salvage chemotherapy in	III	**Active, not recruiting**	367 patients have been accrued. This is the first phase III study showing survival benefit of 24% with single agent quizartinib over salvage chemotherapy in patients with relapsed/refractory Flt3 mutated AML	NCT02039726 [**158]**

patients with Flt3-ITD mutated relapsed/refractory AML				
QuANTUM-First: phase III study of quizartinib versus placebo with induction and consolidation chemotherapy and maintenance in newly diagnosed Flt3-ITD mutated AML	III	**Active, recruiting**	First phase III study enrolling newly diagnosed Flt3 ITD mutated AML patients evaluating quizartinib in combination with conventional chemotherapy. Study is expected to enroll >500 patients.	NCT02668653
Combination of quizartinib and omacetaxine mepesuccinate for AML carrying Flt3-ITD	II	**Active, recruiting**	-	NCT03135054
Quizartinib and decitabine in treating participants with untreated or relapsed Flt3-ITD mutated AML or MDS	I/II	**Not yet recruiting**	-	NCT03661307
DS-3033b plus quizartinib combination study in Flt3-ITD mutant AML	I	**Active, recruiting**	-	NCT03552029

AML: acute myeloid leukemia; ITD: internal tandem duplication; HSCT: hematopoietic stem cell transplantation; ORR: overall response rate; CRc: composite complete remission; MTD: maximum tolerated dose; DLT: dose-limiting toxicity.

4.2 Mechanisms of resistance to quizartinib and other Flt3 inhibitors

One of the obstacles to overcome while treating patients with Flt3 inhibitors is a short response duration due to rapid development of resistance, which leads to the treatment failure. Data from trials in which Flt3 inhibitors were used as monotherapy indicated a primary resistance rate around 30% of all Flt3 AML patients [159].

One of the potential reasons of resistance to Flt3 inhibitors is the appearance of new mutations. Patients with resistance showed a similar pattern of harbouring Flt3-TKD mutations [160, 161]. The constitutive activation of essential tyrosine residues (Tyr845, Tyr892, Tyr922) in the Flt3 mutants and downstream signalling factors was one of the main resistance mechanisms of Flt3 TKIs [162].

Another reason responsible for the resistance emerging in Flt3-ITD cells is upregulation of RUNX1 expression. Silencing of RUNX1 abrogated the emergence and proliferation of quizartinib-resistant Flt3-ITD cells in the presence of quizartinib [163]. Moreover, reactivation of downstream FGF/Ras/ERK and Wnt signalling pathways have been shown to induce resistance to quizartinib [164]. FGF2 promotes resistance through activation of FGFR1 and downstream MAPK effectors [165]. Other significant factors that seem to be involved in quizartinib resistance are p21Cdkn1a (p21) and pre-B cell leukemia transcription factor 1 (Pbx1). Quizartinib inhibits the p21-mediated inhibitory signal on cell proliferation, allowing Flt3-ITD positive cells to proliferate again. Loss of p21 is accompanied by the upregulation of Pbx1 expression [166]. Moreover, the effect of Flt3-TKD on drug resistance may be due to perturbation of deactivation of the protein, which is necessary for drug binding, leading to the reduced affinity of the drug to the mutants [167]. Crystal structure of quizartinib attached to Flt3 suggested that such contact depends on the basic aromatic interactions with the gatekeeper F691 and F830 residues and therefore, any alterations in F691 and F830 may result in a significant loss of binding affinity [168]. Furthermore, Flt3-ITD mutations in most AML patients are activated when becoming resistant to the quizartinib, accompanying large clonal diversity. Besides, high patient genetic heterogeneity also remarkably reduces the response to the targeted therapeutics with quizartinib [169].

A promising solution in clinical trials to overcome the resistance is to combine Flt3 inhibitors with other agents. A collaborative Flt3 inhibitor, HSD 1169 that acts against Flt3-ITD and sorafenib-resistant cell lines, has already shown an effect [170]. Moreover, TAK-165, an autophagy inhibitor, eliminated tumor cells through the activation of chaperone-mediated autophagy to enhance the efficacy of quizartinib [171]. In another study, inhibition of PI3K-δ showed synergistic anti-tumor activity with Flt3 inhibitors [172]. Combination of novel

inhibitors with established Flt3 inhibitors gives promising signs of efficacy improvements in the near future. Immune checkpoint inhibitors, chimeric antigen receptor (CAR) T cells and bispecific antibodies are important agents in novel cancer immunotherapy [173]. For example, Flt3-targeted CAR T cells have shown to have synergic activity with crenolanib [174]. Taking these examples into consideration, integration of Flt3 inhibitors into cancer immunotherapy seems to be an optimistic method to minimize resistance.

4.3 Adverse effects of quizartinib

Quizartinib is a chronically-administered agent with the potential for cumulative toxicity and/or decreased tolerability over time. FDA analyses [175] recorded that quizartinib treatment was associated with concentration- dependent prolongation of QTcF to levels consistent with an increased risk of arrhythmias. The prominent side effects of the treatment were fatigue (36%), edema (25%), ECG abnormality (25%), dyspnea (18%), hypotension (20%), dizziness (11%), headache (15%), presyncope/syncope (9%), fall (7%), palpitations/arrhythmia (9%), angina (4%), cardiac failure, hypoxia and heart block (2%). QT prolongation (25%) was the most common cardiac adverse event.

Sudden cardiac death or cardiac arrest are the most serious clinical consequences of the pro-arrhythmic potential of quizartinib. Therefore, FDA performed an analysis consisting of the 724 patients with AML not in remission, treated with quizartinib monotherapy across 5 clinical studies and 169 patients with newly-diagnosed AML from the on-going Phase III trial Study AC220-A-U302. Four deaths (1.7%) due to acute or subacute cardiac events attributed to quizartinib treatment were identified.

Overall, due to its unique mechanism for QT prolongation, quizartinib has the potential to trigger sudden death at the time of a rapid rise in heart rate, even without previously observed QTcF prolongation.

5. Cardiotoxicity of tyrosine kinase inhibitors: on-target, off-target

Because of the significant oncologic benefits of the small molecule inhibitors in cancer therapy and the belief that targeted therapeutics have fewer toxic side effects than conventional chemotherapy, the first signs of cardiotoxicity were surprising. The first reports of TKI cardiotoxicity was a case of 10 patients who received treatment with imatinib and developed congestive heart failure (CHF) [176]. In a study conducted on patients with gastrointestinal stromal tumors (GISTs) who were treated with sunitinib, assessments of LVEF and the biomarker troponin I showed that 18% of patients happened to have CHF or a 15% or more decline in LVEF [177]. Cardiotoxicity from TKI treatment was also observed in the patients receiving sorafenib [178].

Toxicity can be categorized into 2 types: on-target and off-target. An optimal target would be the one having an important role in the cancer kinome, but not in other organs, therefore by inhibiting it, function of other organs would not be affected [179]. Such targets are very rare though and usually targets involved in cancer also have a significant role in other organs, including the heart and vasculature. Therefore, inhibiting such targets could lead to on-target toxicity.

An example of on-target toxicity is treatment with sorafenib. It has the ability to inhibit sarcoma RAF-1 and BRAF alongside several growth factor receptors. RAF kinases are a part of the pro-survival ERK (mitogen-activated protein kinase) pathway. Conditional cardiac-specific

deletion of RAF-1 in a mouse model led to LV dilation and reduced contractile function, highlighting the significant role of RAF-1 in the heart [180]. A phase III clinical trial showed that sorafenib is effective for the treatment of advanced clear-cell carcinoma in the kidney. However, cardiotoxicity in the form of cardiac ischemia or infarction occurred in 3% of patients [181].

A few approaches to tackle the unavoidable on-target toxicity have been proposed and they include targeted delivery of the compounds to the cancer, avoiding normal tissue or inhibiting cell death pathways in the heart that are activated by the drug but that are not necessary for tumor cell death [173]. For example, JNK inhibition has been proposed as a strategy to limit imatinib-induced cardiomyocyte death without reducing anti-tumor efficacy [182]. An alternative approach could be to identify and target unique kinases from the cancer kinome that are not present in the heart or are not necessary for the physiological heart function. Target selection in drug discovery has been directed towards previously validated targets. It seems that the majority of agents in development targets kinases for which approved drugs are already available. Genome sequencing and ribonucleic acid interference screens give a new hope for identification of novel uncharacterized kinase targets [183].

Off-target toxicity means that a TKI inhibits a kinase, it was not primarily meant to inhibit and that this kinase plays an essential role in the heart. The majority of the approved TKIs bind to multiple kinases, although with different affinities. Cardiotoxicity of TKIs is correlated with a lack of target specificity [184]. Often, the kinase mediating toxicity is unknown and its identification can be very difficult. Multitargeting (for example, sunitinib has more than 50 targets and sorafenib more than 15) makes it even more challenging [179]. Off -target toxicity induced by sunitinib is a characteristic example of poor selectivity. Sunitinib was designed as

a multikinase inhibitor that targets VEGF1, PDGF, colony-stimulating factor 1 receptor and others. However, it has the capability to inhibit up to 90 kinases [185]. A phase I/II trial investigating the efficacy of sunitinib in 75 patients with gastrointestinal stromal tumor showed an 8% incidence of heart failure and a 28% incidence of LVEF decrease of more than 10% [177]. Toxicity of sunitinib is likely due to both on- and off-target effects. Off-target cardiotoxicity could be reduced by improving selectivity or redesigning the drug so that it no longer inhibits heart-relevant kinases (assuming the kinase does not have a key part in cancer progression). Obviously, off-target toxicity will be more frequent with multitargeted TKIs and combination therapy. Furthermore, a study of potential mechanisms of toxicity in cultured cardiomyocytes *in vitro* showed an evidence of energy compromise [186]. No activation of AMP-activated protein kinase (AMPK), the master regulator of the response of the cardiomyocyte to energy stress, was observed in sunitinib treated cardiomyocytes. Kinase assays showed that sunitinib was a very potent direct inhibitor of AMPK with IC50 values for the catalytic (α) subunits in the very low nanomolar range, being responsible for the failure to recruit the kinase. Adenoviral-mediated gene transfer of a constitutively active α subunit of AMPK partially rescued sunitinib-induced cell death, suggesting off-target inhibition of AMPK accounted for the toxicity [186]. This is an interesting example of off-target inhibition of a kinase that might be unessential for tumor cell elimination, but it is important for cardiac homeostasis. Another study found that several kinase inhibitors, including sunitinib, can directly activate the endoribonuclease activity of IRE1, leading to XBP-1 splicing and a reduction in endoplasmic reticulum stress [187]. Such response can be cytoprotective for both stressed cancer cells and cardiomyocytes. The researchers suggested that sunitinib has to be redesigned to avoid activation of endoribonuclease activity, thereby enhancing cancer cell death, however, this might also enhance cardiotoxicity. These examples illustrate the similar critical roles played by many of these kinases in cancer progression and cardioprotection.

Overall, the use of agents with exceptional pharmacokinetic and pharmacodynamic properties can be promising with regard to the identification of so far unknown biological functions of kinases in the heart. Identification of the roles of a kinase of interest can be achieved by using combinations of inhibitors that all inhibit this kinase, but that have different off-target profiles. Such methods could be applied to study the developing and adult heart as well as stem cell populations [188].

6. Pathophysiology of myocardial infarction and cardiac remodeling

Myocardial infarction (MI) is a major health issue associated with significant mortality and morbidity and a leading cause of the heart failure. During MI due to oxygen deprivation when a coronary artery gets blocked and there is limited supply of blood to the cells, cardiomyocytes die [189]. Hypoxic conditions induce anaerobic respiration and destabilization of the cellular membrane, finally leading to cardiomyocyte death [190-192]. Myofibrillar contraction bands, ruptured mitochondria, destruction of cardiomyocyte membranes, microvascular destruction, haemorrhage and inflammation are the main characteristics of the infarcted myocardium [193]. Necrotic cell death in the infarcted myocardium contributes to the enhanced production of reactive oxygen species (ROS) finally leading to oxidative stress [194, 195]. After the acute MI oxidative stress occurs in both infarcted and non-infarcted myocardium. Neutrophils and macrophages express NADPH oxidase, which is a major source of O_2 in the heart [196], and it is highly increased in the infarcted myocardium [197]. Moreover, nitric oxide (NO) synthase, a major source of NO in the repairing tissue, is produced by macrophages and is also increased in infarcted myocardium, triggering an enhanced production of NO [198]. Moreover, the ability to fight the oxidative stress is impaired in the infarcted heart. Overall, oxidative stress holds an important role in the progression of MI, contributing to myocardial remodelling, including the proinflammatory response, cardiomyocyte apoptosis and hypertrophy.

The healing process after MI consists of inflammatory, proliferative and maturation phases (**figure 8**). The inflammatory response post MI leads to healing and scar formation and is triggered by coordinated activation of different chemokines, cytokines and adhesion molecules. Nuclear factor-kappa B (NF-kB) is a redox-sensitive transcription factor and is one of the most important regulators in the activation of these genes. Under normal conditions it remains inactive, however when the tissue gets injured, NF-kB is triggered by ROS [199]. Activated NF-kB stimulates immune responses by enhancing the gene expression of interstitial and vascular adhesion molecules, as well as monocyte chemoattractant protein-1, leading to leukocyte infiltration into the infarcted myocardium [200]. It also initiates gene expression of pro-inflammatory cytokines, such as tumor necrosis factor (TNF)-α and interleukins, initiating an inflammatory response [201]. In animal models of MI TNF-α expression is upregulated and is responsible for the induction of inflammatory protein synthesis, macrophage phagocytosis, cell growth, differentiation and apoptosis [202]. Furthermore, H_2O_2 may stimulate cardiac TNF-α production through activation of the p38 MAPK pathway and thus mediate myocardial inflammation [203]. Neutrophils and macrophages next digest dead cells and extracellular matrix (ECM) debris [204]. During the proliferative phase monocytes and macrophages release cytokines and growth factors, supress inflammatory factors, promote angiogenesis, proliferation of fibroblasts and production of ECM proteins. While at the final stage of the maturation phase, apoptosis of fibroblasts and vascular cells leads to formation of a collagen scar [205-207]. Such changes in cellular mechanisms induce alterations in ventricular shape and function, thinning of the myocardium, ventricular dilation, hypertrophy of the non-infarcted myocardium and an overall deterioration in cardiac function. These features contribute to adverse ventricular remodelling that over time increases the chances of heart failure and mortality [208].

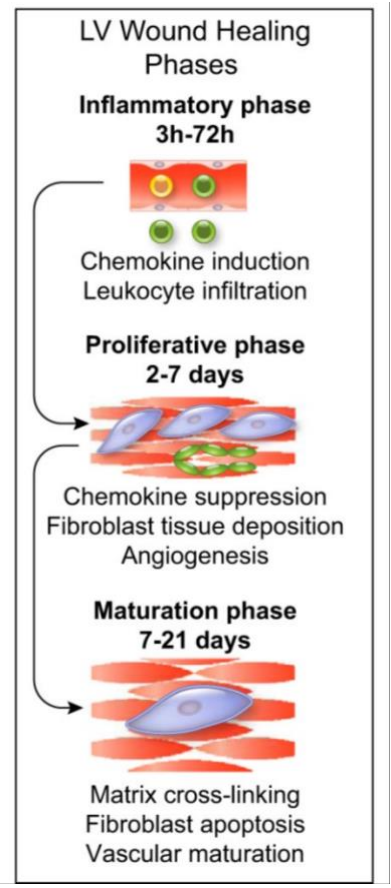

Figure 8. Phases of post MI healing process [209]

Cardiac remodelling may occur as an adaptive or maladaptive mechanism not only after MI, but also due to pathophysiological stimulation, which leads to an elevation in wall stress and reduction in contractility, such as ischemia, pressure and volume overload, neuroendocrine activation or genetic background [210, 211]. Adaptive remodelling allows the physiological cardiac function to be maintained due to compensatory structural and functional alterations of the heart [212, 213]. However, due to persistent stress, cardiac remodelling becomes maladaptive over time and culminates in irreversible cardiac damage [214]. The main features of the cardiac remodeling are cardiomyocyte loss due to apoptosis, necrosis, necroptosis or autophagy; compensatory cardiomyocyte hypertrophy; fibroblast proliferation and ECM reorganisation leading to fibrosis; mitochondrial dysfunction and metabolic aberrations that

lead to reduction of contractility (**figure 9**) [215]. Cardiac remodelling is also accompanied by increased LV mass and reduction in LV ejection fraction [216].

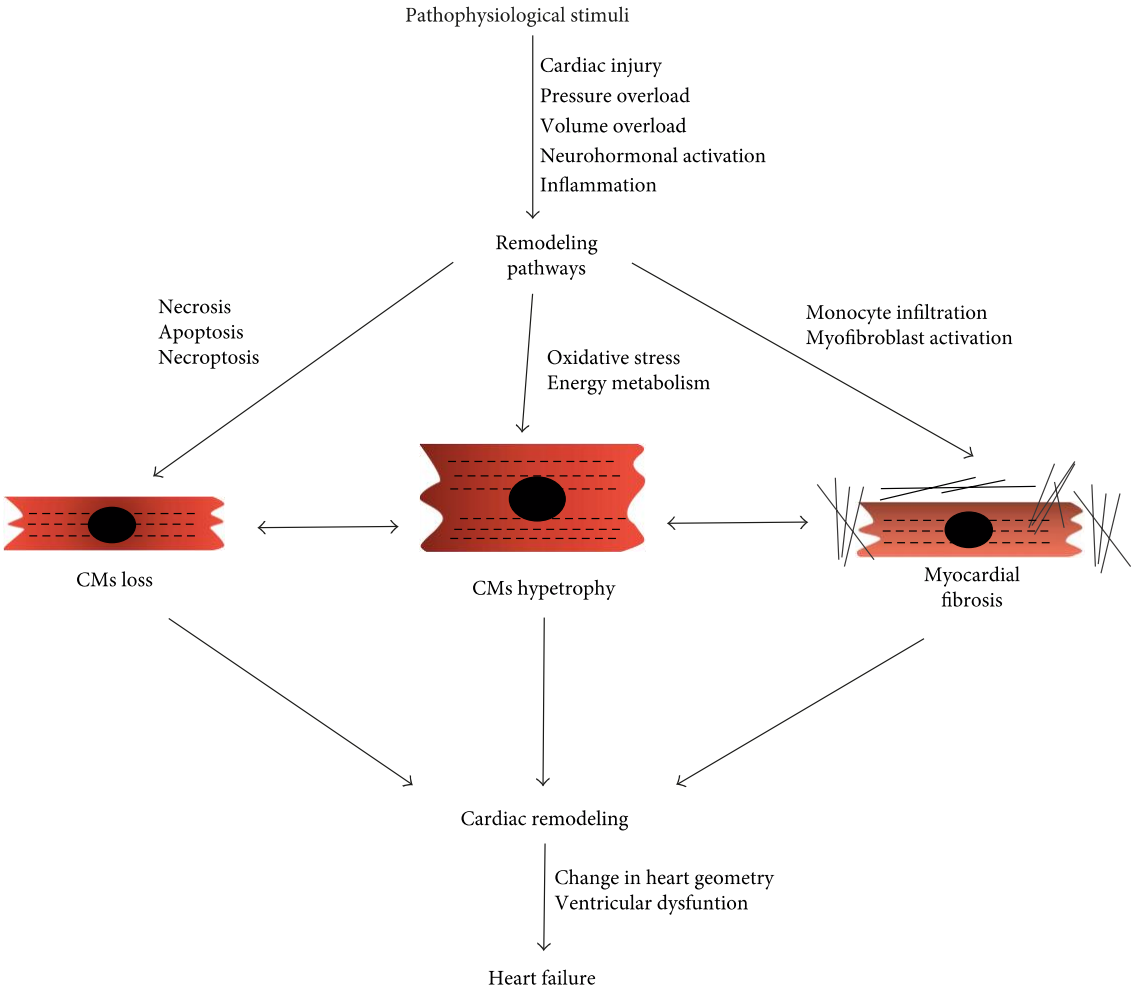

Figure 9. Overview of the main factors contributing to cardiac remodeling [217]

Progressive loss of myocytes plays an important role in remodeling. There are three main mechanisms that are involved in myocyte death: apoptosis or programmed cell death, necrosis and autophagy [218]. Despite the debates how apoptosis or necrosis are involved in the progression of cardiac dysfunction, recent evidence suggested that both mechanisms are closely related and are different versions of the same process called necroptosis [215].

Autophagy is an evolutionary conserved mechanism for cellular homeostasis, where proteins and mitochondria are recycled for energy production and protein synthesis. Activation of autophagy has been shown to constitute cardioprotective effects in cardiovascular pathologies (via ATP production or protein and organelle quality control) [219]. It is an adaptive response of the heart to stress overload. However, prolonged upregulation of autophagy may be damaging for heart function [219].

As a compensatory adaptive response to injury or stress that deteriorates the cardiac output, cardiomyocytes undergo hypertrophy. Persistent hemodynamic overload on the heart walls leads to tissue remodelling, which starts as a compensatory LV hypertrophy. However, such compensatory remodelling will eventually also result into pathological remodelling, leading to heart failure [220]. Adaptive hypertrophic remodelling has to maintain an equilibrium of inflammation, angiogenesis and cardiac muscle growth. If this balance cannot be kept, maladaptive remodelling occurs. During such pathological remodelling, there is a decrease in cardiomyocyte force generation, which consequently is responsible for ventricular dilation, contractile abnormality and arrythmias [220]. Chronic hypertrophy is characterized by apoptosis and interstitial and perivascular fibrosis. Deposition of type I and III collagen and ECM crosslinking stiffen the walls, diminishing the heart elasticity and diastolic function [221]. Fibrosis further reduces contractility and disturbs the cardiac chemoelectrical conductance, resulting in inefficient contractions [222]. During fibrotic deposition, in both adaptive and pathological responses, there is monocyte infiltration that enhances the local macrophage population. Monocytes are considered to regulate the myocardial inflammatory response that is triggered by cytokines, macrophages and lymphocytes [223]. Endothelial cells also play an important role in the profibrotic inflammatory environment by initiating a proinflammatory secretory phenotype [224]. Additionally, subpopulations of lymphocytes and

mast cells contribute to activation of fibroblasts within the myocardium maintaining the inflammation [225, 226].

Aim and hypothesis of the study

Tyrosine kinase inhibitors are successfully used in cancer therapy, however they may exert cardiotoxicity through on-target or off-target effects in the patients.

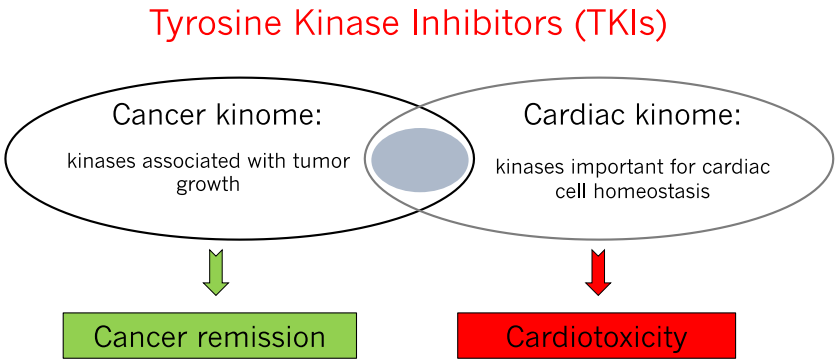

Given that Flt3 exerts a cytoprotective role in the heart and that cardiac Flt3 activation is beneficial for cardiomyocyte survival under ischemic conditions [79], the inhibition of this signaling pathway might lead to further cardiomyocyte damage in already injured heart, resulting in additional cardiac dysfunction. Therefore, the aim of the study was to investigate whether quizartinib aggravates cardiac damage after myocardial infarction and whether this is related to the inhibition of the Flt3-dependent signaling pathway

We hypothesized that wild type mice treated with quizartinib are more susceptible to ischemic damage and show worse remodeling and function after myocardial infarction than vehicle-treated mice and that there is no additional deterioration after MI in quizartinib treated flt3 (-/-) mice.

The Fms-like tyrosine kinase 3-targeting inhibitor quizartinib decreases cardiomyocyte viability and potentiates hypoxic cell death *in vitro* and *in vivo*

Daria Monogiou Belik, Lifen Xu, Giacomo Della Verde, Vera Lorenz, Melania Balzarolo, Aleksandra Wodnar-Filipowicz, Michika Mochizuki, Otmar Pfister and Gabriela M. Kuster

Manuscript Draft

Abstract

Aims: Tyrosine kinase inhibitors (TKIs) targeting fms-like tyrosine kinase 3 (Flt3) have been developed for treatment of hematologic malignancies such as acute myeloid leukemia. Flt3 is also expressed in the heart and its activation is cytoprotective in myocardial infarction (MI). We sought to test whether pharmacological inhibition of Flt3 aggravates cardiac injury and worsens outcome after MI. **Methods and Results:** Five week-old male C57BL/6NRj mice were administered quizartinib (10 mg/kg) or vehicle (captisol) once daily by gavage for three weeks. Mice were then randomly assigned to MI or sham surgery and drug administration was continued for another three weeks. Quizartinib did not affect cardiac dimensions or function after one week post-MI compared to vehicle. However, after one week, apoptotic cell death was significantly enhanced in both the infarct border zone and the remote myocardium of quizartinib-treated vs. vehicle-treated mice. There were no differences in cardiomyocyte size or fibrotic area. In a longitudinal analysis over three weeks post-MI, cardiac dilation and decline in cardiac function appeared more consistent in quizartinib-treated infarcted mice vs. quizartinib-treated sham mice than in vehicle-treated infarcted mice vs. their corresponding sham. Histology showed no differences in apoptosis or fibrosis after three weeks between quizartinib and vehicle-treated mice. Myocardial infarction caused less damage in non-conditional Flt3-deficient mice irrespective of quizartinib treatment, suggesting that functional Flt3 is required for quizartinib toxicity. Quizartinib dose-dependently decreased cell viability and increased apoptosis in H9c2 cells *in vitro*. In addition, quizartinib at both high (20μM) and low concentrations (5μM) augmented H_2O_2-induced cell death and apoptosis beyond additive degree. **Conclusions:** In contrast to non-conditional Flt3-deficiency, short-term pharmacological inhibition of Flt3 decreases cell viability and potentiates hypoxic cardiomyocyte death *in vitro* and *in vivo*. These findings raise concerns regarding potential cardiotoxicity in patients with underlying ischemic heart disease.

Introduction

Improvements in cancer therapy have impressively increased the lifespan of cancer patients. However, cardiovascular complications remain a primary and potentially life-limiting side effect of cancer treatment [1]. Cardiomyopathy and heart failure are among the most important manifestations of cardiotoxicity [2]. They may occur during or immediately after cancer therapy or up to several years later as it is frequently the case for anthracycline-induced cardiomyopathy [3, 4]. Cardiac dysfunction and heart failure can also be observed under targeted therapies, such as tyrosine kinase inhibitors (TKIs) [5]. TKIs are small molecules that inhibit the enzymatic activity of tyrosine kinases and block downstream signaling activation [6].

Fms-like tyrosine kinase 3 is a membrane-bound receptor tyrosine kinase (RTK) that has a crucial role in normal haematopoiesis [7]. Stimulation of the receptor with its ligand activates signal transduction pathways involving phosphatidylinositol 3 kinase (PI3K)/Akt and Ras-Raf-MEK-ERK, which trigger the proliferation and survival of hematopoietic progenitor cells [8, 9]. Flt3 is also expressed in the heart and upregulated after myocardial infarction (MI) in mice [10]. We recently demonstrated that stimulation of Flt3 with recombinant Flt3 ligand exerts cytoprotective effects after MI in mice when administered at therapeutic concentrations into the infarct border zone. Flt3 activation decreased cardiomyocyte apoptosis *in vivo* and improved post-MI function and remodelling by reducing the infarct size. Flt3 ligand also activated Akt-dependent pro-survival signalling and reduced oxidative stress-induced apoptosis in cardiomyocytes *in vitro* [11].

Activity-enhancing mutations of Flt3 have been found in 15-35% of patients with acute myeloid leukaemia (AML), making Flt3 one of the most frequently mutated genes in

haematological malignancies [12]. In recent years, several TKIs targeting aberrant Flt3 signaling to decrease relapse rate and improve survival have been developed. First generation TKIs lacked specificity for Flt3 and cardiac toxicity has been reported. Specifically, sorafenib and sunitinib can cause mitochondrial dysfunction and cell death, which is mostly attributed to inhibition of RAF I, VEGFRs and PDGFRs, respectively [5, 13]. Second generation compounds (quizartinib, gilteritinib, crenolanib) are more selective and potent inhibitors of Flt3 with a narrower kinome profile in order to improve their activity and tolerability in patients with AML [14, 15]. Quizartinib (also known as AC220) is the first drug specifically designed to selectively inhibit Flt3 [6]. It has higher *in vivo* potency than first generation inhibitors [14, 16, 17] and is highly selective for Flt3 already at nanomolar concentrations [18]. Quizartinib has been studied in a number of clinical trials as a single drug for treatment of AML demonstrating promising results with sufficient tolerance and controllable safety [19-21]. However, because patients with cardiovascular disease are mostly excluded from clinical trials, knowledge about the cardiovascular toxicity of quizartinib is scarce. Still, quizartinib failed to obtain FDA approval in 2019 with the FDA citing cardiac side effects as one of the major concerns. Besides ECG abnormalities and arrhythmias, these also included dyspnea, cardiomyopathy and heart failure [22]. Given the cytoprotective role of Flt3 in the infarcted mouse heart we now sought to test whether treatment of mice with quizartinib during MI worsens outcome and – if yes – whether this is related to Flt3 signaling.

Materials and methods

Animals and in vivo model

Studies were conducted using five-week-old male C57BL/6NRj (WT) and 129S/SvEv-Flt3tm1Irl (Flt3-KO) mice. Flt3-KO mice were kindly provided by Prof. Aleksandra Wodnar-

Filipowicz from the Department of Biomedicine of the University Hospital and University of Basel, and used with the permission of their creators [23]. The breeding and the animal care were carried out in the Animal Facility of the Department of Biomedicine, University Hospital Basel (ZLF, Basel, Switzerland). The procedures were performed according to guidelines of the Swiss Federal Act on Animal Protection and the National Institutes of Health Guide for the Care and Use of Laboratory Animals and approved by the Veterinary Department of Basel (Switzerland).

Quizartinib dosing and treatment

Quizartinib was purchased from Selleck Chemicals (Houston, TX, USA). It was diluted via sonication in 15% polyanionic beta-cyclodextrin Captisol (Cidex pharmaceuticals) to the concentration of 2mg/ml and administered through oral gavage once per day. The drug was given in the dosage of 10mg/kg/day based on preclinical animal studies of pharmacokinetic properties and efficacy after administration of a single dose. Zarrinkar and colleagues showed that a single dose was well absorbed achieving a maximum plasma level of 3.8μM within 2h. The peak concentration of free quizartinib after a single 10mg/kg dose was more than 30-fold above the IC50 for Flt3-ITD inhibition in cellular assays. After 24 hours estimated free drug was present at a concentration of the cellular IC50, indicating that once a day oral dosage is sufficient for continuous inhibition of Flt3 activity in mice [14]. Moreover, a test for antitumor efficacy of the drug in a MV4-11 tumor xenograft model showed that treatment with 10 mg/kg leads to rapid and complete regression of tumors in mice and no tumor regrowth was observed during the 60-day posttreatment observation period [14]. The overall experimental set up included 80 WT mice among which 40 mice received quizartinib and 40 mice received vehicle only (in form of captisol) for 21 consecutive days. Five animals died for technical reasons before or during the surgery. Animals that survived the myocardial infarction surgery (see below)

continued in the experiment for the next 7 consecutive days. A subpopulation of 13 mice continued quizartinib administration and of 12 mice vehicle administration for 14 additional days after the surgery and before sacrifice. Another experimental set up included 31 Flt3-KO mice, among which 16 Flt3-KO mice received quizartinib and 15 Flt3-KO mice received vehicle for 21 consecutive days. One animal died before surgery. After the surgery the surviving animals continued the treatment for 21 additional days.

Echocardiography

Transthoracic echocardiography was conducted prior to quizartinib treatment initiation, before myocardial infarction (MI), and one and three weeks post MI using a Vevo 2100 Ultrasound device (VisualSonics, Tororno, ON, Canada) equipped with a MS-550 linear-array probe working at a central frequency of 40 MHz. Mice were anesthetized with 5% isoflurane in pure oxygen for induction and 2% isoflurane for the maintenance through a nose cone. The body temperature was maintained at 37°C by a rectal thermometer on a warming pad. Chest hair was removed with a depilatory cream (Nair). Parasternal long-axis views in B-mode and parasternal short-axis views at mid-papillary muscle level in both B- and M-mode were acquired. Data were transferred to an offline computer and analysed with Vevo 2100 1.6.0 software by an investigator who was blinded to the experimental details including treatment allocation and surgical group. Left ventricular (LV) anterior (LVAW) and posterior (LVPW) wall thickness and internal dimensions (LVID) were derived from the measurement of M-Mode. Values were averages of three cardiac cycles. Left ventricular ejection fraction (EF) was calculated from derived volumes (Vol), which are computed based on the Teichholz formulas:

$LV\ Vol;d=(7.0 / (2.4 + LVID;d)) \times LVID;d^3$,

$LV\ vol;s=(7.0 / (2.4 + LVID;s)) \times LVID;s^3$,

EF%=100 x ((LV Vol;d – (LV Vol;s) / LV Vol;d), whereby d denotes diastole and s denotes systole.

LV mass was calculated based on the corrected cube formula:

LV mass=1.053 × [(LVID;d + LVPW;d + LVAW;d)^3 – LVID;d^3] × 0.8.

Echocardiographic 2D strain and strain rate measurement based on speckle-tracking was used to assess the global changes of left ventricular function. For this purpose, the endocardium was manually traced on a parasternal long axis view. Manual adjustments were done when needed. Endocardial strain values were then calculated with the strain package (Vevo Strain Package, Vevo 2100 version 1.6.0).

Myocardial infarction (MI) model

Eight-week-old C57B6/J male mice were randomly assigned to sham or MI group. Before the surgery animals were anesthetized with intraperitoneal injection of ketamin/xylazine/acepromazin (65/15/2 mg/kg). Occlusion of the left anterior descending (LAD) coronary artery was conducted according to previous reports [24, 25]. Briefly, anesthetized mice were intubated endotracheally and connected to a rodent MiniVent ventilator (Model 845, Harvard Apparatus, Holliston MA, USA). A small chest incision was made between the third and fourth left intercostal space, which provided access to the beating heart. After carefully cutting open the pericardium, the heart was exposed and the LAD was permanently occluded with a 8/0 polypropylene suture (B. Braun). The successful ligation was verified by immediate discoloration of the affected myocardium. Then, the chest was closed, the lungs were reinflated and a subcutaneous injection of saline was given for liquid compensation. The mice were then transferred to a warmed chamber for waking up. Sham-operated mice underwent thoracotomy and pericardial incision without LAD ligation. After recovery from operation, subcutaneous injections of buprenorphine (0.1mg/kg in 0.9% NaCl solution) were given every 6h for two

consecutive days. An additional dose of buprenorphine was provided per os during the night (for 2 nights) in the drinking water (9μg/ml). Changes of body weight, physical condition and behaviour were monitored and recorded daily. The mice were sacrificed immediately after the last echocardiography for heart collection.

Perfusion and paraffin embedding

At the time of sacrifice 350mM potassium chloride (KCl) diluted in water was injected intravenously through the jugular vein to arrest the heart in diastole. The thoracic cavity was opened with scissors. A small incision was made on the right atrium to release the blood. A 23G needle, which was connected to a syringe attached to a pressure-controlled perfusion pump, was gently inserted through the apex into the LV. Afterwards, the heart was perfused with 15mL of cold 4% paraformaldehyde (PFA) under a pressure between 70-100 mmHg. The heart was cut free from the main vessels and surrounding tissues. The atria were removed and the weight of the ventricles was measured. The value was normalized to the tibia length. The right ventricle was discarded and the LV was fixed in 4% freshly prepared PFA at 4°C overnight. The next morning the hearts were transferred to 70% EtOH for approximately 6-7 hours and then cut transversally into 2 sections with a razor blade, processed and embedded in paraffin according to routine procedures. The embedded tissue was cut into 4μm sections on a Microm HM 340E Electronic Rotary Microtome (ThermoFisher Scientific, Michigan, USA) and used for histology.

Picrosirius staining

The tissue was incubated at 55°C for 30min, then deparaffinized and rehydrated, and treated with haematoxylin solution, Gill No.3 (Richard-Allan Scientific, #GHS316) for 12min followed by bluing with running tap water. Afterwards, it was dipped into 100% EtOH for

1min and incubated in Sirius Red f3B (diluted in 0.1% picric acid) for 1 hour. The tissue was then dehydrated and mounted in embedding medium (J.T.Baker, #E3921). The stained tissue was scanned using Widefield Fluorescence Nikon Ti2 microscope and analysed with Fiji.

Terminal deoxynucleotidyl transferase dUTP nick end labelling (TUNEL) assay

The tissue was incubated at 55°C for 30min, then deparaffinized and rehydrated and permeabilized using 10mM TrisHCl and 20μg/ml proteinase K (ThermoFisher Scientific, #EO0491) for 25min. The tissue was then washed with tris-buffered saline (TBS) and incubated with *in situ* cell death detection kit, Fluorescein (Roche Diagnostics AG, #12-156-792-910), for 1h at 37°C in the dark. The nuclei were stained with 4',6-diamidino-2-phenylindole (DAPI) (Invitrogen, #D1306). The tissue was mounted with 2.5% 1,4-Diazabicyclo[2.2.2]-octane (DABCO) (Sigma-Aldrich, #D27802) in 66% Tris-HCl 0.2M, 33% glycerol, 13% polyvinyl alcohol for preservation. Apoptotic cells were detected by Widefield Fluorescence Nikon Ti2 microscope and quantified with NIS-Elements AR Analysis 5.11.00 64-bit (Nikon).

Cleaved Caspase-3 staining

Deparaffinized and rehydrated tissue was processed for antigen retrieval using Antigen Unmasking Solution (Vectorlabs, #H3300) at 97°C for 25min, left to cool down for 1h, then permeabilized with 0.2%Triton X-100 in phospahate-buffered saline (PBS) for 45min, washed with PBS and blocked with 0.2% gelatine and 0.5% bovine serum albumin (BSA) in PBS for 30min. The tissue was incubated with polyclonal rabbit anti-mouse cleaved caspase-3 primary antibody (1:100 Cell Signalling, #9661) overnight at 4°C, washed with PBS the next day and incubated with secondary anti-rabbit Alexa 555 antibody (diluted 1:400 in blocking buffer) for 1h at room temperature. Cell nuclei were stained with DAPI (Invitrogen, #D1306). After

washing with PBS the tissue was mounted with 2.5% DABCO (Sigma-Aldrich, #D27802) in 66% Tris-HCl 0.2M, 33% glycerol, 13% polyvinyl alcohol for preservation. Apoptotic cells were detected by Widefield Fluorescence Nikon Ti2 microscope and quantified with Fiji.

Wheat germ agglutinin (WGA) staining

Deparaffinized and rehydrated tissue was processed for antigen retrieval as described, then washed with TBS 0.1% Tween 20 and blocked with 10% goat serum (Life Technologies, #50-062Z) for 1h. Heart tissue was stained with the following antibodies: FITC-conjugated lectin from Triticum vulgaris (wheat germ agglutinin (WGA)) (1:100 Sigma, #4895) and monoclonal mouse α-sarcomeric-actinin (1:20 Sigma, #A7811). Goat Alexa Fluor (Invitrogen) (1:100 to 1:800 according to primary antibody) was used as secondary antibody. Cell nuclei were detected with DAPI (Invitrogen, #D1306). Tissue was mounted with SlowFade Antifade kit (Invitrogen, #S2828). The stained samples were visualized using Widefield Fluorescence Nikon Ti microscope and quantified with NIS-Elements AR Analysis 5.11.00 64-bit (Nikon).

Cell culture and treatment

The rat embryonic myoblast cell line H9c2 was purchased from American Type Culture Collection (Manassas, US). The cells were cultured in Dulbecco`s Modified Eagle`s Medium (DMEM) high glucose L-glutamine, pyruvate (Gibco, #31885-023) supplemented with fetal bovine serum (FBS) to a final concentration of 10% (Gibco, #102170-106), 25mM HEPES (Gibco, #15630-056), 1% penicillin and streptomycin (Gibco, #15140) in a humidified incubator containing 5% CO_2 at 37°C. Subconfluent cells (80-90%) were trypsinized and plated in 35mm or 60mm dishes or 96-well plates for treatment with different concentrations of quizartinib and H_2O_2 at different time points according to the set-up of each experiment.

Neonatal Rat Ventricular Myocyte (NRVM) isolation

NRVM were isolated from 1-3 days old Sprague-Dawley rats. Pups were sacrificed by decapitation and the hearts were quickly removed. Atria, vessels and lung tissue were removed and ventricles were transferred into Trypsin-EDTA 0.05% (Gibco, #25300) and incubated at 4°C on a slow shaker overnight. Hearts were washed with 7ml of DMEM low glucose L-glutamine, pyruvate (Gibco, #31885-023) supplemented with FBS to a final concentration of 7% (Gibco, #102170-106), 25mM HEPES (Gibco, #15630-056), 1% penicillin and streptomycin (Gibco, #15140) and then digested with collagenase type 2 (36mg/50ml HBSS) (Worthington, #LS004174) via shaking in the water bath at 37°C. The cell suspension was filtered through a 100μm cell strainer to remove undigested tissue. Cells were resuspended in FCS- containing DMEM and preplated in a cell culture flask for 1h at 37°C to remove most of fibroblasts and endothelial cells. Preplating was repeated one more time. Afterwards, cells were counted using the Neubauer chamber and plated in FCS-containing DMEM with 100μM of 5-bromo-2`- desoxyuridine (BrdU) (Sigma, #B5002) to prevent proliferation of non-myocytes. The cells were kept in FCS-containing DMEM for 24 hours and then incubated in serum free (SF) DMEM overnight. Afterwards, the experiments were performed.

Cell viability assay

Cell viability was measured based on the 3-(4,5-dimethylthiazol-2-yl)-2,5-diphenyltetrazolium bromide (MTT) assay according to the Cell Proliferation Kit I protocol from Roche (#11-465-007-001). H9c2 and NRVM cells were seeded in a 96-well plate at a density of $4x10^3$ and $4x10^4$ cells/well, respectively. The following day the medium was changed to serum free and the cells were incubated overnight. After treatment with 200nM-20μM quizartinib for up to 72h depending on the experimental set-up, 10μl of the MTT labeling reagent (final concentration 0.5mg/ml) was added to each well and the plate was incubated for

4h at 37°C. Then 100µl of the Solubilization solution was added into each well and the plate was incubated overnight at 37°C. The next day absorbance was measured using the Synergy H1 Hybrid Multi-Mode Reader (BioTek, Switzerland) at 570nm.

Detection of cell death with AnnexinV and Propidium Iodide (PI)

H9c2 cells were treated with 2-20µM of quizartinib for 24h, H_2O_2 (as a control) for 6h or both. Apoptotic and non-apoptotic cell death was assessed using FITC-AnnexinV (BioLegend, #640905) and PI (Sigma-Aldrich, #P-4864). The cells were trypsinized using Trypsin-EDTA 0.05% (Gibco, #25300) for 1-3min and then 10% FCS-containing DMEM was added to inactivate Trypsin. Both the trypsinized cells and the medium containing the detached cells were collected, pooled and centrifuged at 1500 rpm for 5min in a Heraeus Megafuge 1.0R centrifuge (ThermoFischer Scientific, Michigan, USA). The pellet was washed with PBS and resuspended in FITC-AnnexinV (2.25µg/ml)/PI (5µg/ml) staining mix. The cells were incubated for 15min in the dark at room temperature and cell death was assessed using a BD LSRFortessa™ cell analyzer (BD Biosciences).

Data presentation and statistical analyses

Data are presented as mean±SEM. Statistical analyses were performed with GraphPad Prism version 8 software (GraphPad). The D`Agostino-Pearson normality test was applied to assess the values for Gaussian distribution. Parametric tests were used for normally distributed and non-parametric tests for non-normally distributed data and data sets with $n<8$. Unpaired t-test and Mann Whitney-U test were used to compare two groups and ordinary one-way ANOVA and Kruskal-Wallis followed by Sidak`s and Dunn`s, respectively, to compare the multiple groups. For echocardiography data, two-way ANOVA followed by Tukey`s (comparison between groups) or Sidak`s (comparison between time points) multiple

comparison tests were used. Development over time was tested for significance using a linear mixed effect model on R (version 3.4.1) and R Studio (1.0.153).

Results

Quizartinib does not lead to measurable changes in cardiac function one week after myocardial infarction

Given the cardioprotective effects of Flt3 stimulation in the infarcted heart [11], we sought to test whether the pharmacological inhibition of Flt3 during myocardial infarction (MI) leads to more pronounced cardiac injury and dysfunction. Five week old mice were randomly assigned to quizartinib (10 mg/kg/day per gavage) or vehicle (15% captisol) administration. Mice were subjected to LAD ligation or sham surgery after three weeks and quizartinib or vehicle treatment was continued for another three weeks. Echocardiography was performed before the initiation of drug administration, before the surgery and at one and three weeks after surgery (**Supplemental Figure S1**). A subset of mice was sacrificed one week after surgery and the remaining mice three weeks after surgery. Less animals survived after MI than after sham surgery, but mortality was not significantly different between any of the groups (**Figure 1**).

Echocardiography before surgery, i.e. after three weeks of drug treatment, showed no differences in cardiac morphology and function between quizartinib- and vehicle treated mice. One week after the surgery conventional echocardiography showed a significant decrease in global systolic function as assessed by left ventricular ejection fraction (LVEF) in the quizartinib-treated animals relative to quizartinib-treated animals before the surgery. Vehicle-treated mice that underwent MI surgery also showed a significant decrease in LVEF at one

week post-MI in comparison to vehicle-treated animals before the surgery. Likewise, cardiac function was significantly lower after MI compared to sham-operated mice for both treatment groups, whereas there was no difference in LVEF between vehicle-treated and quizartinib-treated infarcted mice (**Figure 2A**).

Myocardial infarction leads to thinning of the infarcted myocardial wall. Left anterior diastolic wall thickness (LVAW;d) was significantly decreased in both quizartinib- and vehicle-treated animals one week post MI in comparison to the wall thickness before the surgery and in comparison to sham-operated mice. For both comparisons the differences were more pronounced for quizartinib- than for vehicle-treated mice. However, there was no significant difference between the two groups. The weakening of the infarcted wall may lead to cardiac dilation. Cardiac dilation in terms of an increase in LV internal diameters was present in both quizartinib- and vehicle-treated animals in comparison to the same animals before the surgery. Similarly, LVID;d was significantly larger in both infarct groups compared to sham, with no difference between the two infarct groups.

Quizartinib increases apoptosis one week post MI

Infarct damage may be augmented by ongoing apoptotic cell death, which occurs predominantly in the infarct border zone during the first week post-MI [26]. A subset of mice was therefore sacrificed one week after MI and myocardial tissue was stained to assess apoptotic cell death, cardiomyocyte size and amount of fibrosis. Interestingly, the LV weight to tibia length ratio was significantly increased for vehicle-treated mice one week after MI compared to sham, but not for quizartinib-treated mice after MI compared to sham.

Apoptotic cell death was assessed in the infarct border zone by TUNEL staining and in whole myocardial cross-sections by cleaved caspase 3 staining. Apoptosis was significantly increased in the infarct border zone of quizartinib-treated compared to vehicle-treated mice (**Figure 3A**). Moreover, there was also more apoptosis in the remote myocardium as assessed by cleaved caspase 3-positive nuclei, which were significantly more frequent in quizartinib-treated than in vehicle-treated infarcted hearts (**Figure 3B**).

Quizartinib does not alter the extension of fibrosis and cardiomyocyte size one week post MI

To further test whether the enhanced cell death led to a measurable increase in scar size, the deposition of collagen was assessed by picrosirius staining and the percentage of total myocardial tissue that was picrosirius positive was determined. We observed no difference in the fibrotic scar size between the quizartinib- and vehicle-treated mice at one week after MI (**Figure 3C**).

Because LV weight/tibia length ratio was increased after MI, but only significantly for vehicle-treated mice, we sought to assess whether there was a difference in compensatory cardiomyocyte hypertrophy by measuring cell size using wheat germ agglutinin (WGA) staining of cellular membranes. Cardiomyocyte size was markedly increased in the hearts of animals that underwent MI surgery compared to sham animals, and this was true for both quizartinib-treated and vehicle-treated mice. However, there were no differences between drug- and vehicle-treated MI animals (**Figure 3D**). These experiments indicate that quizartinib does not seem to enhance scar size or compensatory cardiomyocyte hypertrophy after MI.

Quizartinib accentuates cardiac dysfunction over three weeks after MI

Because the enhanced cell death at one week post-MI may translate into aggravated cardiac injury and dysfunction at a later time, we followed a subset of mice up to three weeks. None of the animals died during the prolonged follow-up. Cardiac function remained impaired at three weeks post MI. In particular, LVEF was significantly diminished in both quizartinib- and vehicle-treated mice in comparison to their LVEF before the surgery (**Figure 4A**). LVEF was also significantly decreased for quizartinib-treated mice after MI compared to sham. However, when assessing the development of cardiac function over time by fitting an R studio linear mixed effect model, only the deterioration in quizartinib-treated infarcted mice compared to quizartinib-treated sham mice remained significant, whereas this was not the case for vehicle-treated infarcted versus sham mice. However, the development of LVEF over time was again not significantly different between quizartinib-treated and vehicle-treated MI mice. Very similar observations were made for all other parameters that were altered after MI. Specifically, LVAW thickness remained significantly decreased compared to pre-surgery values (**Figure 4B**) and was also significantly lower in quizartinib-treated infarcted vs. sham mice. In addition, wall thinning over time was only significant for quizartinib-treated mice after MI compared to sham. Ventricular dilation also further progressed and remained significant compared to pre-surgery status for both vehicle- and quizartinib-trated mice after three weeks. This again appeared to be more pronounced for quizartinib-treated infarcted mice, which showed a significant progression of LVID;d over time compared to quizartinib-treated sham mice (**Figure 4C**). In contrast to the one week data, there were no significant differences for LV weight to tibia length ratio between the groups at three weeks. Taken together, these data suggest that cardiac dysfunction persisted over the three week period post-MI and was slightly accentuated in quizartinib-treated mice, when taking the development over time of all individual animals into consideration.

Quizartinib does not increase the low rate of apoptosis and scar size three weeks after MI

The percentage of TUNEL-positive nuclei in the infarct border zone was approximately 10 times lower at three weeks compared to one week after MI and there was no significant difference any more between the quizartinib-treated and vehicle-treated mice (**Supplemental Figure S2A**). We also observed no significant difference in scar size between the treatment groups three weeks post MI (**Supplemental Figure S2B and C**).

Quizartinib does not affect cardiac morphology and function up to three weeks post-MI in Flt3 receptor knock out mice

We further sought to investigate how the observed effects of quizartinib relate to Flt3 receptor signaling. For this purpose, we used 5-week-old Flt3 receptor knock out (Flt3-KO) mice in an identical model as described for wild type mice (**Supplemental Figure 1**). Overall mortality was again lower in Flt3-KO mice after MI than after sham surgery and there was no difference between quizartinib-treated and vehicle-treated mice (**Supplemental Figure S3**). In contrast to wild type mice, however, the decline in LVEF, thinning of the infarcted wall (decrease of LVAW;d) and cardiac dilation (increase of LVID;d) were all less pronounced in Flt3-KO mice and did not reach statistical significance for any comparison over three weeks post-MI (**Supplemental Figure S4A-C**). Specifically, this was also the case for quizartinib-treated mice, in which quizartinib did not appear to aggravate outcome with respect to any of the above parameters. Importantly, the LV weight to tibia length ratio was significantly increased in both quizartinib-treated and vehicle-treated animals (**Supplemental Figure S4D**). These data indicate that in the absence of the Flt3 receptor, quizartinib does not affect post-MI outcome, suggesting that the quizartinib-related effects observed in wild type mice may in fact relate to the inhibition of Flt3 signaling.

Quizartinib decreases cardiomyocyte viability in a dose-dependent manner in vitro

Because of the observed increase in apoptotic cell death in quizartinib-treated compared to vehicle-treated mice one week after MI, we further examined the effect of quizartinib on primary neonatal cardiomyocytes and H9c2 cells *in vitro*. NRVM were cultured for 24 hours in 96-well plates containing 7% FCS DMEM medium, then kept in serum free DMEM medium overnight before being exposed to 200nM-20μM quizartinib or DMSO for another 24 hours (**Supplemental Figure S5A**). 100μM H_2O_2 was used as positive control. After 24 hours the MTT assay showed that – compared to DMSO – the high concentration range of quizartinib, i.e. 2μM and 20μM impaired cardiomyocyte viability in a dose-dependent manner, whereas lower concentrations (20nM and 200nM) did not have any effect (**Supplemental Figure S5B**). In contrast, in H9c2 cells, only the highest concentration of quizartinib significantly decreased metabolic activity and all lower concentrations including 2μM had no effect (**Supplemental Figure S5C**). These observations suggest that primary cardiomyocytes may be more susceptible to potential toxic effects of quizartinib than the H9c2 cell line. Next, we wanted to explore whether a longer exposure of cells to low concentrations of quizartinib may also decrease cell viability. H9c2 cells were treated with 2nM-200nM of quizartinib and cell viability was assessed at 24, 48 and 72 hours (**Supplemental Figure S5E**). 1mM H_2O_2 was used as positive and 0.1% FCS as negative control. We saw that cell viability was not affected in response to various low concentrations of quizartinib at any time point (**Supplemental Figure S5D**). Taken together, these experiments show that high concentrations of quizartinib can reduce cell viability, whereas lower concentrations have no significant effect even over time. Given the comparable responses of NRVM and H9c2 cells to 20μM quizartinib and in consideration of the three Rs principle of animal experimentation, H9c2 were used for all further *in vitro* studies.

Quizartinib induces apoptosis in a dose-dependent manner in vitro

Quizartinib inhibits cell proliferation and induces apoptosis in leukemia cell lines that are dependent on Flt3 [18]. Because of the decreased cell viability above concentrations of 2 μM *in vitro* and the enhanced apoptosis observed in our quizartinib-treated mice *in vivo*, we proceeded to identify whether the decrease in cell viability can be attributed to apoptosis. Apoptotic cell death in response to 2-20μM quizartinib for 24 hours was measured by flow cytometry using Annexin V and PI double staining. Consistent with the data obtained by MTT, quizartinib dose-dependently decreased the amount of viable cells (**Figure 5A**). Quizartinib also increased the amount of apoptotic cells in a dose-dependent manner with a roughly two-fold increase in response to 20μM versus DMSO (**Figure 5B**). These findings suggest that at least part of the quizartinib-induced loss of cell viability is caused by apoptosis.

Quizartinib potentiates H_2O_2-induced cell death and apoptosis in vitro

Ischemia/reperfusion injury contributes to apoptotic cell death in the infarct border zone [27], which is mediated by oxidative stress [28]. We therefore pretreated H9c2 cells with 5 and 20μM quizartinib for 18 hours before adding 100μM H_2O_2 for additional 6 hours. The combination of quizartinib with H_2O_2 markedly enhanced the decrease in viable cells and the increase in Annexin V and PI double positive cells. In fact, H_2O_2 on top of 20μM quizartinib approximately led to a doubling of the amount of apoptotic cells versus quizartinib alone and a tripling versus H_2O_2 alone (**Figure 6A and B**). These findings suggest that quizartinib potentiates oxidative stress-induced apoptosis.

Discussion

In the present study we show that the Flt3-targeting TKI quizartinib enhances oxidative stress-associated apoptotic cell death *in vitro* and *in vivo* and may accentuate the decline in cardiac function over three weeks post-MI in mice. Comparable studies in Flt3 receptor deficient mice, which do not show differences in cardiac function and remodeling upon quizartinib, suggest that these effects could be related to the inhibition of Flt3 rather than be unspecific.

Despite the success of small molecule TKIs in the treatment of malignancies, there is an increasing number of studies revealing a high rate of adverse cardiac events occurring in patients during or even after the therapy, with systolic dysfunction and heart failure being among the most prevalent and severe side effects [13, 29-33]. As in other organs, cardiac homeostasis and function are maintained by a highly coordinated network of molecular signaling pathways. Many of these pathways are common to various different cells and organs. In particular, kinases involved in the regulation of cell survival and proliferation may be part of a shared kinome between cancer cells and the heart [34]. However, our understanding of the specific roles of many cancer drug targets in the healthy or injured heart is limited and side effects of TKIs may occur apparently unforeseeably when the drug is already in clinical use [35].

In our study we examined the second-generation Flt3 inhibitor quizartinib, which has shown high potency in the treatment of AML either as a single agent or in combination with conventional chemotherapy regimens [36], but also potentially relevant cardiotoxicity in preclinical trials [22]. Because we previously found that Flt3 exerts protective effects in the infarcted heart through the inhibition of apoptotic cell death [11], we focused our studies on

cardiomyocyte viability. We found that quizartinib-treated mice had significantly enhanced apoptotic cell death at one week post-MI, and this was the case both in the infarct border zone as well as in the remote myocardium. Apoptotic cell death in infarcted myocardium plays an important role in the progression of adverse LV remodeling and dysfunction after MI [26, 27, 37, 38]. Even if we could not observe significant differences in cardiac morphology and function between quizartinib- and vehicle-treated mice up to three weeks post-MI, this increased apoptosis most likely reflected in the diminished compensatory hypertrophy (LV weight/tibia length ratio) of quizartinib-treated hearts at one week post-MI and has the potential to translate into more severe functional impairment in the more chronic phase of ischemic heart disease. Earlier studies in mice have shown that although rapidly declining within the first two weeks after MI, cardiac function continues to deteriorate up to at least nine weeks [39], with another group showing slow but progressive worsening of cardiac function even up to 4 months [40]. Although further studies are needed to examine whether quizartinib worsens post-MI outcome in the chronic phase of the disease, this assumption is supported by previous observations that apoptotic cell death, even at a very low level, is in itself sufficient to cause cardiomyopathy and heart failure [41].

Previous studies using the multi-targeting TKI sorafenib showed similar results [42] in that sorafenib led to a significant increase in cardiomyocyte death, at least *in vitro*. Importantly, no differences in cardiac function or infarct size up to two weeks post-MI were observed in mice treated with sorafenib compared to vehicle while undergoing MI [42], which is consistent with our findings. However, there are also important differences between the study by Duran and colleagues and ours. Firstly, whereas they observed a higher mortality of sorafenib-treated mice after MI, survival of quizartinib- and vehicle-treated mice was comparable in our study up to three weeks post-MI. Secondly, sorafenib-induced cardiomyocyte death was mostly

attributable to necrosis and not to apoptosis. We observed an increase in TUNEL-positive and cleaved caspase-3 positive cells in the hearts of quizartinib-treated compared to vehicle treated mice at one week post-MI. To further differentiate the type of cell death and confirm quizartinib-dependent myocyte apoptosis, *in vitro* studies were performed on NRVM and H9c2 cells. Whereas these studies showed that a considerable amount of cell death is most likely due to necrosis, we also found a dose-dependent increase in apoptosis as assessed by Annexin V/PI double-positivity in response to quizartinib. Given that quizartinib is more specific for Flt3 than sorafenib, and that Flt3 signaling inhibits apoptotic cell death in both leukemia cells [43] and cardiomyocytes [11], the differences in the mechanism of myocyte death between sorafenib and quizartinib are most likely attributable to the balance of inhibition of Flt3 signaling and inhibition of other TKs.

Consistent with our previous findings that Flt3 activation inhibits hypoxia- and oxidative-stress induced cardiomyocyte apoptosis *in vitro* and *in vivo* [11], we observed a potentiation of both apoptotic and non-apoptotic cell death in cardiomyocytes exposed to oxidative stress in the presence of quizartinib. From a translational aspect, this observation compatible with the multi-hit hypothesis of cardiotoxicity [44], stating that additional cardiac stressors are needed to unmask latent cardiotoxicity of cancer drugs. Furthermore, because Flt3 is upregulated in the ischemic heart, our findings are consistent with a Flt3 signaling related effect of quizartinib.

Although more specific for Flt3 than previous TKIs, quizartinib also targets other receptor TKs including colony stimulating factor 1 receptor [14], stem cell factor receptor (SCFR/c-kit) [14, 18] and platelet derived growth factor receptor (PDGFR) [14, 18]. At least for some of these receptors, cardioprotective effects have been shown [45, 46]. In addition, off-target effects

through inhibition of unrelated kinases or unspecific drug toxicity could also contribute to quizartinib toxicity. We did not find any differences between quizartinib- and vehicle-treated mice that do not possess a functional Flt3 receptor while undergoing MI. Consistent with previous, unpublished observations in our laboratory, Flt3-KO mice showed mitigated responses to MI injury as they appear to be protected through mechanisms related to non-cardiac functions of Flt3. Whereas studies to precisely elucidate these mechanisms are still ongoing in our laboratory, our preliminary findings in Flt3-KO mice argue against unspecific toxicity of quizartinib.

Study Limitations

We followed the mice for three weeks post-MI. However, longer follow-up might be needed to detect structural or functional differences caused by the early enhanced cell death in quizartinib-treated mice. The use of a non-conditional Flt3 knock out mouse model may introduce additional effects due to compensatory processes or heart-extrinsic mechanisms. Furthermore, Flt3 deficiency may be potently protective due to yet to be identified mechanisms, which may mask the cardiotoxic effect of quizartinib in Flt3 knock out mice. Finally, the study has been conducted in mice and due to differences in physiology, extrapolations to humans must be done with caution.

Conclusion

In conclusion, quizartinib potentiates hypoxic apoptotic cell death *in vitro* and after MI *in vivo*, which could explain at least in part some of the toxicity observed in preclinical trials. More work will be needed to understand to what degree these effects are specific for the

inhibition of Flt3 signaling or attributable to Flt3 unrelated mechanisms. Improved understanding of the mechanisms underlying TKI toxicity is urgently needed to advance future drug design and to develop cardioprotective strategies to improve cardiovascular health in cancer patients requiring TKI therapy.

Figures

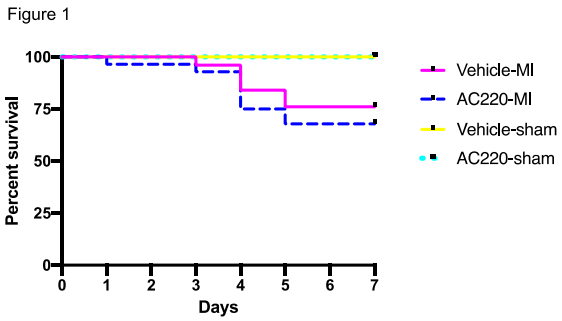

Figure 1. Peri- and post-procedural survival up to 7 days. Kaplan Meier survival curves for C57BL/6N mice treated with quizartinib (AC220) or vehicle undergoing sham surgery or MI up to 7 days. Vehicle-MI n=25; AC220-MI n=28; vehicle-sham n=10; AC220-sham n=12.

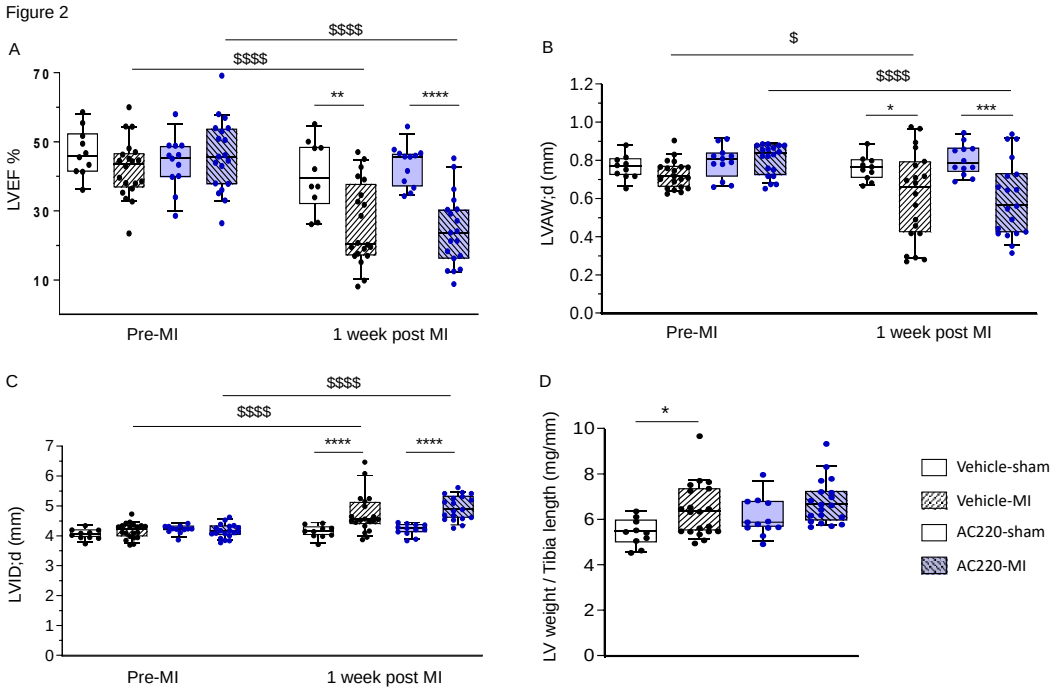

Figure 2. Cardiac function and morphology by echocardiography one week post MI. Serial echocardiography was performed before surgery and at one week after surgery. Groups were compared using 2-way ANOVA followed by Tukey's and Sidak`s multiple comparison test (symbols and asterisks, respectively). **(A)** Cardiac function in terms of left ventricular ejection fraction (LVEF). **(B)** Wall thickness of the left anterior wall in diastole (LVAW;d). **(C)** Left ventricular inner diameter in diastole (LVID;d). **(D)** Left-ventricular weight normalized to tibia length. Data are presented as mean ± SEM; Vehicle-MI n=20; AC220-MI n=19; vehicle-sham n=10; AC220-sham n=12; */$ $p<0.5$; ** $p<0.01$; *** $p<0.001$; ****/$$$$ $p<0.0001$.

Figure 3

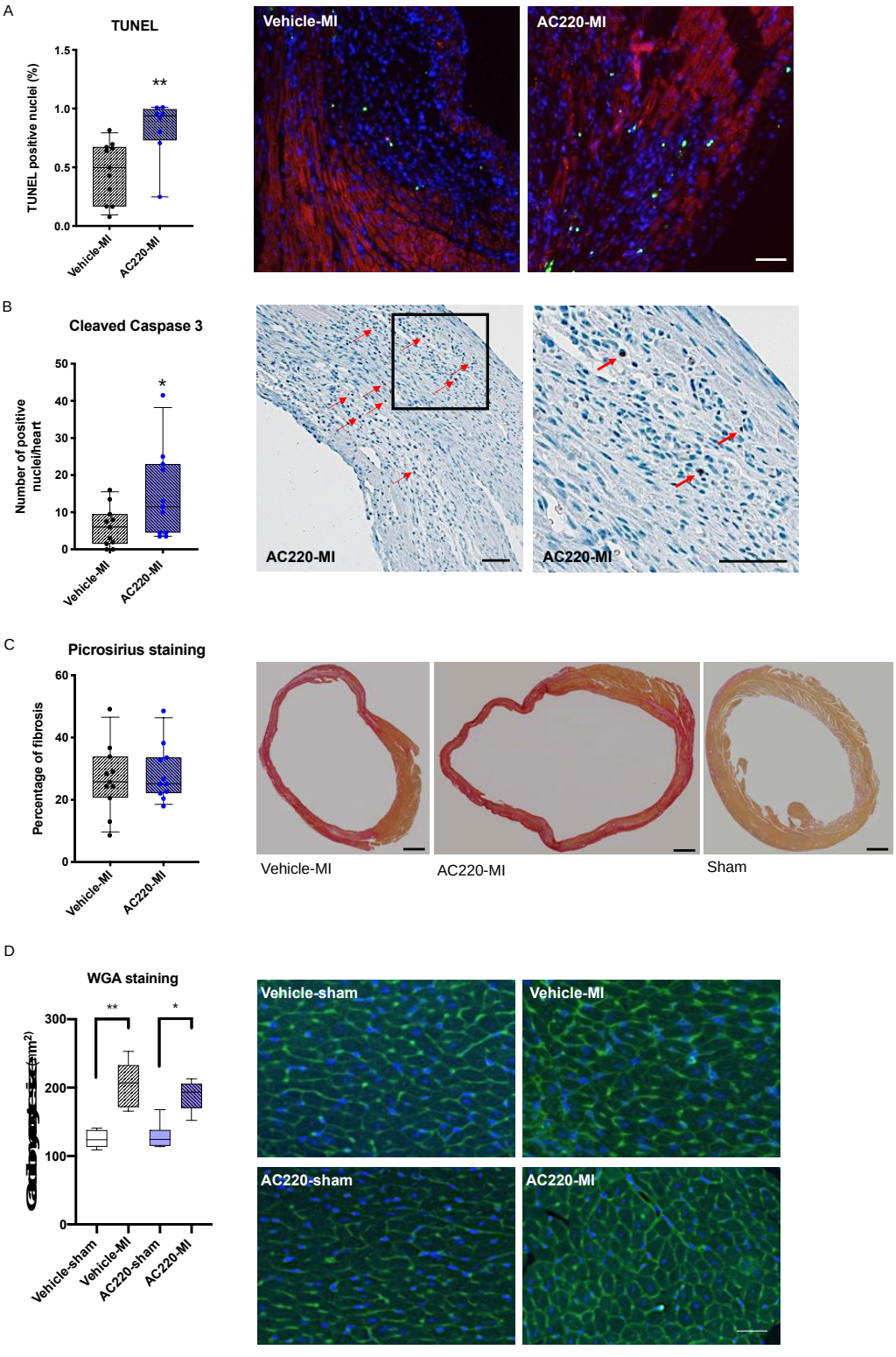
A
TUNEL
TUNEL positive nuclei (%)
1.5
1.0
0.5
0.0
**
Vehicle-MI
AC220-MI
Vehicle-MI
AC220-MI
B
Cleaved Caspase 3
Number of positive nuclei/heart
50
40
30
20
10
0
*
Vehicle-MI
AC220-MI
AC220-MI
AC220-MI
C
Picrosirius staining
Percentage of fibrosis
60
40
20
0
Vehicle-MI
AC220-MI
Vehicle-MI
AC220-MI
Sham
D
WGA staining
300
200
100
0
**
*
Vehicle-sham
Vehicle-MI
AC220-sham
AC220-MI
Vehicle-sham
Vehicle-MI
AC220-sham
AC220-MI

Figure 3. Apoptotic cell death, infarct size and cardiomyocyte size at one week post-MI. A preassigned subset of mice was sacrificed after one week. Apoptotic cell death was increased in the infarct border zone and also in the remote myocardium of quizartinib-treated mice. **(A)** TUNEL-positive nuclei in the infarct border zone: quantification and representative microscopic images; red: alpha-sarcomeric actinin, blue: DAPI-positive nuclei; green: TUNEL-positive nuclei; scale bar=100μM; nonparametric Mann-Whitney test. **(B)** Cleaved caspase 3-positive cells in the remote myocardium: quantification and representative microscopic image of AC220-MI sample in two magnifications; scale bar=50μM; unpaired two-tailed t test. **(C)** Fibrotic area by picrosirius staining: quantification and representative microscopic images of vehicle-MI, AC220-MI and respective sham groups; scale bar=500 μM; unpaired two-tailed t test. **(D)** Cardiomyocyte size assessed by wheat germ agglutinin (WGA) staining: quantification and representative microscopic images; green: cardiomyocyte borders (WGA), blue: nuclei (DAPI); scale bar=20μM; unpaired Kruskal-Wallis test. AC220: quizartinib; * $p<0.05$; **<0.01.

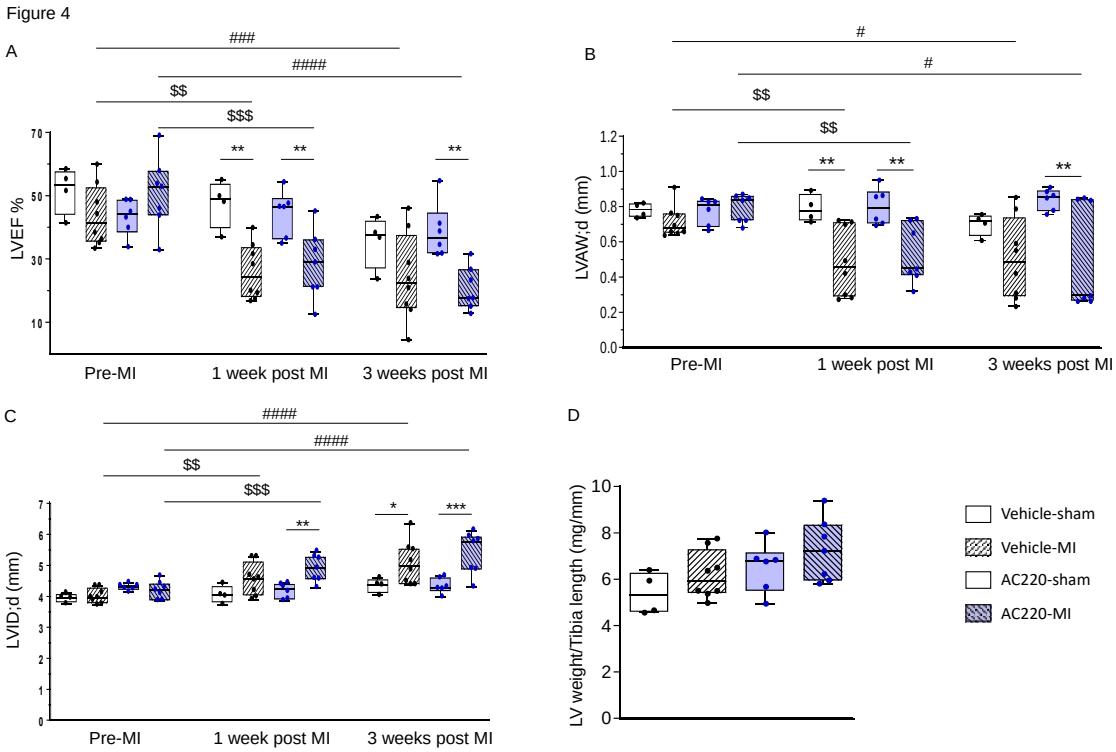

Figure 4. Cardiac function and morphology by echocardiography three weeks post-MI. Serial echocardiography was performed before surgery and at one and three weeks after surgery. Groups were compared using 2-way ANOVA followed by Tukey's and Sidak`s multiple comparison test (symbols and asterisks, respectively) and for development over time by fitting an R-Studio linear mixed effect model (p values in brackets). Only animals completing the three week follow-up were included to allow for paired analyses of development over time. **(A)** Cardiac function in terms of left ventricular ejection fraction (LVEF; **p=0.00939 AC-MI vs. AC-sham**; p=0.99979 V-MI vs. V-sham; p=0.48864 V-MI vs. AC-MI). **(B)** Left anterior wall thickness in diastole (LVAW;d; **p=0.0485 AC-MI vs. AC-sham**; p=0.8866 V-MI vs. V-sham; p=0.6409 AC-MI vs. V-MI). **(C)** Left ventricular inner diameter in diastole (LVID;d; **p<0.001 AC-MI vs. AC-sham;** p=0.134 V-MI vs. V-sham; p=0.670 AC-MI vs. V-MI). **(D)** Left-ventricular weight normalized to tibia length. Data are presented as mean ± SEM; Vehicle-MI n=8; AC220-MI n=7; vehicle-sham n=4; AC220-sham n=6; */# p<0.5; **/$$ p<0.01; ###/$$$ p<0.001; #### p<0.0001.

Figure 5

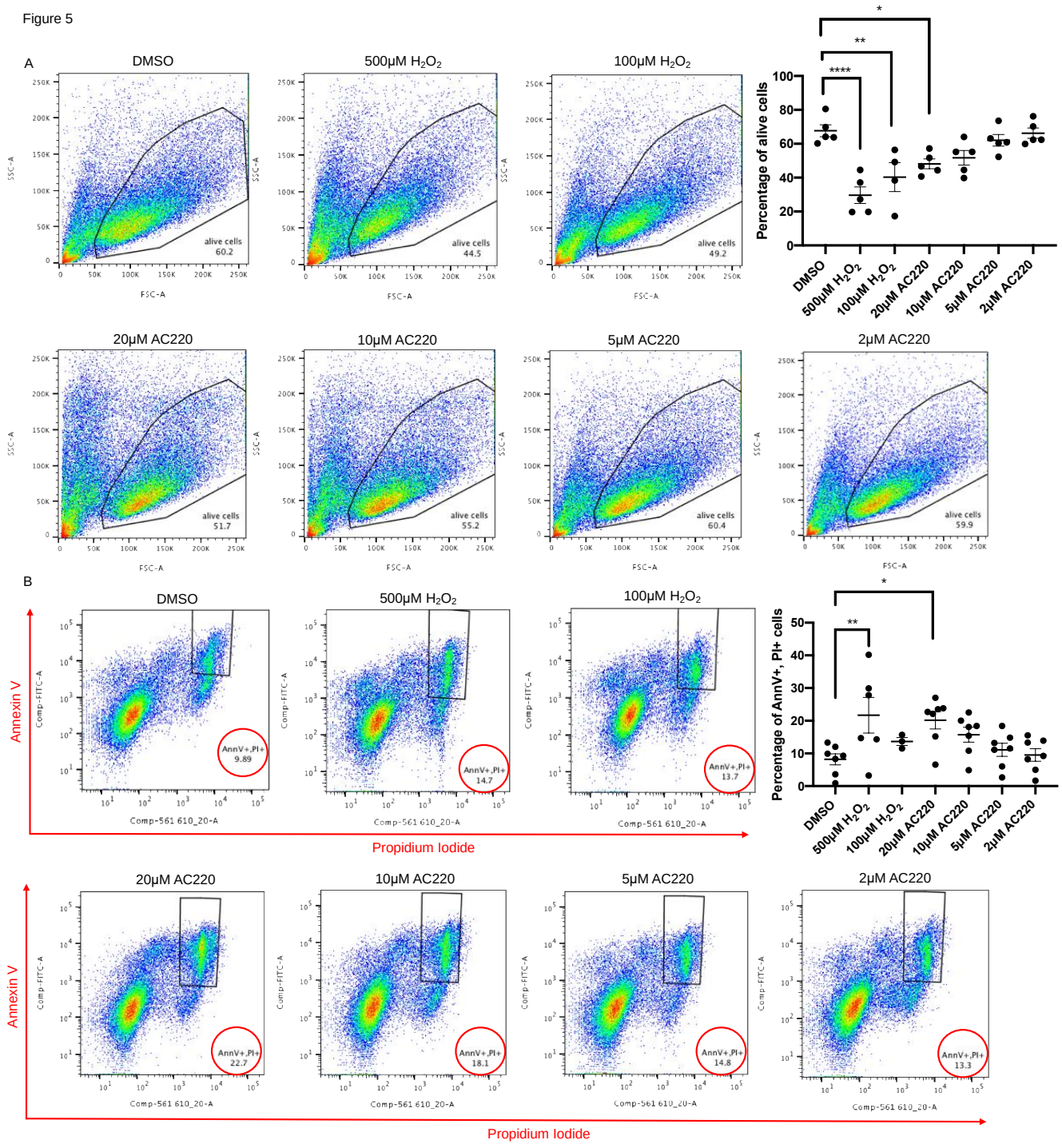
A
DMSO
500μM H2O2
100μM H2O2
20μM AC220
10μM AC220
5μM AC220
2μM AC220
alive cells 60.2
alive cells 44.5
alive cells 49.2
alive cells 51.7
alive cells 55.2
alive cells 60.4
alive cells 59.9
SSC-A
FSC-A
Percentage of alive cells
DMSO
500μM H2O2
100μM H2O2
20μM AC220
10μM AC220
5μM AC220
2μM AC220
B
Annexin V
Propidium Iodide
Comp-FITC-A
Comp-561 610_20-A
AnnV+,PI+ 9.89
AnnV+,PI+ 14.7
AnnV+,PI+ 13.7
AnnV+,PI+ 22.7
AnnV+,PI+ 18.1
AnnV+,PI+ 14.8
AnnV+,PI+ 13.3
Percentage of AnnV+, PI+ cells

Figure 5. Viable and apoptotic H9c2 cells after treatment with different concentrations of quizartinib *in vitro*. H9c2 cells were treated with quizartinib in the dosage range of 2µM to 20µM for 24h. DMSO, 100µM and 500µM H_2O_2 were used as control. AnnexinV and PI staining was performed and analysed by flow cytometry. **(A)** Representative images and quantification of viable cells. **(B)** Representative images and quantification of AnnexinV/PI-double positive apoptotic cells. The data are presented as mean ± SEM, n = 4-5; ****p<0.0001; **p < 0.01; *p < 0.5, ordinary one-way ANOVA followed by Sidak`s test.

Figure 6

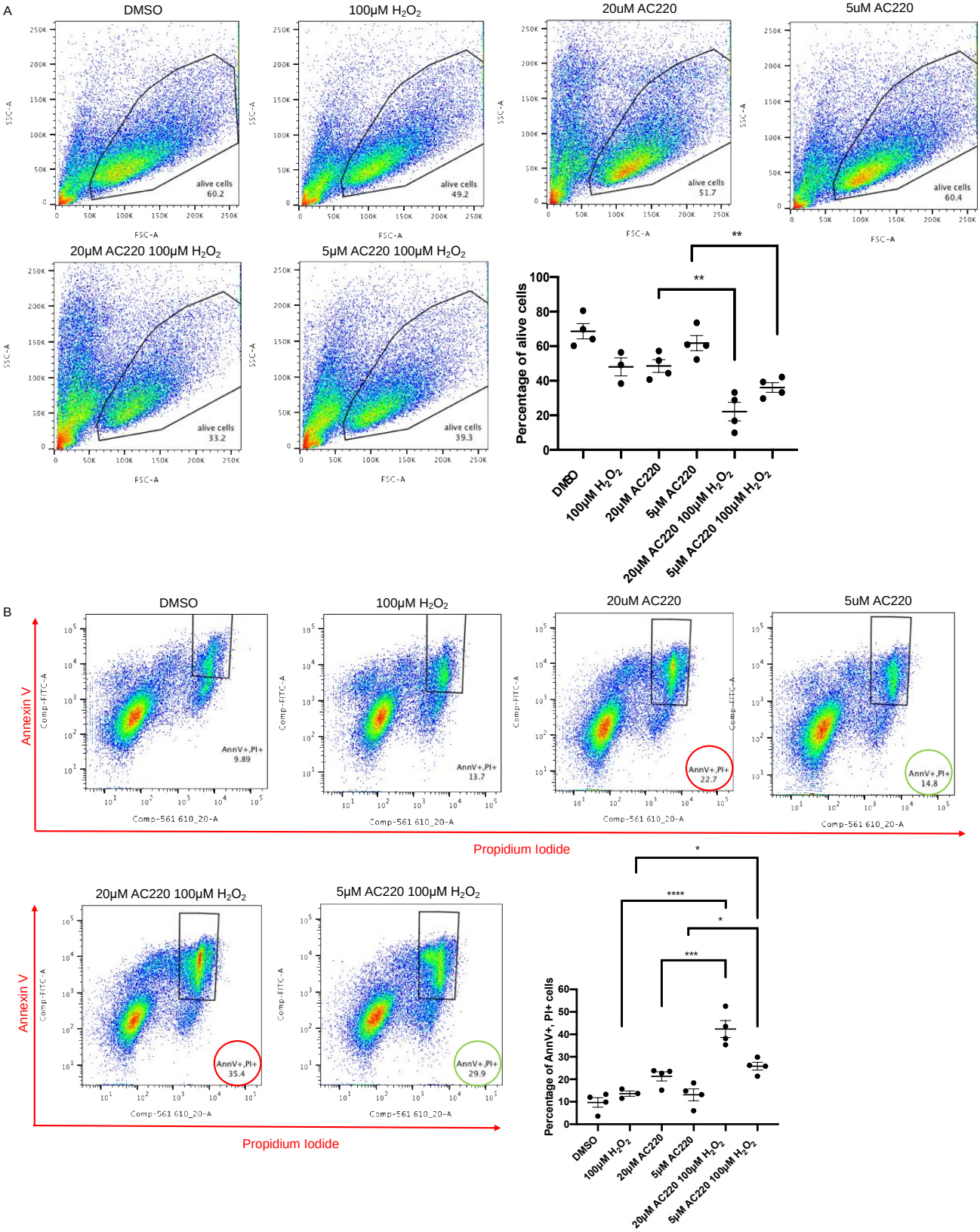
A
DMSO
100μM H2O2
20uM AC220
5uM AC220
alive cells 60.2
alive cells 49.2
alive cells 51.7
alive cells 60.4
20μM AC220 100μM H2O2
5μM AC220 100μM H2O2
alive cells 33.2
alive cells 39.3
SSC-A
FSC-A
Percentage of alive cells
DMSO
100μM H2O2
20μM AC220
5μM AC220
20μM AC220 100μM H2O2
5μM AC220 100μM H2O2
B
Annexin V
Propidium Iodide
AnnV+,PI+ 9.89
AnnV+,PI+ 13.7
AnnV+,PI+ 22.7
AnnV+,PI+ 14.8
AnnV+,PI+ 35.4
AnnV+,PI+ 29.9
Comp-FITC-A
Comp-561 610_20-A
Percentage of AnnV+, PI+ cells

Figure 6. Viable and apoptotic H9c2 cells after treatment with different concentrations of quizartinib in combination with H_2O_2 *in vitro.* H9c2 cells were treated with 5 and 20μM quizartinib for 18h and H_2O_2 was added for additional 6h. DMSO and 100μM H_2O_2 were used as control. **(A)** Representative images and quantification of viable cells. **(B)** Representative images and quantification of AnnexinV/PI-double positive apoptotic cells. The data are presented as mean ± SEM, n = 3-4; ****p<0.0001; ***p<0.001; *p<0.05; ordinary one-way ANOVA followed by Sidak`s test.

Supplemental figures

Supplemental Figure S1

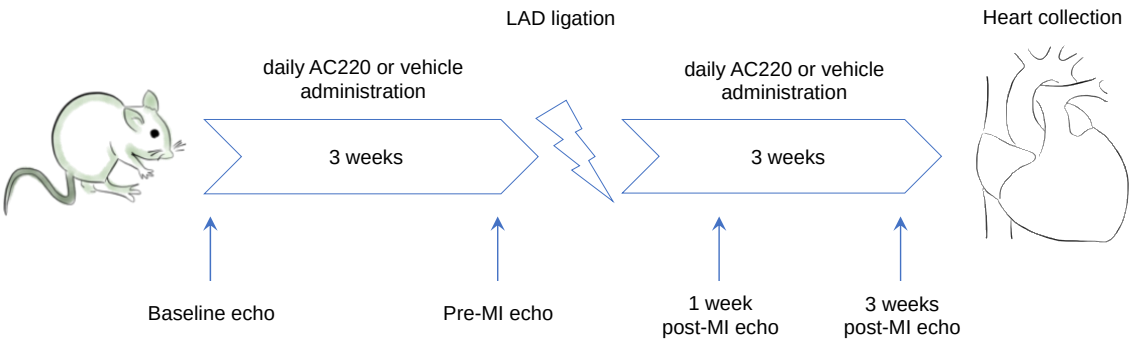

Supplemental figure S1. Experimental setup. Five-week-old male C57BL/6N and 129S1/SvlmJ Flt3-KO out mice received quizartinib or vehicle through oral gavage once a day for six weeks. After three weeks of treatment animals were randomly assigned to left ventricular anterior descending artery (LAD) ligation or sham operation. Three weeks after surgery hearts of all surviving animals were perfused and embedded in paraffin for further immunohistochemistry. A preassigned subset of mice was sacrificed at one week post-surgery and hearts were collected in a similar manner. Echocardiography was performed before initiation of the treatment, before the surgery and one and three weeks after the surgery.

Supplemental Figure S2

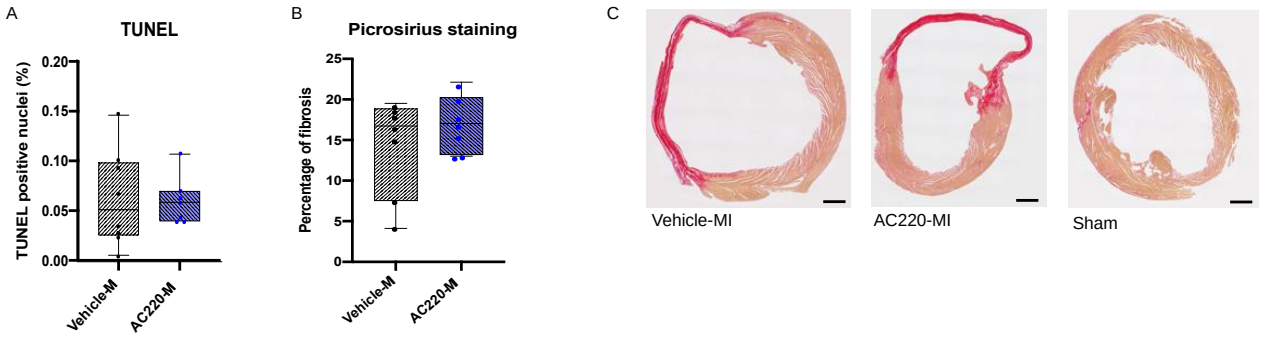

Supplemental figure S2. Apoptotic cell death in the infarct border zone and infarct size at three weeks post-MI. (A) Quantification of TUNEL-positive nuclei. **(B)** Quantification of fibrotic area by picrosirius staining. (**C)** Representative microscopic images of vehicle-MI, AC220-MI and sham; scale bar=500 μM.

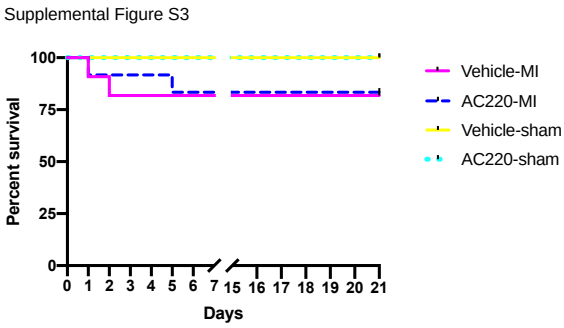

Supplemental figure S3. Peri- and post-procedural survival up to 21 days in Flt3-KO mice. Kaplan Meier survival curves for Flt3-KO mice treated with quizartinib (AC220) or vehicle undergoing sham surgery or MI up to 21 days. Vehicle-MI n=11; AC220-MI n=12; vehicle-sham n=3; AC220-sham n=4.

Supplemental Figure S4

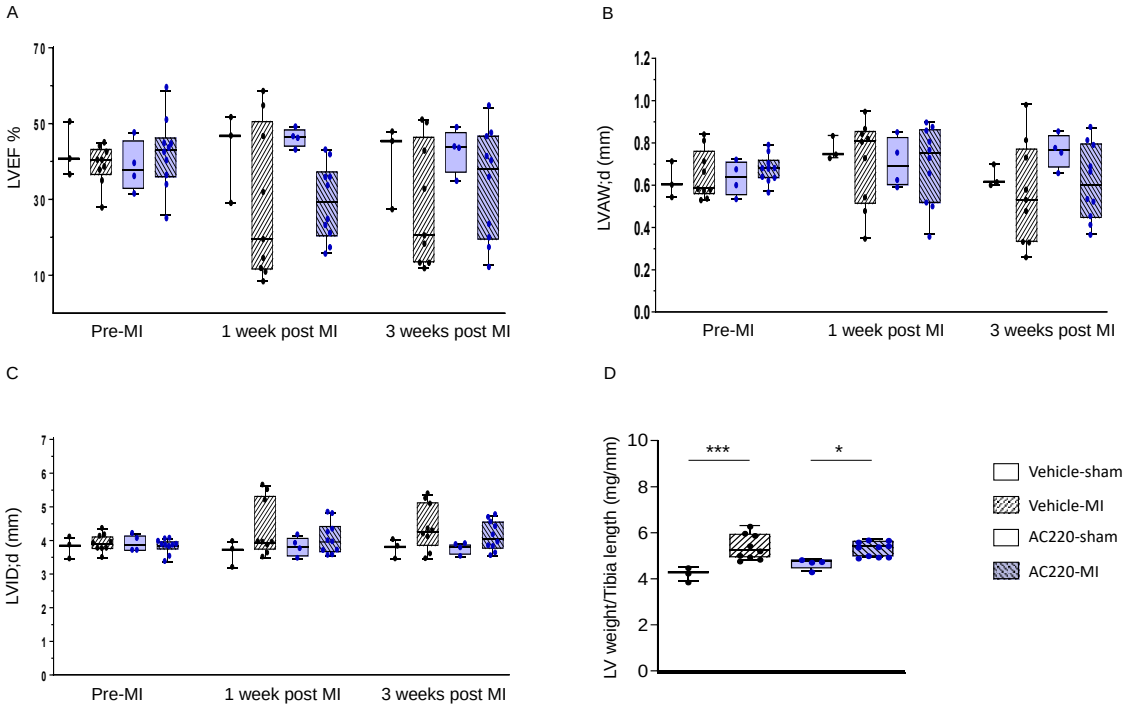

Supplemental figure S4. Cardiac function and morphology by echocardiography in Flt3-KO mice one and three weeks post-MI. Serial echocardiography was performed before surgery and at one and three weeks after surgery. Groups were compared using 2-way ANOVA followed by Tukey's and Sidak`s multiple comparison test and for development over time by fitting an R-Studio linear mixed effect model. For echocardiography, none of the comparisons was significant. **(A)** Cardiac function in terms of left ventricular ejection fraction. **(B)** Left anterior wall thickness in diastole. **(C)** Left ventricular inner diameter in diastole. **(D)** Left-ventricular weight normalized to tibia length. Data are presented as mean ± SEM; Vehicle-MI n=9; AC220-MI n=10; vehicle-sham n=3; AC220-sham n=4; * $p<0.5$; *** $p<0.001$.

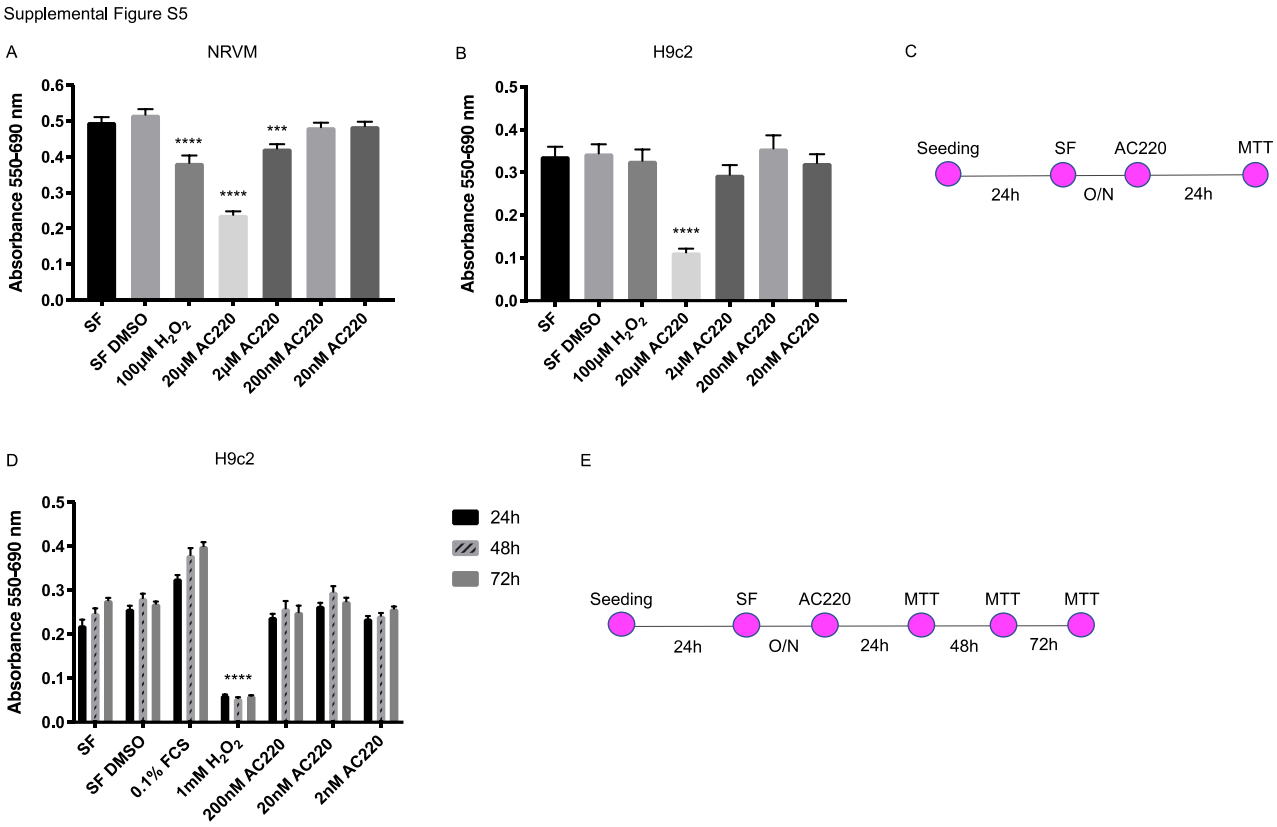

Supplemental figure S5. NRVM and H9c2 viability after treatment with different concentrations of quizartinib. MTT assay was performed after 24h, 48h, 72h of quizartinib treatment. DMSO, 100µM and 1mM H_2O_2 were used as control. In a higher dose-range *in vitro*, quizartinib decreases cardiac myocyte viability, whereas low doses do not have any effect over time. **(A)** Quantification of absorbance in NRVM after 24h, n=6 of 6 replicates per each condition; Kruskal-Wallis test followed by Dunn`s test. **(B)** Quantification of absorbance in H9c2 cells after 24h, n=4 of 6 replicates per each condition; Kruskal-Wallis test followed by Dunn`s test. **(C)** Experimental set-up of quizartinib treatment for 24h. **(D)** Quantification of absorbance in H9c2 cells treated with low concentrations of quizartinib up to 72h, n=2 of 6 replicates per each condition and time point; 2-way ANOVA followed by Tukey`s test. **(E)** Experimental set-up of low doses quizartinib treatment up to 72h. The data are presented as mean ± SEM; ****p<0.0001; ***p<0.001.

References

1. Zamorano J. An ESC position paper on cardio-oncology. *Eur Heart J* 2016;**37**:2739-2740.
2. Perez IE, Taveras Alam S, Hernandez GA, Sancassani R. Cancer Therapy-Related Cardiac Dysfunction: An Overview for the Clinician. *Clin Med Insights Cardiol* 2019;**13**:1179546819866445.
3. Perrino C, Schiattarella GG, Magliulo F, Ilardi F, Carotenuto G, Gargiulo G, Serino F, Ferrone M, Scudiero F, Carbone A, Trimarco B, Esposito G. Cardiac side effects of chemotherapy: state of art and strategies for a correct management. *Curr Vasc Pharmacol* 2014;**12**:106-116.
4. Raschi E, Vasina V, Ursino MG, Boriani G, Martoni A, De Ponti F. Anticancer drugs and cardiotoxicity: Insights and perspectives in the era of targeted therapy. *Pharmacol Ther* 2010;**125**:196-218.
5. Chaar M, Kamta J, Ait-Oudhia S. Mechanisms, monitoring, and management of tyrosine kinase inhibitors-associated cardiovascular toxicities. *Onco Targets Ther* 2018;**11**:6227-6237.
6. Sexauer AN, Tasian SK. Targeting FLT3 Signaling in Childhood Acute Myeloid Leukemia. *Front Pediatr* 2017;**5**:248.
7. Gilliland DG, Griffin JD. The roles of FLT3 in hematopoiesis and leukemia. *Blood* 2002;**100**:1532-1542.
8. Lyman SD, James L, Vanden Bos T, de Vries P, Brasel K, Gliniak B, Hollingsworth LT, Picha KS, McKenna HJ, Splett RR, et al. Molecular cloning of a ligand for the flt3/flk-2 tyrosine kinase receptor: a proliferative factor for primitive hematopoietic cells. *Cell* 1993;**75**:1157-1167.
9. Veiby OP, Jacobsen FW, Cui L, Lyman SD, Jacobsen SE. The flt3 ligand promotes the survival of primitive hemopoietic progenitor cells with myeloid as well as B lymphoid potential. Suppression of apoptosis and counteraction by TNF-alpha and TGF-beta. *J Immunol* 1996;**157**:2953-2960.

10. Ayach BB, Yoshimitsu M, Dawood F, Sun M, Arab S, Chen M, Higuchi K, Siatskas C, Lee P, Lim H, Zhang J, Cukerman E, Stanford WL, Medin JA, Liu PP. Stem cell factor receptor induces progenitor and natural killer cell-mediated cardiac survival and repair after myocardial infarction. *Proc Natl Acad Sci U S A* 2006;**103**:2304-2309.

11. Pfister O, Lorenz V, Oikonomopoulos A, Xu L, Hauselmann SP, Mbah C, Kaufmann BA, Liao R, Wodnar-Filipowicz A, Kuster GM. FLT3 activation improves post-myocardial infarction remodeling involving a cytoprotective effect on cardiomyocytes. *J Am Coll Cardiol* 2014;**63**:1011-1019.

12. Stirewalt DL, Radich JP. The role of FLT3 in haematopoietic malignancies. *Nat Rev Cancer* 2003;**3**:650-665.

13. Orphanos GS, Ioannidis GN, Ardavanis AG. Cardiotoxicity induced by tyrosine kinase inhibitors. *Acta Oncol* 2009;**48**:964-970.

14. Zarrinkar PP, Gunawardane RN, Cramer MD, Gardner MF, Brigham D, Belli B, Karaman MW, Pratz KW, Pallares G, Chao Q, Sprankle KG, Patel HK, Levis M, Armstrong RC, James J, Bhagwat SS. AC220 is a uniquely potent and selective inhibitor of FLT3 for the treatment of acute myeloid leukemia (AML). *Blood* 2009;**114**:2984-2992.

15. Karaman MW, Herrgard S, Treiber DK, Gallant P, Atteridge CE, Campbell BT, Chan KW, Ciceri P, Davis MI, Edeen PT, Faraoni R, Floyd M, Hunt JP, Lockhart DJ, Milanov ZV, Morrison MJ, Pallares G, Patel HK, Pritchard S, Wodicka LM, Zarrinkar PP. A quantitative analysis of kinase inhibitor selectivity. *Nat Biotechnol* 2008;**26**:127-132.

16. Chao Q, Sprankle KG, Grotzfeld RM, Lai AG, Carter TA, Velasco AM, Gunawardane RN, Cramer MD, Gardner MF, James J, Zarrinkar PP, Patel HK, Bhagwat SS. Identification of N-(5-tert-butyl-isoxazol-3-yl)-N'-{4-[7-(2-morpholin-4-yl-ethoxy)imidazo[2,1-b][1 ,3]benzothiazol-2-yl]phenyl}urea dihydrochloride (AC220), a uniquely potent, selective, and efficacious FMS-like tyrosine kinase-3 (FLT3) inhibitor. *J Med Chem* 2009;**52**:7808-7816.

17. Pratz KW, Sato T, Murphy KM, Stine A, Rajkhowa T, Levis M. FLT3-mutant allelic burden and clinical status are predictive of response to FLT3 inhibitors in AML. *Blood* 2010;**115**:1425-1432.

18. Kampa-Schittenhelm KM, Heinrich MC, Akmut F, Dohner H, Dohner K, Schittenhelm MM. Quizartinib (AC220) is a potent second generation class III tyrosine kinase inhibitor that displays a distinct inhibition profile against mutant-FLT3, -PDGFRA and -KIT isoforms. *Mol Cancer* 2013;**12**.

19. Sandmaier BM, Khaled S, Oran B, Gammon G, Trone D, Frankfurt O. Results of a phase 1 study of quizartinib as maintenance therapy in subjects with acute myeloid leukemia in remission following allogeneic hematopoietic stem cell transplant. *Am J Hematol* 2018;**93**:222-231.

20. Cortes JE, Kantarjian H, Foran JM, Ghirdaladze D, Zodelava M, Borthakur G, Gammon G, Trone D, Armstrong RC, James J, Levis M. Phase I study of quizartinib administered daily to patients with relapsed or refractory acute myeloid leukemia irrespective of FMS-like tyrosine kinase 3-internal tandem duplication status. *J Clin Oncol* 2013;**31**:3681-3687.

21. Cortes JE, Tallman MS, Schiller GJ, Trone D, Gammon G, Goldberg SL, Perl AE, Marie JP, Martinelli G, Kantarjian HM, Levis MJ. Phase 2b study of 2 dosing regimens of quizartinib monotherapy in FLT3-ITD-mutated, relapsed or refractory AML. *Blood* 2018;**132**:598-607.

22. FDA. FDA Briefing Document Oncologic Drugs Advisory Committee (ODAC) Meeting: NDA 212166 Quizartinib https://www.fda.gov/media/124896/download. May 14, 2019.

23. Mackarehtschian K, Hardin JD, Moore KA, Boast S, Goff SP, Lemischka IR. Targeted disruption of the flk2/flt3 gene leads to deficiencies in primitive hematopoietic progenitors. *Immunity* 1995;**3**:147-161.

24. Virag JA, Lust RM. Coronary artery ligation and intramyocardial injection in a murine model of infarction. *J Vis Exp* 2011.

25. Degabriele NM, Griesenbach U, Sato K, Post MJ, Zhu J, Williams J, Jeffery PK, Geddes DM, Alton EW. Critical appraisal of the mouse model of myocardial infarction. *Exp Physiol* 2004;**89**:497-505.

26. Palojoki E, Saraste A, Eriksson A, Pulkki K, Kallajoki M, Voipio-Pulkki LM, Tikkanen I. Cardiomyocyte apoptosis and ventricular remodeling after myocardial infarction in rats. *Am J Physiol Heart Circ Physiol* 2001;**280**:H2726-2731.

27. Zhao ZQ, Nakamura M, Wang NP, Wilcox JN, Shearer S, Ronson RS, Guyton RA, Vinten-Johansen J. Reperfusion induces myocardial apoptotic cell death. *Cardiovasc Res* 2000;**45**:651-660.

28. Galang N, Sasaki H, Maulik N. Apoptotic cell death during ischemia/reperfusion and its attenuation by antioxidant therapy. *Toxicology* 2000;**148**:111-118.

29. Force T, Krause DS, Van Etten RA. Molecular mechanisms of cardiotoxicity of tyrosine kinase inhibition. *Nat Rev Cancer* 2007;**7**:332-344.

30. Mellor HR, Bell AR, Valentin JP, Roberts RR. Cardiotoxicity associated with targeting kinase pathways in cancer. *Toxicol Sci* 2011;**120**:14-32.

31. Schmidinger M, Zielinski CC, Vogl UM, Bojic A, Bojic M, Schukro C, Ruhsam M, Hejna M, Schmidinger H. Cardiac toxicity of sunitinib and sorafenib in patients with metastatic renal cell carcinoma. *J Clin Oncol* 2008;**26**:5204-5212.

32. Chen MH, Kerkela R, Force T. Mechanisms of cardiac dysfunction associated with tyrosine kinase inhibitor cancer therapeutics. *Circulation* 2008;**118**:84-95.

33. Armstrong GW, Chen AJ, Linakis JG, Mello MJ, Greenberg PB. Motor vehicle crash-associated eye injuries presenting to U.S. emergency departments. *West J Emerg Med* 2014;**15**:693-700.

34. Lal H, Kolaja KL, Force T. Cancer genetics and the cardiotoxicity of the therapeutics. *J Am Coll Cardiol* 2013;**61**:267-274.

35. Yang B, Papoian T. Tyrosine kinase inhibitor (TKI)-induced cardiotoxicity: approaches to narrow the gaps between preclinical safety evaluation and clinical outcome. *J Appl Toxicol* 2012;**32**:945-951.

36. Zhou F, Ge Z, Chen BA. Quizartinib (AC220): a promising option for acute myeloid leukemia. *Drug Des Dev Ther* 2019;**13**:1117-1125.

37. Fliss H, Gattinger D. Apoptosis in ischemic and reperfused rat myocardium. *Circ Res* 1996;**79**:949-956.

38. Sam F, Sawyer DB, Chang DL, Eberli FR, Ngoy S, Jain M, Amin J, Apstein CS, Colucci WS. Progressive left ventricular remodeling and apoptosis late after myocardial infarction in mouse heart. *Am J Physiol Heart Circ Physiol* 2000;**279**:H422-428.

39. Gao XM, Dart AM, Dewar E, Jennings G, Du XJ. Serial echocardiographic assessment of left ventricular dimensions and function after myocardial infarction in mice. *Cardiovasc Res* 2000;**45**:330-338.

40. Yang F, Liu YH, Yang XP, Xu J, Kapke A, Carretero OA. Myocardial infarction and cardiac remodelling in mice. *Exp Physiol* 2002;**87**:547-555.

41. Wencker D, Chandra M, Nguyen K, Miao W, Garantziotis S, Factor SM, Shirani J, Armstrong RC, Kitsis RN. A mechanistic role for cardiac myocyte apoptosis in heart failure. *J Clin Invest* 2003;**111**:1497-1504.

42. Duran JM, Makarewich CA, Trappanese D, Gross P, Husain S, Dunn J, Lal H, Sharp TE, Starosta T, Vagnozzi RJ, Berretta RM, Barbe M, Yu D, Gao E, Kubo H, Force T, Houser SR. Sorafenib cardiotoxicity increases mortality after myocardial infarction. *Circ Res* 2014;**114**:1700-1712.

43. Lisovsky M, Braun SE, Ge Y, Takahira H, Lu L, Savchenko VG, Lyman SD, Broxmeyer HE. Flt3-ligand production by human bone marrow stromal cells. *Leukemia* 1996;**10**:1012-1018.

44. Khakoo AY, Liu PP, Force T, Lopez-Berestein G, Jones LW, Schneider J, Hill J. Cardiotoxicity due to cancer therapy. *Tex Heart Inst J* 2011;**38**:253-256.

45. Xiang FL, Lu X, Hammoud L, Zhu P, Chidiac P, Robbins J, Feng Q. Cardiomyocyte-specific overexpression of human stem cell factor improves cardiac function and survival after myocardial infarction in mice. *Circulation* 2009;**120**:1065-1074, 1069 p following 1074.

46. Chintalgattu V, Ai D, Langley RR, Zhang J, Bankson JA, Shih TL, Reddy AK, Coombes KR, Daher IN, Pati S, Patel SS, Pocius JS, Taffet GE, Buja LM, Entman ML, Khakoo AY. Cardiomyocyte PDGFR-beta signaling is an essential component of the mouse cardiac response to load-induced stress. *J Clin Invest* 2010;**120**:472-484.

Additional materials and methods

Western blot

H9c2 cells were scraped from 60mm dishes and cell lysates were prepared using RIPA buffer (Cell Signaling, #9803/9806) containing PhosSTOP (Roche, #04-906-845-001) and Complete Protease Inhibitor Cocktail (Roche, #11-697-498-001). Protein samples were reduced with Dithiothreitol and boiled at 95°C with shaking. Samples were loaded on 12% SDS-PAGE and run at 120 Volt. Protein samples were transferred onto PVDF membranes that were previously activated with Methanol. Membranes were blocked for 1 hour with 2% bovine serum albumin (BSA) or 5% skim milk (depending on the antibody) and then probed with appropriate primary antibodies diluted in BSA or milk at 4°C overnight on a shaker. The dilutions of primary antibodies were used as follows: rabbit anti-rat whole PARP (1:1000 Cell Signaling #9542), rabbit anti-rat cleaved PARP (1:1000 Cell Signaling, #9545), rabbit anti-rat cleaved caspase 3 (1:1000 Cell Signaling, #9661), mouse anti-rat GAPDH (1:2000 Sigma, #G8795). The next day the membranes were washed 3 times with TBS-Tween 20 (TBST) buffer, incubated in BSA or skim milk with horseradish peroxidase-conjugated secondary antibody (diluted 1:5000) for 1 hour at room temperature on a shake and then washed again with TBST solution for three times. The immunoreactions were visualized by Western Lightning Plus-ECL Enhanced Chemiluminescence (Perkin Elmer, NEL105001EA) and exposed to CL-XPosure™ film (ThermoScientific, Belgium). Image SXM software (University of Liverpool, UK) was used to quantify protein expression. For multiple staining the membranes were re-blotted with Re-Blot Plus Strong Solution (Millipore, #2504).

Additional results

Animals treated with quizartinib are more susceptible to death when handled by an inexperienced surgeon

In an additional experimental set up and due to absence of our routine surgeon, LAD ligation was performed by a different, newly-trained surgeon. We observed that animals that received quizartinib for three weeks prior surgery were more vulnerable than those treated with vehicle. In particular, only 38% of the quizartinib-treated mice survived up to 7 days post MI, whereas the remainder mice died during or immediately after LAD ligation. In comparison, 69% of vehicle-treated mice undergoing LAD ligation survived. Moreover, among sham operated animals, survival was only 50% among those who received quizartinib, whereas all sham operated animals receiving vehicle survived (**figure 10**).

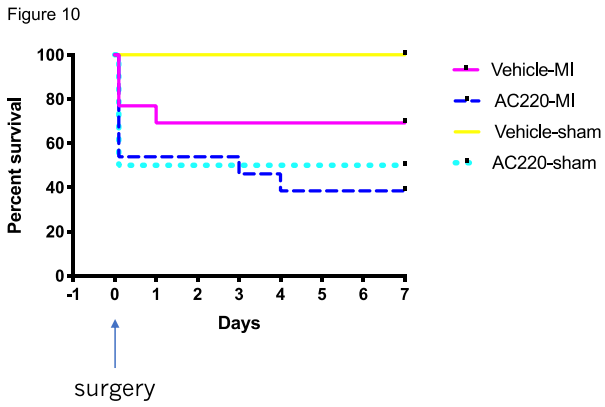

Figure 10. Peri- and post-procedural survival up to 7 days after surgery conducted by an inexperienced surgeon. Kaplan Meier survival curves for C57BL/6N mice treated with quizartinib (AC220) or vehicle undergoing sham surgery or MI up to 7 days. Vehicle-MI n=13; AC220-MI n=13; vehicle-sham n=4; AC220-sham n=4.

Apoptotic cell death declines in quizartinib treated mice from one week to three weeks post-MI

Apoptotic cell death, which is one of the responsible factors inducing cardiac damage and dysfunction, was assessed in the infarct border zone by TUNEL staining one and three weeks post MI. We saw that in mice treated with quizartinib the number of cells undergoing apoptosis was significantly higher after one week compared to three weeks post MI (0.8262% ± 0.09056 vs 0.06006% ± 0.009045, ***p<0.001, n=7-8) (**figure 11**).

Figure 11

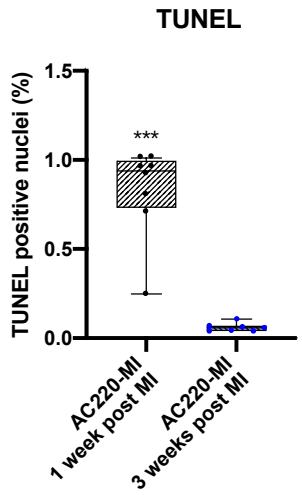

Figure 11. Apoptotic cell death in the infarct border zone at one and three weeks post MI. Apoptotic cell death in the infarct border zone of quizartinib-treated mice is higher one week compared to three weeks post MI. Quantification of TUNEL-positive nuclei, ***p<0.001, n=8, 7 respectively. Shapiro-Wilk normality test, nonparametric Mann-Whitney test.

High dose of quizartinib may induce cleavage of caspase 3 and PARP after 24h

To further investigate whether the cell death is attributed to apoptosis, we assessed cleaved caspase 3 and cleaved poly ADP ribose (PAR) polymerase (PARP) protein expression by Western Blot in H9c2 cells treated with 20μM of quizartinib. Caspases exist within the cytoplasmic compartment of the cells as inactive pro-forms that can be cleaved to form active enzymes following the induction of apoptosis [227] and be translocated to the nucleus [228].

One of the substrates for active caspase is poly ADP ribose (PAR) polymerase (PARP) [229], which is involved in DNA damage repair. It catalyzes the synthesis and binding of PAR to DNA strand breaks, modifying nuclear proteins. The ability of PARP to repair damaged DNA is prevented following cleavage of PARP by caspase-3 [230] (**figure 12A**). This experiment showed that treatment with a high dose of quizartinib for 24 hours may induce activation of the pro-apoptotic caspase pathway as evident by elevated caspase-3 and PARP cleavage (**figure 12B and C**). However, these experiments were not always reproducible. Overall, these data may suggest that cardiomyocyte death may occur at least in part due to activation of the apoptotic cascade.

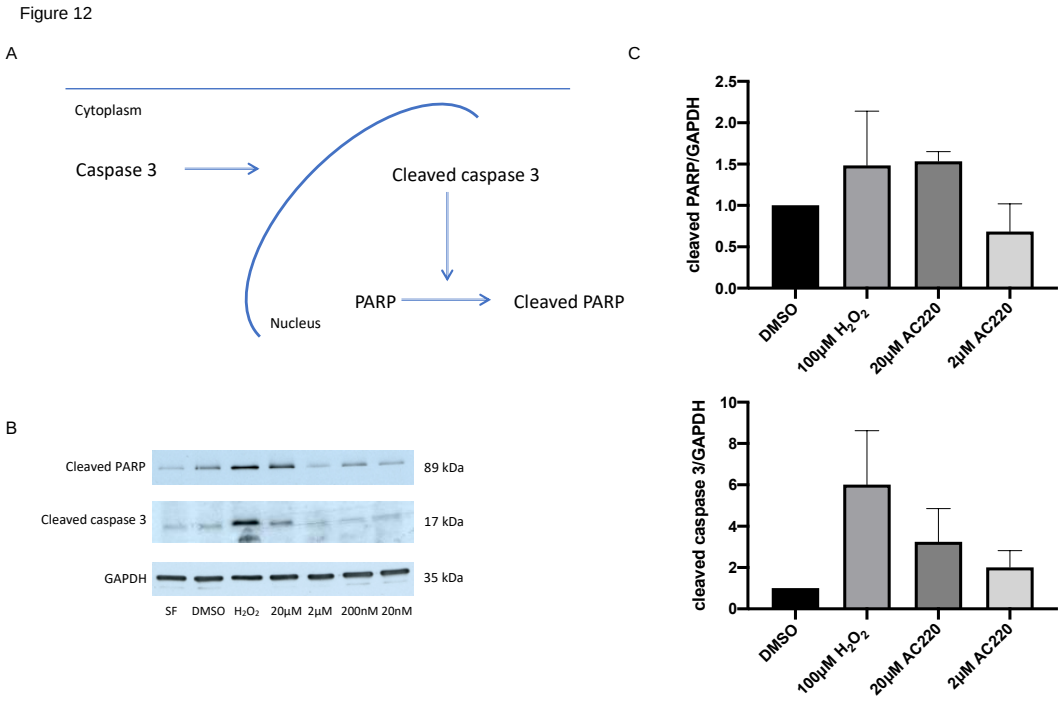

Figure 12. Protein expression of cleaved PARP and cleaved caspase 3 after treatment with quizartinib. H9c2 cells were treated with different doses of quizartinib for 24 hours. Immunoblotting was performed using anti-cleaved PARP and anti-cleaved caspase 3 antibodies. GAPDH was used as reference protein. High dose of quizartinib may induce cleavage of caspase 3 and PARP after 24h. **(A)** In unstimulated cells caspase-3 is present in the cytoplasm. After stimulation (for example, drug treatment) caspase 3 is cleaved and translocates to the nucleus in the catalytically active state.

Furthermore, active caspase 3 induces cleavage of the nuclear enzyme poly ADP ribose polymerase (PARP) to its 89-kDa fragment. **(B)** Representative western blot of one of the successful experiments. The experiment was not always reproducible. **(C)** Quantification of cleaved PARP and cleaved caspase 3 by Image SXM 203, normalized to GAPDH, n=2

Pretreatment with the cleaved caspase 3 inhibitor Z-DEVD-FMK may rescue the cells from apoptosis

We further thought to test whether quizartinib-induced apoptotic cell death could be rescued by inhibition of cleaved caspase 3. H9c2 cells were pretreated with the caspase 3 inhibitor Z-DEVD-FMK before treatment with quizartinib and H_2O_2. After 24 hours we observed a reduction in Annexin V/PI double-positive cells after Z-DEVD-FMK (**figure 13**). These data suggest that inhibition of caspase 3 may be a strategy to rescue cardiomyocytes from quizartinib-induced apoptosis.

Figure 13

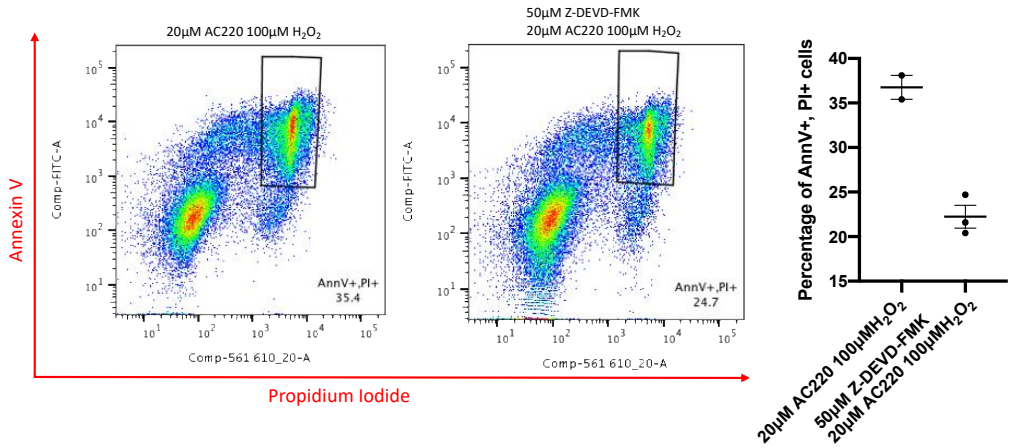

Figure 13. Apoptotic H9c2 cells after pretreatment with the caspase 3 inhibitor Z-DEVD-FMK followed by quizartinib in combination with H_2O_2 *in vitro*. H9c2 cells were pretreated with the caspase 3 inhibitor Z-DEVD-FMK and then treated with quizartinib in combination with H_2O_2.

AnnexinV and PI staining was performed and analysed by flow cytometry. Caspase 3 inhibition reduces the number apoptotic H9c2 cells. Representative images and quantification of apoptotic cells, n=2-3.

Additional data

Table 3. Additional echocardiographic parameters before surgery, and one and three weeks after surgery in wild type mice (WT)

Time point	Before MI			
Groups (WT)	Vehicle-sham	Vehicle-MI	AC220-sham	AC220-MI
Conventional measures (mm)				
LVAW;d	0.7684 ± 0.01999	0.7316 ± 0.01641	0.7955 ± 0.02400	0.8087 ± 0.01870
LVPW;d	0.6381 ± 0.01808	0.5821 ± 0.01588	0.6223 ± 0.01243	0.6518 ± 0.02187
LVAW;s	1.056 ± 0.03587	0.9929 ± 0.02503	1.101 ± 0.03801	1.12 ± 0.02912
LVID;s	3.128 ± 0.07179	3.328 ± 0.06853	3.328 ± 0.06469	3.228 ± 0.08975
LVPW;s	0.8971 ± 0.03025	0.8103 ± 0.02205	0.8818 ± 0.03265	0.8809 ± 0.03614
Strain measures				
Short axis (-%)				
Radial strain	28.78 ± 1.498	25.29 ± 1.215	26.11 ± 1.967	29.04 ± 1.760
Circumferential strain endo	20.75 ± 0.7670	17.92 ± 0.8529	17.76 ± 1.006	18.96 ± 1.209
Circumferential strain epi	7.842 ± 0.3891	6.706 ± 0.3301	6.098 ± 0.4059	6.041 ± 0.5188
Long axis (-%)				
Radial strain	25.26 ± 1.863	24.45 ± 1.277	23.8 ± 1.214	24.25 ± 1.655
Longtitudinal strain endo	14.85 ± 0.4939	13.98 ± 0.7164	13.39 ± 0.8693	12.64 ± 0.6972
Longtitudinal strain epi	8.011 ± 0.4636	7.881 ± 0.3890	7.187 ± 0.3347	6.906 ± 0.4125
Time point	1 week post MI			
Groups (WT)	Vehicle-sham	Vehicle-MI	AC220-sham	AC220-MI
Conventional measures (mm)				
LVAW;d	0.7637 ± 0.02060	0.6149 ± 0.05233	0.8078 ± 0.02375	0.6029 ± 0.04564
LVPW;d	0.6403 ± 0.02610	0.6629 ± 0.04697	0.6437 ± 0.02159	0.6873 ± 0.03186
LVAW;s	0.9795 ± 0.03351	0.7248 ± 0.06914	1.087 ± 0.03323	0.7073 ± 0.06790
LVID;s	3.345 ± 0.09501	4.189 ± 0.1783	3.341 ± 0.07346	4.414 ± 0.1307
LVPW;s	0.8607 ± 0.04587	0.8389 ± 0.05603	0.8918 ± 0.03243	0.8726 ± 0.05059
Strain measures				
Short axis (-%)				
Radial strain	24.24 ± 1.709	13.23 ± 1.716	24.34 ± 1.698	10.7 ± 1.168
Circumferential strain endo	15.22 ± 1.104	10.41 ± 1.254	15.42 ± 1.160	7.964 ± 0.7591
Circumferential strain epi	5.456 ± 0.4843	4.672 ± 0.4119	5.647 ± 0.3805	3.921 ± 0.2771
Long axis (-%)				
Radial strain	21.78 ± 1.482	11.31 ± 1.232	24.47 ± 1.519	10.41 ± 0.7814
Longtitudinal strain endo	11.49 ± 0.6155	7.824 ± 0.8445	12.84 ± 0.8751	6.3 ± 0.5364
Longtitudinal strain epi	6.673 ± 0.3048	4.547 ± 0.4947	6.647 ± 0.5314	3.547 ± 0.2851
Time point	3 weeks post MI			
Groups (WT)	Vehicle-sham	Vehicle-MI	AC220-sham	AC220-MI
Conventional measures (mm)				
LVAW;d	0.701 ± 0.03219	0.5051 ± 0.08200	0.8413 ± 0.02450	0.5201 ± 0.1143
LVPW;d	0.5915 ± 0.02417	0.5878 ± 0.06707	0.6277 ± 0.01741	0.5417 ± 0.09896
LVAW;s	0.8595 ± 0.07975	0.5601 ± 0.1059	1.12 ± 0.03240	0.6234 ± 0.1581
LVID;s	3.609 ± 0.1458	4.521 ± 0.3279	3.529 ± 0.1613	4.883 ± 0.2861
LVPW;s	0.768 ± 0.04892	0.7465 ± 0.08631	0.8163 ± 0.01535	0.6471 ± 0.1163
Strain measures				
Short axis (-%)				
Radial strain	23.03 ± 4.786	10.4 ± 1.921	19.89 ± 2.550	11.49 ± 1.733
Circumferential strain endo	13.96 ± 2.441	8.694 ± 1.521	13.5 ± 1.459	7.274 ± 0.9667
Circumferential strain epi	5.09 ± 0.3807	4.625 ± 0.6700	5.04 ± 0.4413	3.836 ± 0.3625
Long axis (-%)				
Radial strain	15.91 ± 1.050	12.58 ± 1.798	16.17 ± 2.073	12.91 ± 1.912
Longtitudinal strain endo	9.932 ± 1.373	7.707 ± 1.237	9.293 ± 1.035	6.324 ± 1.067
Longtitudinal strain epi	5.72 ± 0.6554	4.851 ± 0.6175	5.028 ± 0.5129	3.664 ± 0.5889

Table 4. Additional echocardiographic parameters before surgery, and one and three weeks after surgery in knock out mice (KO)

Time point	Before MI			
Groups (KO)	Vehicle-sham	Vehicle-MI	AC220-sham	AC220-MI
Conventional measures (mm)				
LVAW;d	0.6213 ± 0.04983	0.6499 ± 0.03897	0.6345 ± 0.04123	0.6778 ± 0.02104
LVPW;d	0.6373 ± 0.02978	0.6123 ± 0.02964	0.6433 ± 0.02282	0.6225 ± 0.01902
LVAW;s	0.8917 ± 0.09581	0.8564 ± 0.03427	0.8903 ± 0.06402	0.9182 ± 0.04363
LVID;s	3.001 ± 0.1399	3.171 ± 0.07449	3.186 ± 0.1678	3.035 ± 0.1035
LVPW;s	0.8373 ± 0.04433	0.8111 ± 0.03542	0.8258 ± 0.02884	0.8209 ± 0.03764
Strain measures				
Short axis (-%)				
Radial strain	24.85 ± 3.802	23 ± 1.850	21.72 ± 1.483	22.04 ± 0.9420
Circumferential strain endo	16.48 ± 2.175	13.23 ± 0.8671	13.36 ± 1.121	13.61 ± 0.9431
Circumferential strain epi	6.675 ± 1.576	4.894 ± 0.4299	4.863 ± 0.7882	5.061 ± 0.4425
Long axis (-%)				
Radial strain	21.36 ± 3.536	21.39 ± 1.034	20.76 ± 2.028	20.88 ± 1.221
Longtitudinal strain endo	12.16 ± 0.4400	12.87 ± 0.8323	10.84 ± 1.822	11.99 ± 0.5308
Longtitudinal strain epi	7.35 ± 0.06604	7.958 ± 0.4171	7.432 ± 0.8589	6.863 ± 0.3746
Time point	1 week post MI			
Groups (KO)	Vehicle-sham	Vehicle-MI	AC220-sham	AC220-MI
Conventional measures (mm)				
LVAW;d	0.771 ± 0.03287	0.7106 ± 0.06830	0.7068 ± 0.06021	0.6983 ± 0.05835
LVPW;d	0.6647 ± 0.04433	0.6456 ± 0.07762	0.6368 ± 0.01667	0.6294 ± 0.05622
LVAW;s	0.9917 ± 0.01884	0.8682 ± 0.09541	0.9375 ± 0.09875	0.8232 ± 0.07193
LVID;s	2.857 ± 0.09103	3.786 ± 0.3672	2.946 ± 0.1285	3.518 ± 0.1895
LVPW;s	0.8757 ± 0.07704	0.8172 ± 0.1074	0.8668 ± 0.01589	0.8048 ± 0.07647
Strain measures				
Short axis (-%)				
Radial strain	25.87 ± 3.979	13.66 ± 2.410	28.58 ± 5.739	12.24 ± 1.259
Circumferential strain endo	15.66 ± 3.295	9.237 ± 1.967	16.18 ± 1.879	8.733 ± 0.8356
Circumferential strain epi	4.381 ± 0.8657	3.6 ± 0.6161	5.945 ± 0.4564	3.481 ± 0.3625
Long axis (-%)				
Radial strain	23.6 ± 2.960	15.97 ± 1.819	19.98 ± 4.450	13.58 ± 1.596
Longtitudinal strain endo	13.07 ± 1.765	8.153 ± 1.056	13.25 ± 1.220	8.184 ± 0.5864
Longtitudinal strain epi	6.972 ± 0.6129	4.441 ± 0.5541	8.169 ± 0.4703	4.217 ± 0.3773
Time point	3 weeks post MI			
Groups (KO)	Vehicle-sham	Vehicle-MI	AC220-sham	AC220-MI
Conventional measures (mm)				
LVAW;d	0.6397 ± 0.03093	0.5607 ± 0.08132	0.7628 ± 0.04078	0.6138 ± 0.05693
LVPW;d	0.6777 ± 0.008413	0.6084 ± 0.06364	0.6368 ± 0.01810	0.6282 ± 0.03339
LVAW;s	0.8687 ± 0.008413	0.6961 ± 0.1165	0.9943 ± 0.07008	0.7454 ± 0.08644
LVID;s	3.01 ± 0.02454	3.843 ± 0.3080	2.978 ± 0.1044	3.472 ± 0.2114
LVPW;s	0.8947 ± 0.04751	0.7748 ± 0.08697	0.811 ± 0.01312	0.851 ± 0.06789
Strain measures				
Short axis (-%)				
Radial strain	24.85 ± 2.282	13.66 ± 2.026	23.51 ± 2.678	19.02 ± 3.312
Circumferential strain endo	14.61 ± 2.552	9.87 ± 1.847	16.05 ± 2.221	12.68 ± 2.090
Circumferential strain epi	4.349 ± 1.207	4.356 ± 0.7222	6.595 ± 1.270	5.088 ± 0.6838
Long axis (-%)				
Radial strain	17.28 ± 2.312	15.87 ± 2.255	19.85 ± 3.132	15.77 ± 1.664
Longtitudinal strain endo	10.99 ± 1.634	9.635 ± 1.191	11.41 ± 1.842	9.524 ± 1.070
Longtitudinal strain epi	6.808 ± 1.067	6.175 ± 0.6259	6.181 ± 0.8781	5.632 ± 0.5997

Photograph of a heart with LAD ligation and a sham heart

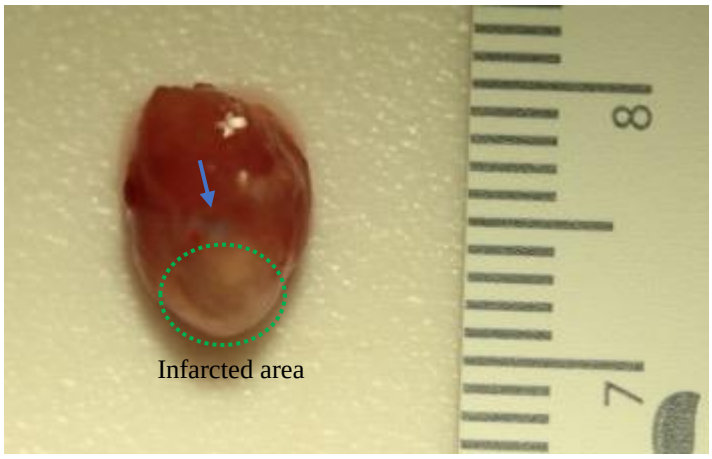

LAD ligation (shown with an arrow)

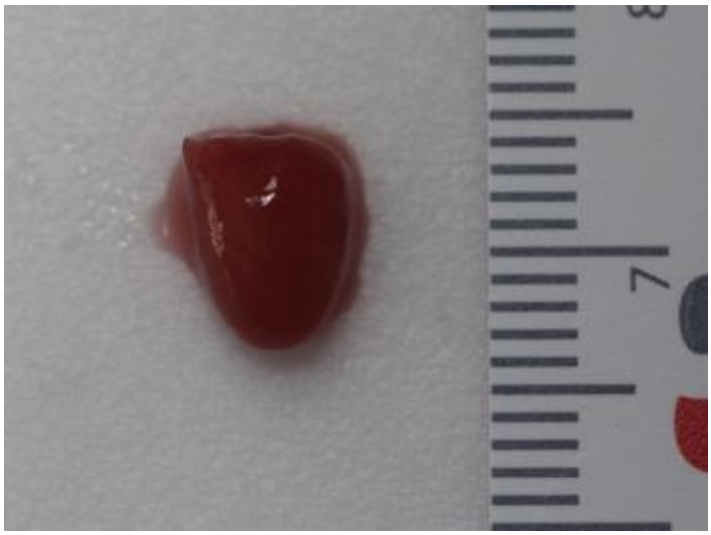

Sham

Discussion

Cardiotoxicity is a term used to describe a broad range of adverse effects on heart function induced by therapeutic molecules. Kinases involved in the regulation of cell survival and proliferation may be part of a shared kinome between cancer cells and the heart [231]. Small molecule TKIs show promising results in the treatment of cancer, however there is an increasing number of studies revealing a relatively high rate of adverse cardiac events in the clinic, with systolic dysfunction and resultant heart failure as one of the most prevalent side effects [86, 176, 178, 232-234]. The cardiac function is maintained by a highly coordinated network of molecular signaling events and our understanding of how drug molecules can perturb the signaling pathways, which maintain cardiac homeostasis and contractile function, requires further exploration. There are gaps in current preclinical drug testing for predicting the development of cardiac toxicities in humans. These gaps include a lack of a comprehensive identification of TKI mechanisms of action and appropriate evaluation of cardiac function [235]. As a result, the majority of the molecular mechanisms underlying therapy-induced cardiotoxicity observed in preclinical drug development, or which emerge clinically, remain to be explained.

Moreover, early preclinical safety evaluation of TKIs very often did not predict cardiovascular risk, thus subsequent clinical trials with TKIs did not include predefined cardiac endpoints, such as measurement of LVEF at baseline and during treatment. The identification of TKI-induced cardiotoxicity and potential heart failure have been based largely on medical history and physical examination, which are insensitive, particularly in patients with underlying mild chances of heart failure or with asymptomatic LV dysfunction. Because of these clinical limitations, rates of cardiotoxicity associated with TKIs may be underestimated [86]. As a

consequence, a thorough preclinical safety evaluation of TKIs with more comprehensive preclinical studies is needed to predict potential cardiotoxicity of TKIs.

In our study we examined the second-generation Flt3 inhibitor, quizartinib, which has shown high potency in the treatment of AML either as a single agent or in combination with conventional chemotherapy regimens, but also potential cardiotoxic effects in preclinical studies [175]. Due to our previous findings on Flt3 exerting protective effects in the infarcted heart through the inhibition of apoptotic cell death [79], we focused our studies on cardiomyocyte viability and heart function after treatment with quizartinib.

We used an animal model of MI that provides a novel approach in the investigation of the function of the Flt3 signaling pathway beyond its role in both normal hematopoiesis and as a crucial regulator of tumor growth and survival. Only a small number of studies has recently studied Flt3 in the heart. They found that Flt3 mRNA and protein expression is upregulated in the injured hearts, but also that it exerts a protective role in alleviating cardiac dysfunction and reducing cardiomyocyte apoptosis in the infarct border zone, thus reducing the expansion of fibrotic scar tissue [77-79]. Therefore, it is an interesting perspective to evaluate the importance of Flt3 in maintaining cardiac homeostasis, while also assessing the potential cardiac toxicity of Flt3-targeting cancer therapies. Moreover, clinical studies exclude patients with pre-existing cardiovascular disease or heart failure, or do not include predefined cardiac endpoints or the assessment of left ventricular function before and during treatment, therefore the consequences of drug administration to patients with underlying cardiac diseases are not clear. Thus, preclinical disease models as ours could contribute to our understanding of potential drug effects in the diseased heart.

We noticed that treatment with quizartinib did not affect the mortality rate, as similar percentages of animals treated with the drug or vehicle died within the first week after MI. The mortality could exclusively be attributed to the induction of infarction and its sequelae, rather than treatment with quizartinib, as both vehicle and drug treated sham animals had 100% survival. Interestingly, one additional set of animals that was operated by a newly trained and, hence, inexperienced surgeon showed 50% mortality of quizartinib treated animals already during the surgical procedure (both sham and MI). Some more animals undergoing LAD and treated with quizartinib also died post-MI, prompting survival to drop to 40% only. These observations suggest that animals treated with quizartinib become more susceptible to additional stressors compared to vehicle-treated mice. However, the cause of death and underlying mechanisms remain to be investigated. Given the fact that TKIs including quizartinib can lead to echocardiographic (ECG) alterations, a possible explanation could be sudden cardiac death due to lethal arrhythmia [175].

Surviving animals showed deterioration in cardiac function and left ventricular remodeling at one and three weeks after MI and this was true when compared to before surgery as well as when compared to sham operated animals. Importantly, mice administered quizartinib showed the most persistent changes. Despite vehicle treated animals having the same degree of cardiac dysfunction and ventricular dilation, the differences between quizartinib-treated MI and sham mice were more pronounced. Most importantly, quizartinib-treated mice exhibited significantly increased numbers of apoptotic nuclei as assessed by TUNEL staining in the infarct border zone and by cleaved caspase 3 staining in the remote myocardium. Apoptotic cell death after MI, which mostly occurs during the first week in rodents, has been previously reported to play an important role in the progression of LV remodeling and cardiac dysfunction after MI [236-239]. Moreover, several TKIs were shown to induce cardiomyocyte apoptosis in

animal models, which is considered an important cellular substrate of their cardiotoxicity. For example, zebrafish embryos treated with 5μM and 10μM ponatinib, which is a multi-targeted kinase inhibitor that primary inhibits Bcr-Abl, but also suppresses other kinases, such as c-Kit, SFK, PDGFR, Flt3, showed apoptotic cardiomyocytes in the heart in a dose-dependent manner as assessed by acridine orange staining and confirmed by TUNEL staining [240]. Treatment of Wistar rats with 30mg/kg of gefitinib, a TKI that targets epidermal growth factor receptor (EGFR), induced mRNA and protein expression of caspase 3 and p53 in cardiomyocytes, indicative of apoptotic cardiomyocyte death [241]. Moreover, sunitinib is suggested to exert its cardiotoxicity through inhibition of ribosomal S6 kinase (RSK), leading to the release of the pro-apoptotic factor BCL2-antagonist of cell death (BAD) and subsequent BCL2-associated X protein (BAX) activation and cytochrome c (Cyt c) release. This results in the activation of the intrinsic apoptotic pathway and to ATP depletion, which both contribute to LV dysfunction [86].

Quizartinib enhances apoptotic cell death during the acute phase after MI. Such loss of cardiac cells may explain the thinning of the LV wall and LV dilation, which were more pronounced in drug treated animals. It has been shown that there is a direct correlation between apoptotic rates, wall thickness and LV chamber size [242]. Thus, myocardial apoptosis that is enhanced through quizartinib after MI can be a crucial determinant of LV remodeling and one of the major factors of quizartinib toxicity. Consistent with the dynamics of apoptotic cell death after MI, the number of apoptotic cells in the infarct border zone of the hearts of animals treated with the drug was impressively lower after three than one week post-MI, and also not different any more from vehicle-treated mice. Still, the increased apoptotic cell death observed early on could translate into more severe remodeling and dysfunction in the chronic phase post-MI, but further studies are needed to clarify whether this is indeed the case. Finally, the fibrotic area

was not significantly different between the treatment groups neither after one nor after three weeks post-MI. However, a higher number of experimental animals may increase the sensitivity of the picrosirius staining to verify this observation.

We next investigated the specificity of quizartinib for Flt3 inhibition, as the majority of the first generation TKIs have multiple targets, therefore leading to extensive cardiotoxicity, whereas the second generation drugs promise to be more exclusive. Flt3 receptor knock out mice from all the treatment groups did not show any significant deterioration in cardiac function or remodeling post MI either after one week or three weeks after the surgery. This experiment strongly suggests that quizartinib exerts its actions through inhibition of the Flt3 signaling pathway, which is also referred to as "on-target" toxicity. Moreover, ablation of the Flt3 receptor might be considered protective after MI, as Flt3 KO mice that underwent LAD ligation did not show significant changes in heart function and morphology compared to sham. These results come to agreement with previous observations from our group, where Della Verde *et al.* showed that ablation of Flt3 ligand (Flt3L-/-) is protective during post MI cardiac remodeling. Whereas the underlying mechanisms are currently being further investigated in our laboratory, possible immune-modulatory effects elicited or suppressed in the absence of Flt3 may be responsible. However, because quizartinib enhanced apoptotic cell death post-MI in wild type mice, it will be important to perform immunohistochemistry after 1 week to assess apoptotic cell death also in our Flt3-KO mice. Quizartinib failing to enhance apoptosis after MI in Flt3-KO-mice would further strengthen the hypothesis of on-target toxicity.

Our investigation of the quizartinib effect on cultured cardiomyocytes (NRVMs and H9c2) showed that only the higher (20μM) concentration of the drug induces a significant decrease in cell viability. These results are compatible with the *in vitro* toxicity screening of four FDA-

approved TKIs, crizotinib, sunitinib, erlotinib and nilotinib, which showed that all of the inhibitors induced reduction in human cardiomyocyte viability at the highest concentration tested (10μM) [243]. However, crizotinib, sunitinib, and nilotinib also significantly decreased cell viability at a lower concentration of 3μM. Another study [240] examined lower concentrations in the range 50nM to 1μM of imatinib, dasatinib, nilotinib, bosunitib and ponatinib on rat cardiomyocyte survival and showed a dose-dependent decrease in cell viability up to 72h of treatment. In our *in vitro* experiments, low doses of quizartinib did not affect cell viability over time. However, we also observed a dose-dependency in the decrease of cell viability for the doses ranging between therapeutic (2μM) and high (20μM).

There is a variety of evidence in the literature regarding the type of cell death attributed to TKI toxicity *in vitro*. For example, Duran and colleagues [244] showed that necrosis was responsible for the death of adult feline left ventricular myocytes after exposure to high concentrations of sorafenib (10-50 μmol/L), as they did not observe cleavage of caspase 3. Chu and colleagues [177] demonstrated that sunitinib at the concentration of 1μM led to activation of caspase 9, an initiator caspase of the mitochondrial apoptotic pathway, in cultured NRVMs. Apoptosis was also confirmed by TUNEL staining. Furthermore, Kerkela and colleagues [176] observed that NRVMs treated with 5μM of imatinib initially led to cleavage of caspase 3 and TUNEL positivity, indicating apoptotic death, however the cells were directed to necrotic death due to progressive ATP depletion, nuclear pyknosis and loss of sarcolemmal integrity. In contrast, Zhao and colleagues [245] showed that H9c2 cells treated with sunitinib underwent autophagy, as was supported by presence of autophagosomes (when treated with 2.5μM) shown by fluorescence microscopy and expression of the autophagy-related proteins LC3-II and Beclin 1 (when treated with 1.3-10μM).

In order to confirm that cardiomyocytes undergo apoptosis after treatment with quizartinib we measured protein expression of cleaved PARP and cleaved caspase 3, which are important members of the apoptotic pathway [227, 230]. Whereas we saw cleavage of both caspase and PARP at the highest concentration of the drug (20μM) as assessed by Western Blotting in some experiments, this was not always reproducible. A possible explanation might be that given the small fraction of cells undergoing apoptosis (AnnexinV/PI double positivity in roughly 20% of cells under quizartinib vs. 10% in DMSO), Western Blotting might not be sensitive enough to consistently detect any differences. Further studies using alternative techniques (e.g., flow cytometry) have been initiated.

Ischemia and reperfusion are associated with enhanced oxidative stress, which is thought to be responsible for the ischemia and/or reperfusion damage that occurs predominantly in the infarct border zone [246]. Therefore, in order to support our *in vivo* data, we simulated the *in vivo* effect of MI by treating the H9c2 myocytes with quizartinib before inducing oxidative stress in form of H_2O_2. We saw that the cells treated with quizartinib and subjected to oxidative stress have an enhanced rate of cell death than those treated only with H_2O_2 or quizartinib. Again, this cell death was partially attributed to apoptosis, as half the population of dead cells was positive for AnnexinV and PI. In addition, whereas only high concentrations of quizartinib (20μM) induced apoptosis *per se*, also the lower concentration of 5μM quizartinib was able to potentiate oxidative stress-induced cell death and apoptosis. These *in vitro* experiments are consistent with the *in vivo* data showing that animals treated with quizartinib and undergoing oxidative stress during MI have higher numbers of apoptotic cells.

It has been shown *in vivo* that suppression of apoptosis by various genetic and pharmacological means decreases the pathological remodeling and progression of heart failure in models of

myocardial infarction [247]. Therefore, we tried to rescue the cells treated with quizartinib and H_2O_2 from apoptosis *in vitro* by using the caspase-3 inhibitor Z-DEVD-FMK, which is a cell permeable fluoromethyl ketone (FMK)-derivatized peptide that acts as effective irreversible caspase inhibitor with no cytotoxic effects and has been used broadly to inhibit caspase activity. In these preliminary experiments we saw that the number of apoptotic cells in response to quizartinib and H_2O_2 could significantly be reduced. Therefore, inhibition of the apoptotic pathway in cardiomyocytes could be a potential solution to protect the cells during cardiotoxic drug treatment. It has already been shown in animal models that caspase inhibition can modulate LV remodeling after MI [248] or reduce myocardial infarct size in the ischemic heart [249-252]. Importantly, however, we should take into consideration the fact that suppression of apoptosis in cardiomyocytes with caspase inhibitors might have the same effect on the leukemic cells, therefore compromising the suppression of the tumor. Therefore, when choosing to inhibit the apoptotic pathway to protect or limit cardiomyocyte damage during TKI treatment, such approach should be targeted specifically to the cardiomyocyte compartment to avoid inhibition of apoptosis in the tumor.

Taken together, we showed that the Flt3-targeting TKI quizartinib enhances oxidative stress-associated cell death *in vitro* and *in vivo* and accentuates the decline in cardiac function over three weeks post-MI in mice. Quizartinib has been approved in Japan for the treatment of adult patients with relapsed/refractory Flt3-ITD–positive AML after revision of the latest phase III QuANTUM-R study, in which quizartinib reduced the risk of death by 24% compared with salvage chemotherapy in patients with Flt3-ITD–positive relapsed/refractory AML after first-line treatment with or without hematopoietic stem cell transplantation [253]. At a median follow-up of 23.5 months, the median overall survival was 6.2 months with quizartinib compared with 4.7 months with salvage chemotherapy. However, the FDA conducted its own

efficacy analysis of quizartinib [175] and achieved different results showing lower median overall survival with quizartinib than demonstrated in the QuANTUM-R study. The analysis also did not demonstrate a significant event free survival benefit with quizartinib versus chemotherapy. The most common adverse effects (>10%) included nausea, anemia, changes in the electrocardiogram (in particular QT prolongation), thrombocytopenia, pyrexia, hypokalemia, febrile neutropenia, vomiting, fatigue, diarrhea, neutropenia, white blood cell count decreased, platelet count decreased, neutrophil count decreased, headache, decreased appetite, cardiomyopathy and heart failure. Based on these data that failed to demonstrate the benefits of quizartinib to outweigh the potential risks, the FDA has not approved the drug. Moreover, the drug has been studied only for Flt3-ITD mutations. However, based on early drug testing [124, 138] and from our experiments it seems that it also inhibits the wild type Flt3 receptor as observed here in cardiomyocytes. In addition, there are no data proving safety of the drug in patients with cardiovascular risks or already existing cardiac diseases.

Currently, there are new drugs in the pipeline that have higher potency for Flt3 inhibition in the treatment of AML. One of those promising drugs is gilteritinib that has been approved by the FDA [254]. It has activity against both Flt3 mutation subtypes (ITD and TKD) and weak activity against c-Kit. Gilteritinib also inhibits the tyrosine kinase AXL, which is implicated in Flt3 inhibitor resistance. The phase III clinical trials with 371 patients with relapsed or refractory Flt3-mutated AML, among which 247 were randomly assigned to the gilteritinib group and 124 to the salvage chemotherapy group, showed that gilteritinib provides significantly longer survival and there is a higher percentage of patients with remission in comparison to salvage chemotherapy. The only observed adverse effects included febrile neutropenia, anemia and thrombocytopenia [123]. No data about potential cardiotoxicity of the

drug is available. Therefore, pre-clinical investigation of any potential cardiac risk would provide useful information for the future application of the drug in patient treatment.

In conclusion, our studies showed that quizartinib decreases cardiomyocyte viability and enhances cardiomyocyte apoptosis under hypoxia *in vitro* and *in vivo*. It seems to exert its cardiotoxic action mostly through inhibition of the Flt3 signaling pathway as it failed to worsen outcome in Flt3 receptor knock out mice. Cardiomyocyte apoptosis could be partially rescued by treatment with a caspase 3 inhibitor, which could offer a therapeutic strategy for cardioprotection when deliverable in a heart-specific manner.

Translational perspective

Before the initiation of cancer therapy, a thorough patient history, physical examination and analysis of cardiac morphology and function by echocardiography should be performed to determine the baseline cardiovascular risk and identify preexisting cardiovascular diseases. The risk/benefit ratio of treatment with a TKI should be carefully evaluated in patients at a high risk for cardiotoxicity. During the treatment, constant monitoring of patients for early symptoms or signs of cardiac dysfunction should be performed. Although currently ACE-inhibitors, angiotensin receptor blockers and betablockers are used for cardioprotection, more targeted protective therapies need to be developed based on a deepened understanding of the mechanisms of toxicity. Therefore, studies like yours are important to identify those mechanisms and expect any potential risk of cardiotoxicity.

Chapter 2: Role of Plk2 in cardiomyocyte proliferation

Introduction

Heart failure is a leading cause of death and morbidity worldwide. Currently almost 40 million patients suffer from heart failure [255], which occurs most frequently as a sequel of MI and due to loss of cardiomyocytes and limited ability of the mammalian heart to regenerate [256]. The heart reacts to the loss of cardiomyocytes by cardiomyocyte hypertrophy and excessive fibrotic tissue replacement leading to scar formation [257]. Such processes lead to remodeling of the surrounding myocardium and eventually to impaired cardiac function. The potential of an adult mammalian heart to regenerate after an injury remains a fundamental question in the cardiovascular field and still has to be elucidated.

Lower vertebrates such as the newt and zebrafish display regenerative capacity throughout their life and thus, are able to replace lost cardiac tissue after an injury [258-260]. However, there has been a persistent belief that mammalian heart tissue cannot regenerate due to the inability of adult mammalian cardiac cells to proliferate. A few years ago though, it was shown that mammalian cardiogenesis is possible during adult life, including in humans [261, 262], although at a very low level that is insufficient to compensate for major cell loss.

Studies on the mammalian response to cardiac injury (**figure 14**) show that at embryonic stages, compensatory proliferation of cardiomyocytes can restore the lost tissue, because the embryonic environment and embryonic developmental pathways facilitate cell cycle re-entry and repopulation of the heart based on cardiomyocyte proliferation [263] . Even in neonatal mice there is a time window immediately after birth when the heart exhibits a robust

regenerative capacity. In case of an injured heart (due to MI or ventricular resection), neonatal cardiomyocytes are able to proliferate, while an intense angiogenesis occurs. Despite some scarring, the lost tissue can be replaced within 3 weeks and cardiac function is normal after a few months [264]. Genetic fate mapping has shown that pre-existing cardiomyocytes can re-enter the cell cycle and repopulate the lost cardiac area [265, 266]. Interestingly, such regenerative capacity is lost by day 7 due to terminal cell cycle withdrawal of cardiomyocytes, revealing that there is a rapid decline in cardiac regenerative potential soon after birth. Eventually, adult mice have virtually no regenerative potential and cardiomyocyte proliferation is insufficient to replace lost tissue, resulting in extensive scarring and decrease of cardiac function after injury [267].

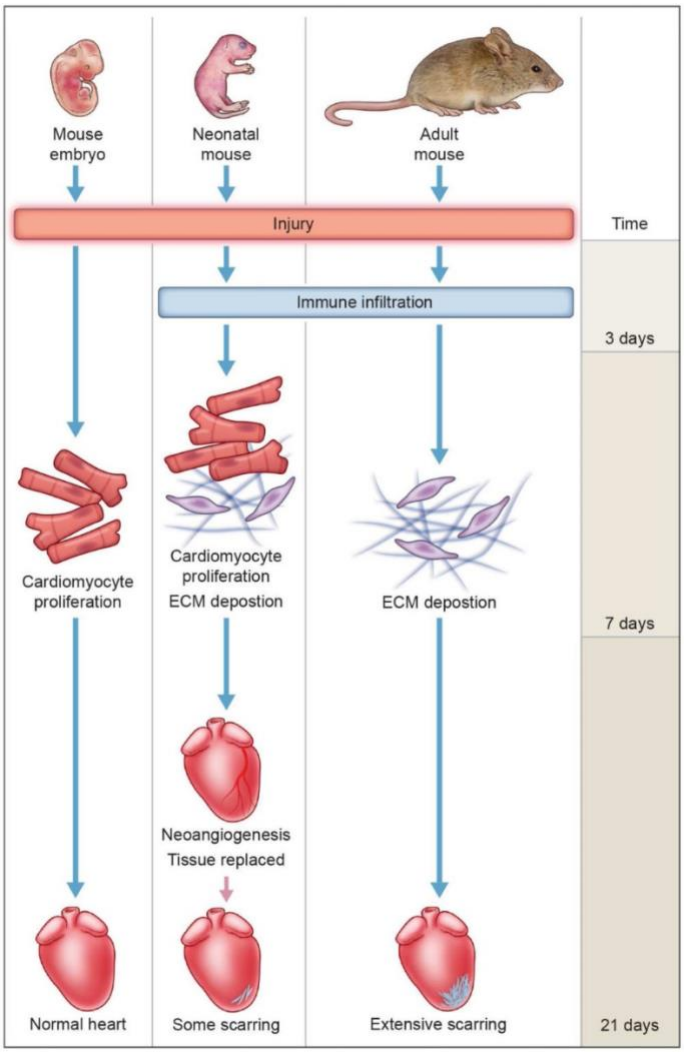

Figure 14. Mouse heart regenerative potential at different stages of life [267]

Interestingly, case reports from corrective heart surgeries in infants [268] and MI in a newborn child [269] have suggested that the human neonatal heart may also have a higher regenerative potential, at least partially maintaining the intrinsic capacity to repair the myocardial damage and thus, recovering the cardiac function.

Consequently, recent studies have aimed to detect cell intrinsic and extrinsic factors that take part in the cell cycle regulation and in control of cell cycle arrest in cardiomyocytes and therefore, could be potential targets for stimulation or reactivation of cardiomyocyte proliferation in the adult heart (**figure 15**). The arrest of dividing cardiomyocytes is conducted by cell cycle regulators and is associated with downregulation of G1/S cyclins (such as cyclins A and D) and G2/M cyclins and cyclin-dependent kinases (CDKs) and upregulation of cell cycle inhibitors [270]. Therefore, overexpression of cyclins D1 and D2 and cyclin A2 can trigger cardiomyocyte DNA synthesis or mitosis, respectively, in adult mice [271, 272]. Deletion of p130 and Rb, which are known for their role in inhibiting cell cycle progression through the regulation of E2F-responsive genes [273], triggers cardiomyocytes to re-enter the cell cycle [274]. Despite the manipulation of these cell cycle regulators to stimulate DNA replication, it is not sufficient for production of new cardiomyocytes in the adult heart. It may be attributed to the fact that in spite of the enhanced DNA synthesis, the cardiomyocytes do not undergo cytokinesis, resulting in multinucleation without complete cell division [275].

The transcriptional factor Meis1 has also been described as a potential key regulator of postnatal cell cycle arrest, maintaining high levels of cyclin-dependent kinase inhibitors and diminishing the expression of positive cell cycle regulators [276]. Moreover, miRNAs have been shown to regulate the cardiomyocyte proliferation during development and regeneration [277], such as miR-195 that is upregulated after birth and controls the expression of checkpoint

kinase 1 and other cell cycle factors [264]. Similarly, the Nrg1/ErbB2 pathway is also involved in the regulation of postnatal cardiac growth [278]. Finally, it has been shown that endocardial Notch signaling is required for zebrafish heart regeneration by supporting cardiomyocyte proliferation [279].

Another essential pathway that is involved in cell cycle regulation is the Hippo signaling pathway [280]. It regulates organ size in different species, partially by inhibiting cellular proliferation [281]. The transcriptional co-activator Yap is a member of the Hippo pathway. When dephosphorylated, it translocates to the nucleus, where its proliferative and oncogenic activity is driven by its association with the TEAD family of transcription factors which induce transcription of Hippo-controlled genes [282], therefore upregulating genes that promote cell proliferation and inhibit apoptosis [283]. It is excluded from the nucleus when phosphorylated, leading to smaller heart size during fetal development in mice. Inactivation of the pathway results in cardiomegaly [284-286]. Studies show that neonatal mouse hearts have low levels of phosphorylated Yap, whereas adult mice have high levels [284]. Moreover, forced expression of a constitutively active Yap in the adult heart stimulates cardiac regeneration and improves contractility after myocardial infarction, whereas cardiac-specific deletion of Yap hinders neonatal heart regeneration, resulting in a fibrotic response after an injury even in young mice [287]. Elevated expression of Igf1 receptor has also been observed in hearts that express a constitutive form of Yap [285]. These studies suggest that the Hippo pathway may restrict the cell cycle and reduce cell sensitivity to mitogens, therefore inhibiting cardiomyocyte proliferation. When Yap is activated in mature cardiomyocytes, cardiomyocyte proliferation is increased and can potentially improve the cardiac function after MI [288]. Overall, manipulating Yap activity seems to be a promising strategy for adult heart regeneration.

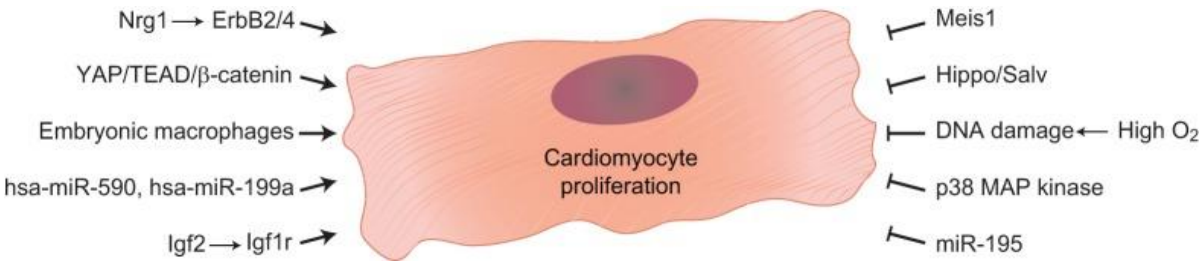

Figure 15. Cell intrinsic and extrinsic factors regulating the cardiomyocyte cell cycle [289]

Mochizuki and colleagues [290] identified the cell cycle regulator polo-like kinase 2 (Plk2) as a coordinator of cell proliferation and early lineage commitment of cardiac progenitor cells that is regulated downstream of YAP. In particular, degradation of YAP results in lower expression of Plk2 on the transcriptional level, associated with lower cell proliferation and higher lineage commitment of cardiac progenitor cells. In this context, the question arose, whether Plk2 may play a role in the cell cycle regulation of cardiomyocytes downstream of YAP.

The Plk proteins (1-5) are members of the serine-threonine kinase family that have been shown to regulate the cell cycle [291], controlling entry into mitosis, centrosome maturation, exit from mitosis and initiation of cytokinesis [292]. Plks carry two conserved domains- the canonical serine/threonine kinase domain and the non-catalytic polo box domain (PBD), which binds to substrates [293]. Plk2, in particular, was identified as an early-growth response gene that regulates cell proliferation in the G1 phase [291]. Plk2 is expressed in post-mitotic neurons [294] controlling dendritic spine sprouting and the density of synapses in neurons [295]. Plk2 transcripts have been also found in human fetal lung, kidney, spleen and heart [291]. Moreover, it is expressed in the vascular system in early developmental stages [296, 297], regulating the vascular development through small GTPases involved in lamelopodia formation of endothelial cells during angiogenesis [298]. Plk2 mainly functions as a regulator of the transition from G1 to early S phase, when both Plk2 mRNA and protein are at their peak [299].

Moreover, Plk2 is required for centriole duplication during S phase [300]. It is a nonessential gene and Plk2 deficient embryos are viable, despite the retarded growth and skeletal development late in gestation [301]. Plk2 silencing with taxol or nocodazole induces apoptosis [302], suggesting that it may prevent from mitotic catastrophe after spindle damage. Furthermore, Plk2 plays role in DNA damage control, as its expression is triggered by DNA-damaging agents [302], and may serve as a tumor suppressor [303].

The Plk family has been found to be associated with the proliferative capacity of cardiac myocytes. In 1997 Plk was first identified to have a role in DNA synthesis of cardiac myocytes [304]. In particular, Plk gene was expressed in abundance in cardiac cells of fetal and neonatal rats, but not in adult cardiomyocytes. Its protein was also detected only in fetal and neonatal hearts. Plk was highly expressed at the earliest stage of development and its mRNA levels decreased gradually during cardiac differentiation. In the same study it was shown to be involved in the progression of cell cycle of cardiomyocytes and to be downregulated by serum deprivation. However, another study indicated that Plk1 specifically, when overexpressed, is not able to promote cell cycle progression in rat cardiomyocytes *in vitro* [305]. Recently, Plk2 was shown to be regulated by miR-128 and to induce cardiac cell apoptosis in response to ischemia reperfusion stress through activation of the nuclear factor κB (NF-κB) signal pathway, thus considering miR-128 and Plk2 as new targets for prevention of cardiac ischemia reperfusion injury or oxidative stress-mediated injury [306].

Thus, we were interested in investigating whether increase in Plk2 expression could be a strategy to promote cell proliferation. For that purpose we studied not only its expression in neonatal versus adult cardiomyocytes (which already has been shown), but also its regulation

in various pro-proliferating or inhibitory conditions (low and high concentration of serum, oxidative stress in form of hypoxia).

Aim and hypothesis of the study

We hypothesized that Plk2 is necessary for cardiomyocyte proliferation and survival and therefore, may contribute to the regenerative capacity of the neonatal mouse heart. The following experiments were designed as a series of pilot studies with the aim to a) examine how Plk2 is regulated in the neonatal and adult heart and b) whether its expression is associated with a proliferative state of the cells.

Materials and Methods

Neonatal Rat Ventricular Myocyte (NRVM) isolation

The procedure of NRVM isolation was performed as described in the Materials and Methods section of the paper draft (page 65).

Cell culture conditions

According to the experimental purpose freshly isolated NRVMs were cultured under 21% or 1% (hypoxia) of oxygen availability in the 5% CO_2 humidified incubator at 37°C. The serum concentration of DMEM was 0% (serum free), 7% or 20% (high serum stimulation).

Western blot

Whole hearts from neonatal and adult rats were cut into small pieces and homogenized with a polytron PT-DA 07/2EC-E107 homogenizer (Kinematica, Switzerland). Whole heart homogenate or NRVM lysates were prepared with radioimmunoprecipitation assay (RIPA) buffer (Cell Signaling, #9803/9806) containing PhosSTOP (Roche, #04-906-845-001) and Complete Protease Inhibitor Cocktail (Roche, #11-697-498-001). Cell lysates were incubated on ice and then subjected to SDS-PAGE and transferred to polyvinylidene difluoride (PVDF) membranes. The membranes were probed with mouse anti-rat GAPDH (1:7000 Sigma, #G8795) and rabbit anti-rat Plk2 (1:2000 Sigma #SAB4500156). Western Lightning Plus-ECL Enhanced Chemiluminescence (Perkin Elmer, NEL105001EA) was used as substrate to develop the membrane in a colorimetric detection. Image SXM software (University of Liverpool, UK) was used to quantify protein expression.

Quantitative Reverse Transcription Polymerase Chain Reaction (PCR)

Total RNA was extracted from NRVMs or homogenized heart tissue using Trizol-Chloroform (Sigma). cDNA was generated using the High Capacity cDNA Reverse Transcription Kit (Applied Biosystems, #4368814) according to the manufacturer's instructions. The amplification was performed using Power SYBR Green PCR Master Mix and the respective primers (Microsynth) (table below), with an ABI PRISM 7500 sequence detection system (Applied Biosystems, #4367659). mRNA levels were calculated using the comparative CT method with 18S rRNA as reference gene.

Reverse Transcriptase PCR:

RT-buffer	2µl
dNTP	0.8µl
Random Primer	2µl
Reverse Transcriptase	1µl
RNasin	0.5µl
ddH_2O	3.7µl

+10µl (up to 2µg) RNA

Program:

10min	94°C
120min	94°C
5sec	4°C
∞	4°C

Real time PCR:

SYBR Green PCR Mix	10µl
Primer forward	0.75µl
Primer reverse	0.75µl
ddH_2O	3.5µl

10µl/tube

+5µl cDNA

Program:

20sec	95°C	
3sec	95°C	
30sec	60°C ← step 2	**40 cycles**
∞	4°C	

Gene	Forward primer 5`-3`	Reverse primer 5`-3
Plk2	CCGAGATCTCGCGGATTATAGT	CTGTCATTTCGTAACACTTTGCAA
18S rRNA	CCATTCGAACGTCTGCCCTAT	GTCACCCGTGGTCACCATG

Cell viability assay

The cell viability was measured based on the 3-(4,5-dimethylthiazol-2-yl)-2,5-diphenyltetrazolium bromide (MTT) assay according to the Cell Proliferation Kit I protocol from Roche (#11-465-007-001). NRVMs were seeded in a 96-well plate at a density of $4x10^4$ cells/well. The following day the medium was changed to serum free and the cells were incubated overnight. After incubation with 0%, 7% and 20% serum containing medium, every 24h (up to 72h) 10µl of the MTT labeling reagent (final concentration 0.5mg/ml) was added to each well and the plate was incubated for 4h at 37°C. Then 100µl of the Solubilization solution

was added into each well and the plate was incubated overnight at 37°C. The next day absorbance was measured using the Synergy H1 Hybrid Multi-Mode Reader (BioTek, Switzerland) at 570nm.

Flow cytometry

Freshly isolated NRVMs were cultured in p60 at a density of $2x10^6$ cells per dish. The following day the medium was changed to serum free and the cells were incubated overnight for cell cycle synchronization. The cells were then incubated in 0% and 7% serum containing medium for 36h. Hoechst in a concentration of 5µl/ml and Verapamil in a concentration of 2µl/ml were added to the plates for 30min, then the cells were trypsinized and washed with HBSS. 1µl 7AAD was added to the samples and incubated on ice for 10min. Flow cytometry for cell cycle evaluation was performed on BD LSRFortessa™ cell analyzer (BD Biosciences).

Data presentation and statistical analyses

Data are presented as mean±SD. Statistical analyses were performed with GraphPad Prism version 8 software (GraphPad). The Shapiro-Wilk normality test was applied to assess the values for Gaussian distribution. Parametric tests were used for normally distributed values and non-parametric tests for non-normally distributed values and data sets with $n<8$. To compare two groups unpaired t-test was used for parametric and Mann Whitney test for non-parametric data. Ordinary one-way ANOVA was used to compare multiple groups of normally distributed data and Kruskal-Wallis test followed by Dunn`s test to compare non-normally distributed data sets.

Results

Plk2 is highly expressed in neonatal but downregulated in adult mouse hearts

Based on the fact that Plk2 has been identified as cell cycle regulator [290] and neonatal hearts have been shown to maintain their regenerative capacity, while the mature hearts do not [267], we wanted to investigate the expression of Plk2 on both the transcriptional and translational level in neonatal and adult mouse hearts. Hearts were isolated from two-day and 12-week-old rats and homogenized in order to extract RNA and protein. Real time PCR showed that there is a 6.71-fold increase of Plk2 mRNA expression in neonatal hearts in comparison to adult hearts (**figure 16A**). Similarly, the results of western blot showed that protein expression of Plk2 is 6.097-fold higher in neonatal hearts (**figure 16B**). These data indicate that Plk2 expression is upregulated in neonatal hearts on both transcriptional and translational levels.

Figure 16

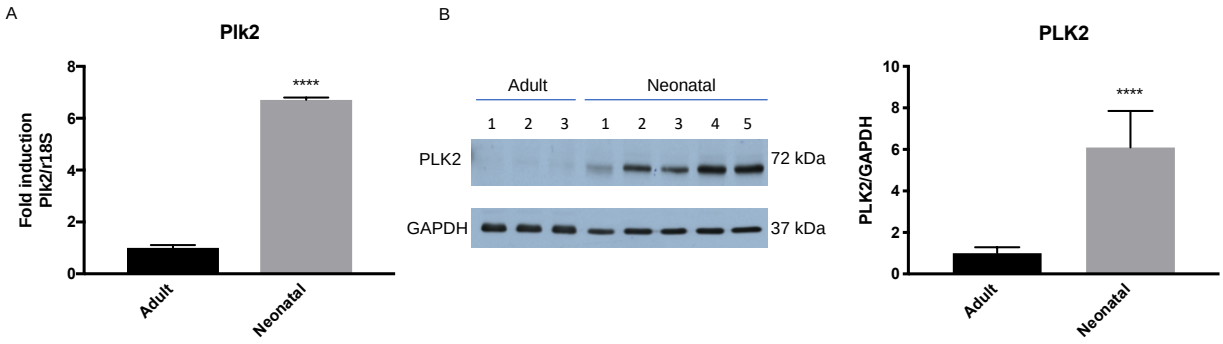

Figure 16. mRNA and protein expression of Plk2 in neonatal and adult rat heart homogenates. The hearts from neonatal and adult rats were homogenized and mRNA and protein were isolated according to the protocol. Plk2 is downregulated in the adult hearts both on transcriptional and translational levels. **(A)** Real time PCR: quantification, **(B)** Western blot: representative bands (GAPDH was used as reference protein) and quantification. Data are presented as mean ± SD; neonatal rats n=10; adult rats n=9; ****p<0.0001; two-tailed unpaired t-test.

Plk2 mRNA expression is hypoxia- and serum-regulated in vitro

Next, we wanted to test whether and how different culture conditions affect Plk2 expression. We chose different concentrations of serum, with 7% being ideal for NRVM growth and culturing, and oxygen availability in order to simulate conditions that could modify the proliferation behavior of neonatal cardiomyocytes. In addition, serum deprivation and hypoxia were used to simulate the environment of an infarcted heart (ischemia). We observed an immediate response (within 2 hours) to low oxygen availability with significant downregulation of Plk2 mRNA under hypoxia (**figure 17A**). Plk2 mRNA was also significantly downregulated after two days in serum free medium (**figure 17C**). Conversely, after incubation of the cells with 20% of serum, Plk2 mRNA expression was rapidly upregulated with a 12.76-fold increase after one hour (**figure 17E**). Interestingly, despite the clear regulation on the gene expression level, we did not see significant differences in Plk2 protein expression under the same conditions (**figure 17B, D, F** respectively). These data show that Plk2 is downregulated under hypoxic conditions and after serum deprivation on the transcriptional level and rapidly increased after serum stimulation.

Figure 17

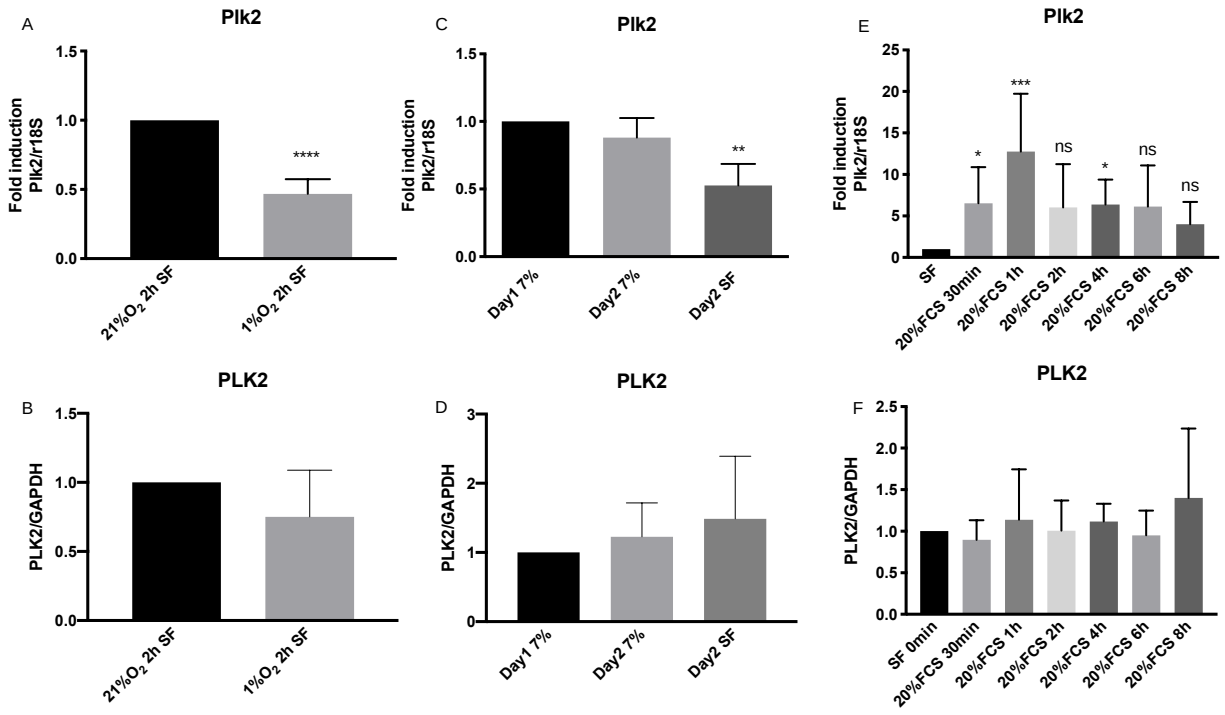

Figure 17. mRNA and protein expression of Plk2 under different conditions of oxygen and serum availability over time. The freshly isolated NRVMs were cultured under hypoxic condition (1% oxygen), 0% (serum free), 7% and 20% serum for different times as indicated. Plk2 mRNA expression is downregulated under low oxygen and serum deprivation, while its expression is upregulated under high serum conditions. There is no difference in PLK2 protein expression. **(A)**, **(C), (E)** Real time PCR: quantification of Plk2 mRNA expression under hypoxia for 2 hours; n= 4; Mann-Whitney test, in serum free medium for 2 days; n= 3; Kruskal-Wallis test, and in high serum medium over time; n=6; Kruskal-Wallis test. **(B), (D), (F)** Western blot: quantification of PLK2 protein expression under the same conditions; (B), (D) n= 3, (F) n=4. Data are presented as mean±SD, fold induction; ****p<0.0001, ***p<0.001, **p<0.01.

Mitochondrial activity is enhanced in NRVMs exposed to high serum

Metabolic activity is an indication of cell viability and proliferation and can be measured by the MTT assay. We evaluated mitochondrial activity in NRVMs under different serum concentrations. Freshly isolated NRVMs were cultured in 96-well plates in serum free, 7% and 20% serum containing medium. After 24h, 48h and 72h we performed the MTT assay. Absorbance significantly increased with higher serum concentrations, suggesting enhanced viability and/or increased proliferation of NRVMs (**figure 18**).

Figure 18

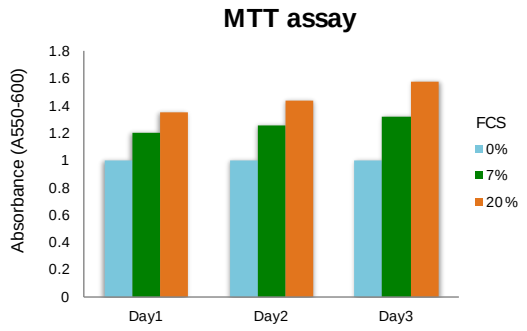

Figure 18. Mitochondrial activity of NRVMs up to 72 hours in different concentrations of serum. NRVMs were isolated and cultured in 0%, 7% and 20% serum. MTT assay was performed after 24h, 48h and 72h and absorbance was measured. Mitochondrial activity is enhanced when NRVMs are cultured in high concentrations of serum. The data is normalized to the 0% serum condition for each day; n=1 of 6 replicates per each condition and time point.

The G1/S-phase transition is limited in the absence of serum

We saw that NRVMs are metabolically active in the presence of high serum concentrations. We therefore assessed how serum affects the cell cycle phases in order to test whether it has the potential to trigger proliferation. After incubation in 0% and 7% serum containing medium, cells were stained with Hoechst and the cell cycle was evaluated by flow cytometry. We observed that in serum-deprived medium the cells are mostly arrested in the G0/G1 phase with little progression to S-phase. Upon serum exposure, a small fraction of NRVMs can transition to S phase of the cell cycle, when DNA synthesis takes place (**figure 19**). This experiment suggests that serum induces cell cycle progression in a subset of NRVMs, providing them the potential ability to proliferate.

Figure 19

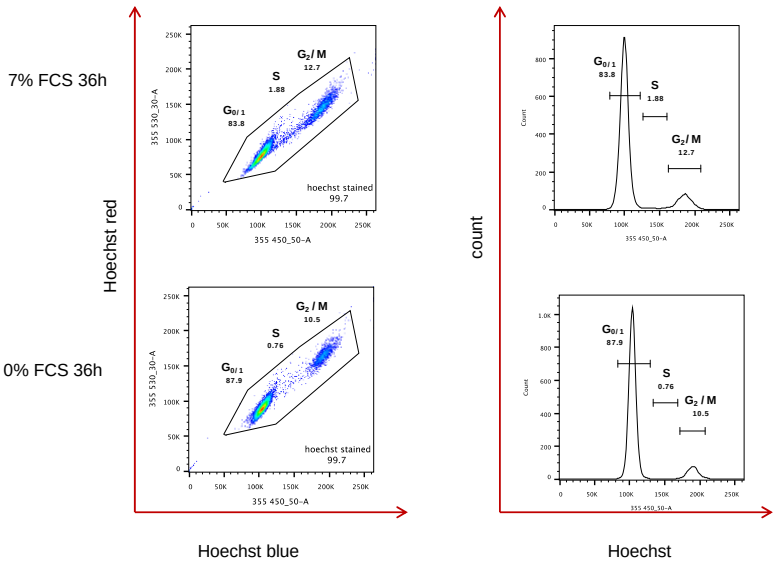

Figure 19. Cell cycle phases in the presence and absence of serum. Freshly isolated NRVMs were cultured in medium with 7% and 0% serum for 36h. Staining with Hoechst 33342 was performed and the cells were analyzed with flow cytometry. G1/S phase transition is limited in serum deprived medium. Representative flow cytometry images and histogram of G0/1, S and G2/M phases of cell cycle.

Discussion

In this set of preliminary experiments, we found that Plk2 expression is downregulated during postnatal development, when cardiomyocyte maturation and cell cycle withdrawal occur. In neonatal cardiomyocytes *in vitro*, Plk2 expression is regulated by the availability of oxygen and serum and it is upregulated under conditions favoring cardiomyocyte viability and cell cycle activity. Finally, we saw that neonatal cardiomyocytes are metabolically active and maintain the ability to proliferate under physiological and high serum conditions.

For many years the heart was considered a post-mitotic organ without the ability to regenerate after an injury. However, such belief started dissipating when studies showed that adult human cardiomyocytes can be regenerated at a low rate. This low rate is however not sufficient to compensate for the lost tissue after a myocardial infarction [261, 262]. Therefore, understanding the cellular and molecular mechanisms that can facilitate cardiomyocyte proliferation throughout life, deciphering the reasons why proliferative capacity is not robust in adult mammals and identifying means that can enhance this limited capacity are major goals in the field of cardiovascular biology.

Plk2 has been identified as a coordinator of cell proliferation and early lineage commitment of cardiac progenitor cells. It is regulated downstream of YAP [290], which is a member of the Hippo pathway and has been described to have an important role in heart development [307]. The Plk2 expression observed in the mouse hearts in our experiments shows similarity with the YAP expression described by others, which demonstrated robust expression in neonatal and juvenile mouse heart and decline to nearly undetectable levels by 12 weeks of age [284], [286]. Moreover, Yap gain-of-function stimulates proliferation of cultured cardiomyocytes *in*

vitro and of postnatal cardiomyocytes *in vivo* [286]. As a downstream substrate of YAP, Plk2 might also be involved in cardiomyocyte proliferation, consequently similar experiments for gain-of-function could be useful in order to reveal Plk2 function in cardiomyocytes.

We found that Plk2 expression was regulated by serum. Indeed, the Plk2 gene was initially identified in the early-1990s as a serum-inducible immediate-early response gene in NIH 3T3 cells [291]. Interestingly, we saw that Plk2 was affected early and only on the transcriptional level. Similar observations have already been made in quiescent murine NIH 3T3 fibroblasts [291], mouse fetal fibroblasts [308], porcine fetal fibroblasts [308] and human lung fibroblasts [309], where Plk2 mRNA levels were transiently increased after serum stimulation with the peak expression at 0.5–1h. None of the above studies attempted to identify the protein expression of Plk (in case of mouse and porcine fetal fibroblasts [308], antibody suitable for Plk1 was available, but it had no reactivity for PLK2). In our experiments we did not detect changes in PLK2 protein expression. A possible explanation could be a decreased translation or degradation of the protein. Moreover, the method of detection might be not sensitive enough in case of only low amount of the PLK2 protein.

Serum contains numerous polypeptide growth factors, such as platelet-derived growth factor (PDGF) and fibroblast growth factor 2 (FGF2), which generally act by binding to specific cell surface receptors and leading to cell cycle progression and DNA replication [310]. FGF2 was one of the first growth factors shown to promote neonatal cardiomyocyte DNA synthesis through protein kinase C activation [311]. PDGF has also been reported to induce proliferation in neonatal cardiomyocyte cultures through downregulation of the cell cycle G1 phase inhibitor p27, activation of AKT and inhibition of GSK-3b activity [312]. Therefore, it would be

interesting to identify, which pathways mediate the Plk2 gene expression after serum stimulation and how they regulate the cardiomyocyte proliferation.

We observed that serum can help the cardiomyocytes to transition to S phase, where they have the chance to induce DNA replication. It is known that centriole duplication is initiated at the G1/S boundary and is completed in S phase of the cell cycle, which coincides with DNA replication [313]. Moreover, Plk2 is activated near the G1/S phase transition and regulates the reproduction of centrosomes [314]. Therefore, we can suggest that Plk2 might be triggered by growth factors in the serum and participates in the DNA proliferation. However, the substrates of Plk2 in the process of centriole duplication are still unknown. Experiments investigating any potential connection of Plk2 with different cell cycle regulators (for example, through loss- or gain-of-function) will be needed to shed more light on whether Plk2 can directly promote cardiomyocyte proliferation. It has been shown that overexpression of cell cycle regulators, such as cyclin-dependent kinase 1 (CDK1), cyclin B1 (CCNB), cyclin dependent kinase 4 (CDK4) and cyclin D (CCND), promote cell cycle re-entry and induce stable cardiomyocyte proliferation in post-mitotic rat, mouse and human cardiomyocytes [315]. Moreover, expression of Cyclin A has been shown to modestly induce cardiomyocyte proliferation *in vitro* and limited cardiomyocyte proliferation *in vivo* [271]. Thus, it would be interesting to explore whether Plk2 has any regulatory connection with such cell cycle molecules, as it has been shown that YAP regulates the expression of cell cycle genes in cardiomyocytes [286].

Finally, Plk2 has been shown to have properties of a tumor suppressor and to be poorly expressed in tumor tissues, such as human hepatocellular carcinoma [316]. It has been shown to be a direct target of p53 on the transcriptional level [302]. Plk2 expression induces apoptosis in Burkitt`s lymphoma cells [317]. Its transcriptional silencing is also found in epithelial

ovarian cancer [318]. However, a recent study showed that Plk2 mRNA and protein expression are high in aggressive colorectal cancer promoting tumor growth and inhibiting apoptosis of cancer cells *in vitro* and *in vivo*, thus suggesting a potential pro-tumor role for Plk2 [319]. Taken together, the contribution of Plk2 in cancer development seems to be controversial and still not well investigated.

In view of future therapeutics, when targeting Plk2, it will be important to more thoroughly investigate its role and function in the tumor. Only then will we be able to anticipate the effects that activation or inhibition of Plk2 might leave in the heart. In particular, if Plk2 is tumor promoting, its inhibition through pharmacological means could further hamper cardiac regeneration, whereas if Plk2 has anti-tumor capacity, its expression should be enhanced in the tumor, which could also help the heart.

To conclude, this set of preliminary experiments showed that Plk2 is highly expressed in neonatal cardiomyocytes, that still maintain the ability to proliferate, as was confirmed with the mitochondrial activity assay performed in neonatal rat cardiomyocytes. Plk2 is regulated by serum and by the availability of oxygen and such factors are essential for cell proliferation. Therefore, we suggest that Plk2 might participate in the regulation of cell cycle of neonatal cardiac myocytes and may play a role in the homeostasis of the neonatal heart. However, further experiments are required to confirm this hypothesis. If Plk2 proves necessary for cardiomyocyte proliferation, its activation in postnatal cardiomyocytes may be a useful strategy to stimulate cardiomyocyte expansion in the context of therapeutic myocardial regeneration after MI. Overall, understanding the molecular mechanisms of cardiac myocyte proliferation during development and the reasons for the inability of these cells to replicate in adult mammals

is important in order to develop innovative approaches that might support dysfunctional or damaged myocardium and promote the formation of new contractile tissue.

Overall conclusions and future perspectives

Targeted cancer therapeutics improved survival and quality of life of cancer patients, however they can lead to numerous cardiovascular toxicities. These toxicities may interfere with the efficacy of the treatment and negatively affect patient survival. Due to the limited number of studies that elucidate the mechanisms of cardiotoxicity related to novel targeted therapies, early detection and prevention still remain challenging. However, with the advancement of the cardio-oncology field, chances to recognize and manage cardiovascular toxicities without compromising cancer treatment outcome are increasing. Oncologists and cardiologists, as well as patients, need to be aware of the potential adverse effects of cancer therapeutics and prepare a plan for baseline assessment and monitoring of symptoms. In addition, multidisciplinary management from basic science over phase I trials of cardiovascular safety to phase III clinical trials is necessary. The implementation of comprehensive cardiovascular care guidelines along with the monitoring of cancer treatment from diagnosis to survivorship is crucial in order to improve patient outcome. Moreover, inclusion of cardiovascular phenotypes in oncology clinical trials is of paramount importance. Finally, identification of patients at high risk who may benefit from prevention strategies remains a challenge that will be answered through further studies and collaborative cardio-oncology trials.

References

1. Wickramasinghe, C.D., et al., *Concepts in cardio-oncology: definitions, mechanisms, diagnosis and treatment strategies of cancer therapy-induced cardiotoxicity.* Future Oncol, 2016. **12**(6): p. 855-70.
2. Ainger, L.E., et al., *Daunomycin: a cardiotoxic agent.* J Natl Med Assoc, 1971. **63**(4): p. 261-7.
3. Lefrak, E.A., et al., *A clinicopathologic analysis of adriamycin cardiotoxicity.* Cancer, 1973. **32**(2): p. 302-14.
4. Miller, K.D., et al., *Cancer treatment and survivorship statistics, 2019.* CA Cancer J Clin, 2019. **69**(5): p. 363-385.
5. Armstrong, G.T., et al., *Aging and Risk of Severe, Disabling, Life-Threatening, and Fatal Events in the Childhood Cancer Survivor Study.* Journal of Clinical Oncology, 2014. **32**(12): p. 1218-+.
6. Mertens, A.C., et al., *Cause-specific late mortality among 5-year survivors of childhood cancer: the Childhood Cancer Survivor Study.* J Natl Cancer Inst, 2008. **100**(19): p. 1368-79.
7. Schmitz, K.H., et al., *Prospective surveillance and management of cardiac toxicity and health in breast cancer survivors.* Cancer, 2012. **118**(8 Suppl): p. 2270-6.
8. Negishi, T., S. Miyazaki, and K. Negishi, *Echocardiography and Cardio-Oncology.* Heart Lung Circ, 2019. **28**(9): p. 1331-1338.
9. Sulpher, J., et al., *An International Survey of Health Care Providers Involved in the Management of Cancer Patients Exposed to Cardiotoxic Therapy.* J Oncol, 2015. **2015**: p. 391848.
10. Daher, I.N., et al., *The prevention of cardiovascular disease in cancer survivors.* Tex Heart Inst J, 2012. **39**(2): p. 190-8.
11. Albini, A., et al., *Cardiotoxicity of anticancer drugs: the need for cardio-oncology and cardio-oncological prevention.* J Natl Cancer Inst, 2010. **102**(1): p. 14-25.
12. McGowan, J.V., et al., *Anthracycline Chemotherapy and Cardiotoxicity.* Cardiovasc Drugs Ther, 2017. **31**(1): p. 63-75.
13. Billingham, M.E., et al., *Anthracycline cardiomyopathy monitored by morphologic changes.* Cancer Treat Rep, 1978. **62**(6): p. 865-72.
14. Thavendiranathan, P., et al., *Reproducibility of echocardiographic techniques for sequential assessment of left ventricular ejection fraction and volumes: application to patients undergoing cancer chemotherapy.* J Am Coll Cardiol, 2013. **61**(1): p. 77-84.
15. Plana, J.C., et al., *Expert consensus for multimodality imaging evaluation of adult patients during and after cancer therapy: a report from the American Society of Echocardiography and the European Association of Cardiovascular Imaging.* J Am Soc Echocardiogr, 2014. **27**(9): p. 911-39.
16. Kendal, W.S., *Dying with cancer: the influence of age, comorbidity, and cancer site.* Cancer, 2008. **112**(6): p. 1354-62.
17. Cardinale, D., et al., *Early detection of anthracycline cardiotoxicity and improvement with heart failure therapy.* Circulation, 2015. **131**(22): p. 1981-8.
18. Cardinale, D., et al., *Prevention of high-dose chemotherapy-induced cardiotoxicity in high-risk patients by angiotensin-converting enzyme inhibition.* Circulation, 2006. **114**(23): p. 2474-81.

19. Abdel-Qadir, H., E. Amir, and P. Thavendiranathan, *Prevention, Detection, and Management of Chemotherapy-Related Cardiac Dysfunction.* Can J Cardiol, 2016. **32**(7): p. 891-9.
20. Thavendiranathan, P., et al., *Use of myocardial strain imaging by echocardiography for the early detection of cardiotoxicity in patients during and after cancer chemotherapy: a systematic review.* J Am Coll Cardiol, 2014. **63**(25 Pt A): p. 2751-68.
21. Curigliano, G., et al., *Cardiotoxicity of anticancer treatments: Epidemiology, detection, and management.* CA Cancer J Clin, 2016. **66**(4): p. 309-25.
22. Cardinale, D., et al., *Prognostic value of troponin I in cardiac risk stratification of cancer patients undergoing high-dose chemotherapy.* Circulation, 2004. **109**(22): p. 2749-54.
23. Blume-Jensen, P. and T. Hunter, *Oncogenic kinase signalling.* Nature, 2001. **411**(6835): p. 355-65.
24. Ullrich, A. and J. Schlessinger, *Signal transduction by receptors with tyrosine kinase activity.* Cell, 1990. **61**(2): p. 203-12.
25. Manning, G., et al., *The protein kinase complement of the human genome.* Science, 2002. **298**(5600): p. 1912-34.
26. Lemmon, M.A. and J. Schlessinger, *Cell signaling by receptor tyrosine kinases.* Cell, 2010. **141**(7): p. 1117-34.
27. Zinkle, A. and M. Mohammadi, *A threshold model for receptor tyrosine kinase signaling specificity and cell fate determination.* F1000Res, 2018. **7**.
28. Small, D., et al., *STK-1, the human homolog of Flk-2/Flt-3, is selectively expressed in CD34+ human bone marrow cells and is involved in the proliferation of early progenitor/stem cells.* Proc Natl Acad Sci U S A, 1994. **91**(2): p. 459-63.
29. Stirewalt, D.L. and J.P. Radich, *The role of FLT3 in haematopoietic malignancies.* Nat Rev Cancer, 2003. **3**(9): p. 650-65.
30. Rosnet, O., et al., *Isolation and chromosomal localization of a novel FMS-like tyrosine kinase gene.* Genomics, 1991. **9**(2): p. 380-5.
31. Rosnet, O. and D. Birnbaum, *Hematopoietic receptors of class III receptor-type tyrosine kinases.* Crit Rev Oncog, 1993. **4**(6): p. 595-613.
32. Agnes, F., et al., *Genomic structure of the downstream part of the human FLT3 gene: exon/intron structure conservation among genes encoding receptor tyrosine kinases (RTK) of subclass III.* Gene, 1994. **145**(2): p. 283-8.
33. Chen, Y., et al., *Tyrosine kinase inhibitors targeting FLT3 in the treatment of acute myeloid leukemia.* Stem Cell Investig, 2017. **4**: p. 48.
34. Matthews, W., et al., *A receptor tyrosine kinase specific to hematopoietic stem and progenitor cell-enriched populations.* Cell, 1991. **65**(7): p. 1143-52.
35. Rosnet, O., et al., *Murine Flt3, a gene encoding a novel tyrosine kinase receptor of the PDGFR/CSF1R family.* Oncogene, 1991. **6**(9): p. 1641-50.
36. Rosnet, O., et al., *Human FLT3/FLK2 gene: cDNA cloning and expression in hematopoietic cells.* Blood, 1993. **82**(4): p. 1110-9.
37. deLapeyriere, O., et al., *Expression of Flt3 tyrosine kinase receptor gene in mouse hematopoietic and nervous tissues.* Differentiation, 1995. **58**(5): p. 351-9.
38. Maroc, N., et al., *Biochemical characterization and analysis of the transforming potential of the FLT3/FLK2 receptor tyrosine kinase.* Oncogene, 1993. **8**(4): p. 909-18.
39. Lyman, S.D. and S.E. Jacobsen, *c-kit ligand and Flt3 ligand: stem/progenitor cell factors with overlapping yet distinct activities.* Blood, 1998. **91**(4): p. 1101-34.

40. McClanahan, T., et al., *Biochemical and genetic characterization of multiple splice variants of the Flt3 ligand.* Blood, 1996. **88**(9): p. 3371-82.
41. Turner, A.M., et al., *FLT3 receptor expression on the surface of normal and malignant human hematopoietic cells.* Blood, 1996. **88**(9): p. 3383-90.
42. Brasel, K., et al., *Expression of the flt3 receptor and its ligand on hematopoietic cells.* Leukemia, 1995. **9**(7): p. 1212-8.
43. Testa, U., et al., *Expression of growth factor receptors in unilineage differentiation culture of purified hematopoietic progenitors.* Blood, 1996. **88**(9): p. 3391-406.
44. Rappold, I., et al., *Functional and phenotypic characterization of cord blood and bone marrow subsets expressing FLT3 (CD135) receptor tyrosine kinase.* Blood, 1997. **90**(1): p. 111-25.
45. Gotze, K.S., et al., *Flt3high and Flt3low CD34+ progenitor cells isolated from human bone marrow are functionally distinct.* Blood, 1998. **91**(6): p. 1947-58.
46. Liu, K., et al., *In vivo analysis of dendritic cell development and homeostasis.* Science, 2009. **324**(5925): p. 392-7.
47. Waskow, C., et al., *The receptor tyrosine kinase Flt3 is required for dendritic cell development in peripheral lymphoid tissues.* Nat Immunol, 2008. **9**(6): p. 676-83.
48. Eidenschenk, C., et al., *Flt3 permits survival during infection by rendering dendritic cells competent to activate NK cells.* Proc Natl Acad Sci U S A, 2010. **107**(21): p. 9759-64.
49. Dong, J., C.M. McPherson, and P.J. Stambrook, *Flt-3 ligand: a potent dendritic cell stimulator and novel antitumor agent.* Cancer Biol Ther, 2002. **1**(5): p. 486-9.
50. Wu, L. and Y.J. Liu, *Development of dendritic-cell lineages.* Immunity, 2007. **26**(6): p. 741-50.
51. Mackarehtschian, K., et al., *Targeted disruption of the flk2/flt3 gene leads to deficiencies in primitive hematopoietic progenitors.* Immunity, 1995. **3**(1): p. 147-61.
52. Grafone, T., et al., *An overview on the role of FLT3-tyrosine kinase receptor in acute myeloid leukemia: biology and treatment.* Oncol Rev, 2012. **6**(1): p. e8.
53. Gilliland, D.G. and J.D. Griffin, *The roles of FLT3 in hematopoiesis and leukemia.* Blood, 2002. **100**(5): p. 1532-42.
54. Annesley, C.E. and P. Brown, *The Biology and Targeting of FLT3 in Pediatric Leukemia.* Front Oncol, 2014. **4**: p. 263.
55. Tsapogas, P., et al., *The Cytokine Flt3-Ligand in Normal and Malignant Hematopoiesis.* Int J Mol Sci, 2017. **18**(6).
56. Rosnet, O., et al., *Human FLT3/FLK2 receptor tyrosine kinase is expressed at the surface of normal and malignant hematopoietic cells.* Leukemia, 1996. **10**(2): p. 238-48.
57. Carow, C.E., et al., *Expression of the hematopoietic growth factor receptor FLT3 (STK-1/Flk2) in human leukemias.* Blood, 1996. **87**(3): p. 1089-96.
58. DaSilva, N., et al., *Expression of the FLT3 gene in human leukemia-lymphoma cell lines.* Leukemia, 1994. **8**(5): p. 885-8.
59. Meierhoff, G., et al., *Expression of FLT3 receptor and FLT3-ligand in human leukemia-lymphoma cell lines.* Leukemia, 1995. **9**(8): p. 1368-72.
60. Nakao, M., et al., *Internal tandem duplication of the flt3 gene found in acute myeloid leukemia.* Leukemia, 1996. **10**(12): p. 1911-8.

61. Breitenbuecher, F., et al., *Identification of a novel type of ITD mutations located in nonjuxtamembrane domains of the FLT3 tyrosine kinase receptor.* Blood, 2009. **113**(17): p. 4074-7.
62. Mizuki, M., et al., *Flt3 mutations from patients with acute myeloid leukemia induce transformation of 32D cells mediated by the Ras and STAT5 pathways.* Blood, 2000. **96**(12): p. 3907-14.
63. Hayakawa, F., et al., *Tandem-duplicated Flt3 constitutively activates STAT5 and MAP kinase and introduces autonomous cell growth in IL-3-dependent cell lines.* Oncogene, 2000. **19**(5): p. 624-31.
64. Calo, V., et al., *STAT proteins: from normal control of cellular events to tumorigenesis.* J Cell Physiol, 2003. **197**(2): p. 157-68.
65. Takahashi, S., et al., *Flt3 mutation activates p21WAF1/CIP1 gene expression through the action of STAT5.* Biochem Biophys Res Commun, 2004. **316**(1): p. 85-92.
66. Sallmyr, A., et al., *Internal tandem duplication of FLT3 (FLT3/ITD) induces increased ROS production, DNA damage, and misrepair: implications for poor prognosis in AML.* Blood, 2008. **111**(6): p. 3173-82.
67. Scheijen, B., et al., *FLT3 receptors with internal tandem duplications promote cell viability and proliferation by signaling through Foxo proteins.* Oncogene, 2004. **23**(19): p. 3338-49.
68. Meshinchi, S., et al., *Prevalence and prognostic significance of Flt3 internal tandem duplication in pediatric acute myeloid leukemia.* Blood, 2001. **97**(1): p. 89-94.
69. Abu-Duhier, F.M., et al., *Identification of novel FLT-3 Asp835 mutations in adult acute myeloid leukaemia.* Br J Haematol, 2001. **113**(4): p. 983-8.
70. Yamamoto, Y., et al., *Activating mutation of D835 within the activation loop of FLT3 in human hematologic malignancies.* Blood, 2001. **97**(8): p. 2434-9.
71. Griffith, J., et al., *The structural basis for autoinhibition of FLT3 by the juxtamembrane domain.* Mol Cell, 2004. **13**(2): p. 169-78.
72. Choudhary, C., et al., *AML-associated Flt3 kinase domain mutations show signal transduction differences compared with Flt3 ITD mutations.* Blood, 2005. **106**(1): p. 265-73.
73. Lacayo, N.J., et al., *Gene expression profiles at diagnosis in de novo childhood AML patients identify FLT3 mutations with good clinical outcomes.* Blood, 2004. **104**(9): p. 2646-54.
74. Grundler, R., et al., *FLT3-ITD and tyrosine kinase domain mutants induce 2 distinct phenotypes in a murine bone marrow transplantation model.* Blood, 2005. **105**(12): p. 4792-9.
75. Muller, T.A., et al., *Lineage-specific STAT5 target gene activation in hematopoietic progenitor cells predicts the FLT3(+)-mediated leukemic phenotype.* Leukemia, 2016. **30**(8): p. 1725-33.
76. Bailey, E., et al., *FLT3/D835Y mutation knock-in mice display less aggressive disease compared with FLT3/internal tandem duplication (ITD) mice.* Proc Natl Acad Sci U S A, 2013. **110**(52): p. 21113-8.
77. Ayach, B.B., et al., *Stem cell factor receptor induces progenitor and natural killer cell-mediated cardiac survival and repair after myocardial infarction.* Proc Natl Acad Sci U S A, 2006. **103**(7): p. 2304-9.
78. Tian, G., et al., *Protective effect of Flt3L on organ structure during advanced multiorgan dysfunction syndrome in mice.* Mol Med Rep, 2015. **11**(6): p. 4135-41.

79. Pfister, O., et al., *FLT3 activation improves post-myocardial infarction remodeling involving a cytoprotective effect on cardiomyocytes.* J Am Coll Cardiol, 2014. **63**(10): p. 1011-9.
80. Lisovsky, M., et al., *Flt3 ligand stimulates proliferation and inhibits apoptosis of acute myeloid leukemia cells: regulation of Bcl-2 and Bax.* Blood, 1996. **88**(10): p. 3987-97.
81. Rowe, J.M. and M.S. Tallman, *How I treat acute myeloid leukemia.* Blood, 2010. **116**(17): p. 3147-56.
82. Sexauer, A.N. and S.K. Tasian, *Targeting FLT3 Signaling in Childhood Acute Myeloid Leukemia.* Front Pediatr, 2017. **5**: p. 248.
83. Weisberg, E., et al., *Inhibition of mutant FLT3 receptors in leukemia cells by the small molecule tyrosine kinase inhibitor PKC412.* Cancer Cell, 2002. **1**(5): p. 433-43.
84. Kiyoi, H., et al., *Internal tandem duplication of the FLT3 gene is a novel modality of elongation mutation which causes constitutive activation of the product.* Leukemia, 1998. **12**(9): p. 1333-7.
85. Li, Y., Z.H. Gao, and X.J. Qu, *The adverse effects of sorafenib in patients with advanced cancers.* Basic Clin Pharmacol Toxicol, 2015. **116**(3): p. 216-21.
86. Force, T., D.S. Krause, and R.A. Van Etten, *Molecular mechanisms of cardiotoxicity of tyrosine kinase inhibition.* Nat Rev Cancer, 2007. **7**(5): p. 332-44.
87. Schwandt, A., et al., *Management of side effects associated with sunitinib therapy for patients with renal cell carcinoma.* Onco Targets Ther, 2009. **2**: p. 51-61.
88. Gallogly, M.M. and H.M. Lazarus, *Midostaurin: an emerging treatment for acute myeloid leukemia patients.* J Blood Med, 2016. **7**: p. 73-83.
89. Hexner, E.O., et al., *Phase I dose escalation study of lestaurtinib in patients with myelofibrosis.* Leuk Lymphoma, 2015. **56**(9): p. 2543-51.
90. Levis, M., et al., *Results from a randomized trial of salvage chemotherapy followed by lestaurtinib for patients with FLT3 mutant AML in first relapse.* Blood, 2011. **117**(12): p. 3294-301.
91. Odia, Y., et al., *A Phase II trial of tandutinib (MLN 518) in combination with bevacizumab for patients with recurrent glioblastoma.* CNS Oncol, 2016. **5**(2): p. 59-67.
92. Weis, T.M., et al., *Clinical considerations for the use of FLT3 inhibitors in acute myeloid leukemia.* Critical Reviews in Oncology Hematology, 2019. **141**: p. 125-138.
93. Usuki, K., et al., *Clinical profile of gilteritinib in Japanese patients with relapsed/refractory acute myeloid leukemia: An open-label phase 1 study.* Cancer Sci, 2018. **109**(10): p. 3235-3244.
94. Matulonis, U.A., et al., *A randomized phase II study of cabozantinib versus weekly paclitaxel in the treatment of persistent or recurrent epithelial ovarian, fallopian tube or primary peritoneal cancer: An NRG Oncology/Gynecologic Oncology Group study.* Gynecol Oncol, 2019. **152**(3): p. 548-553.
95. Wu, M., C.T. Li, and X.P. Zhu, *FLT3 inhibitors in acute myeloid leukemia.* Journal of Hematology & Oncology, 2018. **11**.
96. Liu, T., et al., *Sorafenib Dose Recommendation in Acute Myeloid Leukemia Based on Exposure-FLT3 Relationship.* Clin Transl Sci, 2018. **11**(4): p. 435-443.
97. Mathew, N.R., et al., *Sorafenib promotes graft-versus-leukemia activity in mice and humans through IL-15 production in FLT3-ITD-mutant leukemia cells.* Nat Med, 2018. **24**(3): p. 282-291.

98. Lange, A., et al., *The sorafenib anti-relapse effect after alloHSCT is associated with heightened alloreactivity and accumulation of CD8+PD-1+ (CD279+) lymphocytes in marrow.* PLoS One, 2018. **13**(1): p. e0190525.
99. Feldmann, F., et al., *Sorafenib inhibits therapeutic induction of necroptosis in acute leukemia cells.* Oncotarget, 2017. **8**(40): p. 68208-68220.
100. Zhao, W., et al., *Sorafenib induces apoptosis in HL60 cells by inhibiting Src kinase-mediated STAT3 phosphorylation.* Anticancer Drugs, 2011. **22**(1): p. 79-88.
101. Muppidi, M.R., et al., *Decitabine and Sorafenib Therapy in FLT-3 ITD-Mutant Acute Myeloid Leukemia.* Clin Lymphoma Myeloma Leuk, 2015. **15 Suppl**: p. S73-9.
102. Mahdi, A.J., et al., *Successful molecular targeted treatment of AML in pregnancy with Azacitidine and Sorafenib with no adverse fetal outcomes.* Br J Haematol, 2018. **180**(4): p. 603-604.
103. Uy, G.L., et al., *A phase 2 study incorporating sorafenib into the chemotherapy for older adults with FLT3-mutated acute myeloid leukemia: CALGB 11001.* Blood Adv, 2017. **1**(5): p. 331-340.
104. Tschan-Plessl, A., et al., *Synergistic effect of sorafenib and cGvHD in patients with high-risk FLT3-ITD+AML allows long-term disease control after allogeneic transplantation.* Ann Hematol, 2015. **94**(11): p. 1899-905.
105. Battipaglia, G., et al., *Efficacy and feasibility of sorafenib as a maintenance agent after allogeneic hematopoietic stem cell transplantation for Fms-like tyrosine kinase 3-mutated acute myeloid leukemia.* Cancer, 2017. **123**(15): p. 2867-2874.
106. Metzelder, S.K., et al., *Long-term survival of sorafenib-treated FLT3-ITD-positive acute myeloid leukaemia patients relapsing after allogeneic stem cell transplantation.* Eur J Cancer, 2017. **86**: p. 233-239.
107. O'Farrell, A.M., et al., *SU11248 is a novel FLT3 tyrosine kinase inhibitor with potent activity in vitro and in vivo.* Blood, 2003. **101**(9): p. 3597-605.
108. O'Farrell, A.M., et al., *An innovative phase I clinical study demonstrates inhibition of FLT3 phosphorylation by SU11248 in acute myeloid leukemia patients.* Clin Cancer Res, 2003. **9**(15): p. 5465-76.
109. Yee, K.W., et al., *Synergistic effect of SU11248 with cytarabine or daunorubicin on FLT3 ITD-positive leukemic cells.* Blood, 2004. **104**(13): p. 4202-9.
110. Teng, C.L., et al., *Effector mechanisms of sunitinib-induced G1 cell cycle arrest, differentiation, and apoptosis in human acute myeloid leukaemia HL60 and KG-1 cells.* Ann Hematol, 2013. **92**(3): p. 301-13.
111. Fiedler, W., et al., *A phase I/II study of sunitinib and intensive chemotherapy in patients over 60 years of age with acute myeloid leukaemia and activating FLT3 mutations.* Br J Haematol, 2015. **169**(5): p. 694-700.
112. Fiedler, W., et al., *A phase 1 study of SU11248 in the treatment of patients with refractory or resistant acute myeloid leukemia (AML) or not amenable to conventional therapy for the disease.* Blood, 2005. **105**(3): p. 986-93.
113. Tamaoki, T., et al., *Staurosporine, a potent inhibitor of phospholipid/Ca++dependent protein kinase.* Biochem Biophys Res Commun, 1986. **135**(2): p. 397-402.
114. Propper, D.J., et al., *Phase I and pharmacokinetic study of PKC412, an inhibitor of protein kinase C.* J Clin Oncol, 2001. **19**(5): p. 1485-92.
115. Fabbro, D., et al., *Inhibitors of protein kinases: CGP 41251, a protein kinase inhibitor with potential as an anticancer agent.* Pharmacol Ther, 1999. **82**(2-3): p. 293-301.

116. Walker, A.R., et al., *Midostaurin, bortezomib and MEC in relapsed/refractory acute myeloid leukemia.* Leuk Lymphoma, 2016. **57**(9): p. 2100-8.
117. Ramsingh, G., et al., *Phase I study of cladribine, cytarabine, granulocyte colony stimulating factor (CLAG regimen) and midostaurin and all-trans retinoic acid in relapsed/refractory AML.* Int J Hematol, 2014. **99**(3): p. 272-8.
118. Stone, R.M., et al., *Phase IB study of the FLT3 kinase inhibitor midostaurin with chemotherapy in younger newly diagnosed adult patients with acute myeloid leukemia.* Leukemia, 2012. **26**(9): p. 2061-8.
119. Stone, R.M., et al., *Midostaurin plus Chemotherapy for Acute Myeloid Leukemia with a FLT3 Mutation.* N Engl J Med, 2017. **377**(5): p. 454-464.
120. Mori, M., et al., *Gilteritinib, a FLT3/AXL inhibitor, shows antileukemic activity in mouse models of FLT3 mutated acute myeloid leukemia.* Invest New Drugs, 2017. **35**(5): p. 556-565.
121. Cucchi, D.G.J., et al., *RNA-based FLT3-ITD allelic ratio is associated with outcome and ex vivo response to FLT3 inhibitors in pediatric AML.* Blood, 2018. **131**(22): p. 2485-2489.
122. Perl, A.E., et al., *Selective inhibition of FLT3 by gilteritinib in relapsed or refractory acute myeloid leukaemia: a multicentre, first-in-human, open-label, phase 1-2 study.* Lancet Oncol, 2017. **18**(8): p. 1061-1075.
123. Perl, A.E., et al., *Gilteritinib or Chemotherapy for Relapsed or Refractory FLT3-Mutated AML.* N Engl J Med, 2019. **381**(18): p. 1728-1740.
124. Zarrinkar, P.P., et al., *AC220 is a uniquely potent and selective inhibitor of FLT3 for the treatment of acute myeloid leukemia (AML).* Blood, 2009. **114**(14): p. 2984-92.
125. Chao, Q., et al., *Identification of N-(5-tert-butyl-isoxazol-3-yl)-N'-{4-[7-(2-morpholin-4-yl-ethoxy)imidazo[2,1-b][1 ,3]benzothiazol-2-yl]phenyl}urea dihydrochloride (AC220), a uniquely potent, selective, and efficacious FMS-like tyrosine kinase-3 (FLT3) inhibitor.* J Med Chem, 2009. **52**(23): p. 7808-16.
126. Pratz, K.W., et al., *FLT3-mutant allelic burden and clinical status are predictive of response to FLT3 inhibitors in AML.* Blood, 2010. **115**(7): p. 1425-32.
127. Kampa-Schittenhelm, K.M., et al., *Quizartinib (AC220) is a potent second generation class III tyrosine kinase inhibitor that displays a distinct inhibition profile against mutant-FLT3, -PDGFRA and -KIT isoforms.* Molecular Cancer, 2013. **12**.
128. Naqvi, K. and F. Ravandi, *FLT3 inhibitor quizartinib (AC220).* Leuk Lymphoma, 2019. **60**(8): p. 1866-1876.
129. Zorn, J.A., et al., *Crystal structure of the FLT3 kinase domain bound to the inhibitor Quizartinib (AC220).* PLoS One, 2015. **10**(4): p. e0121177.
130. Knapper, S., et al., *A phase 2 trial of the FLT3 inhibitor lestaurtinib (CEP701) as first-line treatment for older patients with acute myeloid leukemia not considered fit for intensive chemotherapy.* Blood, 2006. **108**(10): p. 3262-70.
131. Hu, S., et al., *Comparison of antitumor effects of multitargeted tyrosine kinase inhibitors in acute myelogenous leukemia.* Mol Cancer Ther, 2008. **7**(5): p. 1110-20.
132. Weisberg, E., et al., *Antileukemic effects of the novel, mutant FLT3 inhibitor NVP-AST487: effects on PKC412-sensitive and -resistant FLT3-expressing cells.* Blood, 2008. **112**(13): p. 5161-70.
133. Zimmerman, E.I., et al., *Crenolanib is active against models of drug-resistant FLT3-ITD-positive acute myeloid leukemia.* Blood, 2013. **122**(22): p. 3607-15.

134. Ke, Y.Y., et al., *Homology modeling of DFG-in FMS-like tyrosine kinase 3 (FLT3) and structure-based virtual screening for inhibitor identification.* Sci Rep, 2015. **5**: p. 11702.
135. Smith, C.C., et al., *FLT3 D835 mutations confer differential resistance to type II FLT3 inhibitors.* Leukemia, 2015. **29**(12): p. 2390-2.
136. Smith, C.C., et al., *Validation of ITD mutations in FLT3 as a therapeutic target in human acute myeloid leukaemia.* Nature, 2012. **485**(7397): p. 260-3.
137. Levis, M., et al., *Plasma inhibitory activity (PIA): a pharmacodynamic assay reveals insights into the basis for cytotoxic response to FLT3 inhibitors.* Blood, 2006. **108**(10): p. 3477-83.
138. Gunawardane, R.N., et al., *Transient Exposure to Quizartinib Mediates Sustained Inhibition of FLT3 Signaling while Specifically Inducing Apoptosis in FLT3-Activated Leukemia Cells.* Molecular Cancer Therapeutics, 2013. **12**(4): p. 438-447.
139. Levis, M., et al., *A FLT3 tyrosine kinase inhibitor is selectively cytotoxic to acute myeloid leukemia blasts harboring FLT3 internal tandem duplication mutations.* Blood, 2001. **98**(3): p. 885-7.
140. Zheng, R., A.D. Friedman, and D. Small, *Targeted inhibition of FLT3 overcomes the block to myeloid differentiation in 32Dcl3 cells caused by expression of FLT3/ITD mutations.* Blood, 2002. **100**(12): p. 4154-61.
141. Radomska, H.S., et al., *Block of C/EBP alpha function by phosphorylation in acute myeloid leukemia with FLT3 activating mutations.* J Exp Med, 2006. **203**(2): p. 371-81.
142. Sexauer, A., et al., *Terminal myeloid differentiation in vivo is induced by FLT3 inhibition in FLT3/ITD AML.* Blood, 2012. **120**(20): p. 4205-14.
143. Yang, X., A. Sexauer, and M. Levis, *Bone marrow stroma-mediated resistance to FLT3 inhibitors in FLT3-ITD AML is mediated by persistent activation of extracellular regulated kinase.* Br J Haematol, 2014. **164**(1): p. 61-72.
144. Ding, L., et al., *Clonal evolution in relapsed acute myeloid leukaemia revealed by whole-genome sequencing.* Nature, 2012. **481**(7382): p. 506-10.
145. Cortes, J., et al., *AC220, a Potent, Selective, Second Generation FLT3 Receptor Tyrosine Kinase (RTK) Inhibitor, in a First-in-Human (FIH) Phase 1 AML Study.* Blood, 2009. **114**(22): p. 264-264.
146. Cortes, J.E., et al., *Final Results of a Phase 2 Open-Label, Monotherapy Efficacy and Safety Study of Quizartinib (AC220) in Patients >= 60 Years of Age with FLT3 ITD Positive or Negative Relapsed/Refractory Acute Myeloid Leukemia.* Blood, 2012. **120**(21).
147. Perl, A.E., et al., *Efficacy and safety of quizartinib (AC220) in patients age >= 70 years with FLT3-ITD positive or negative relapsed/refractory acute myeloid leukemia (AML).* Journal of Clinical Oncology, 2013. **31**(15).
148. Cortes, J.E., et al., *Results Of a Phase 2 Randomized, Open-Label, Study Of Lower Doses Of Quizartinib (AC220; ASP2689) In Subjects With FLT3-ITD Positive Relapsed Or Refractory Acute Myeloid Leukemia (AML).* Blood, 2013. **122**(21).
149. Ravandi, F., et al., *Phase I/II study of combination therapy with sorafenib, idarubicin, and cytarabine in younger patients with acute myeloid leukemia.* J Clin Oncol, 2010. **28**(11): p. 1856-62.
150. Stone, R.M., et al., *A Phase 1b Study of Midostaurin (PKC412) in Combination with Daunorubicin and Cytarabine Induction and High-Dose Cytarabine Consolidation in*

Patients Under Age 61 with Newly Diagnosed De Novo Acute Myeloid Leukemia: Overall Survival of Patients Whose Blasts Have FLT3 Mutations Is Similar to Those with Wild-Type FLT3. Blood, 2009. **114**(22): p. 263-263.
151. Altman, J.K., et al., *Phase 1 study of quizartinib in combination with induction and consolidation chemotherapy in patients with newly diagnosed acute myeloid leukemia.* American Journal of Hematology, 2018. **93**(2): p. 213-221.
152. Abdelall, W., et al., *The Combination of Quizartinib with Azacitidine or Low Dose Cytarabine Is Highly Active in Patients (Pts) with FLT3-ITD Mutated Myeloid Leukemias: Interim Report of a Phase I/II Trial.* Blood, 2016. **128**(22).
153. Cortes, J.E., S. Khaled, and G. Martinelli, *Quizartinib versus salvage chemotherapy in relapsed or refractory FLT3-ITD acute myeloid leukaemia (QuANTUM-R): a multicentre, randomised, controlled, open-label, phase 3 trial (vol 20, pg 986, 2019).* Lancet Oncology, 2019. **20**(7): p. E346-E346.
154. Sandmaier, B.M., et al., *Results of a phase 1 study of quizartinib as maintenance therapy in subjects with acute myeloid leukemia in remission following allogeneic hematopoietic stem cell transplant.* American Journal of Hematology, 2018. **93**(2): p. 222-231.
155. Cortes, J.E., et al., *Phase 2b study of 2 dosing regimens of quizartinib monotherapy in FLT3-ITD-mutated, relapsed or refractory AML.* Blood, 2018. **132**(6): p. 598-607.
156. Cortes, J.E., et al., *Phase I study of quizartinib administered daily to patients with relapsed or refractory acute myeloid leukemia irrespective of FMS-like tyrosine kinase 3-internal tandem duplication status.* J Clin Oncol, 2013. **31**(29): p. 3681-7.
157. Cortes, J., et al., *Quizartinib, an FLT3 inhibitor, as monotherapy in patients with relapsed or refractory acute myeloid leukaemia: an open-label, multicentre, single-arm, phase 2 trial.* Lancet Oncology, 2018. **19**(7): p. 889-903.
158. Cortes, J.E., et al., *Quizartinib in FLT3-ITD-Mutated Relapsed/Refractory Acute Myeloid Leukemia: QuANTUM-R Trial Results.* Annals of Oncology, 2019. **30**: p. 81-81.
159. Stone, R.M., et al., *Patients with acute myeloid leukemia and an activating mutation in FLT3 respond to a small-molecule FLT3 tyrosine kinase inhibitor, PKC412.* Blood, 2005. **105**(1): p. 54-60.
160. Alvarado, Y., et al., *Treatment with FLT3 inhibitor in patients with FLT3-mutated acute myeloid leukemia is associated with development of secondary FLT3-tyrosine kinase domain mutations.* Cancer, 2014. **120**(14): p. 2142-9.
161. Baker, S.D., et al., *Emergence of polyclonal FLT3 tyrosine kinase domain mutations during sequential therapy with sorafenib and sunitinib in FLT3-ITD-positive acute myeloid leukemia.* Clin Cancer Res, 2013. **19**(20): p. 5758-68.
162. Ishiko, J., et al., *Roles of tyrosine residues 845, 892 and 922 in constitutive activation of murine FLT3 kinase domain mutant.* Oncogene, 2005. **24**(55): p. 8144-53.
163. Hirade, T., et al., *Internal tandem duplication of FLT3 deregulates proliferation and differentiation and confers resistance to the FLT3 inhibitor AC220 by Up-regulating RUNX1 expression in hematopoietic cells.* Int J Hematol, 2016. **103**(1): p. 95-106.
164. Hou, P., et al., *A Genome-Wide CRISPR Screen Identifies Genes Critical for Resistance to FLT3 Inhibitor AC220.* Cancer Res, 2017. **77**(16): p. 4402-4413.
165. Traer, E., et al., *FGF2 from Marrow Microenvironment Promotes Resistance to FLT3 Inhibitors in Acute Myeloid Leukemia.* Cancer Res, 2016. **76**(22): p. 6471-6482.

166. Abe, M., et al., *Internal Tandem Duplication in FLT3 Attenuates Proliferation and Regulates Resistance to the FLT3 Inhibitor AC220 by Modulating p21Cdkn1a and Pbx1 in Hematopoietic Cells.* PLoS One, 2016. **11**(7): p. e0158290.
167. Friedman, R., *The molecular mechanism behind resistance of the kinase FLT3 to the inhibitor quizartinib.* Proteins, 2017. **85**(11): p. 2143-2152.
168. Verma, S., et al., *Insight into the inhibitor discrimination by FLT3 F691L.* Chem Biol Drug Des, 2018. **91**(5): p. 1056-1064.
169. Smith, C.C., et al., *Heterogeneous resistance to quizartinib in acute myeloid leukemia revealed by single-cell analysis.* Blood, 2017. **130**(1): p. 48-58.
170. Dayal, N., et al., *Dual FLT3/TOPK inhibitor with activity against FLT3-ITD secondary mutations potently inhibits acute myeloid leukemia cell lines.* Future Med Chem, 2018. **10**(7): p. 823-835.
171. Ouchida, A.T., et al., *Synergistic effect of a novel autophagy inhibitor and Quizartinib enhances cancer cell death.* Cell Death Dis, 2018. **9**(2): p. 138.
172. He, Y., et al., *Combined inhibition of PI3Kdelta and FLT3 signaling exerts synergistic antitumor activity and overcomes acquired drug resistance in FLT3-activated acute myeloid leukemia.* Cancer Lett, 2018. **420**: p. 49-59.
173. Lal, H., K.L. Kolaja, and T. Force, *Cancer genetics and the cardiotoxicity of the therapeutics.* J Am Coll Cardiol, 2013. **61**(3): p. 267-74.
174. Jetani, H., et al., *CAR T-cells targeting FLT3 have potent activity against FLT3(-)ITD(+) AML and act synergistically with the FLT3-inhibitor crenolanib.* Leukemia, 2018. **32**(5): p. 1168-1179.
175. FDA, *FDA Briefing Document Oncologic Drugs Advisory Committee (ODAC) Meeting: NDA 212166 Quizartinib https://www.fda.gov/media/124896/download.* May 14, 2019.
176. Kerkela, R., et al., *Cardiotoxicity of the cancer therapeutic agent imatinib mesylate.* Nat Med, 2006. **12**(8): p. 908-16.
177. Chu, T.F., et al., *Cardiotoxicity associated with tyrosine kinase inhibitor sunitinib.* Lancet, 2007. **370**(9604): p. 2011-9.
178. Schmidinger, M., et al., *Cardiac toxicity of sunitinib and sorafenib in patients with metastatic renal cell carcinoma.* J Clin Oncol, 2008. **26**(32): p. 5204-12.
179. Ghoreschi, K., A. Laurence, and J.J. O'Shea, *Selectivity and therapeutic inhibition of kinases: to be or not to be?* Nat Immunol, 2009. **10**(4): p. 356-60.
180. Yamaguchi, O., et al., *Cardiac-specific disruption of the c-raf-1 gene induces cardiac dysfunction and apoptosis.* J Clin Invest, 2004. **114**(7): p. 937-43.
181. Escudier, B., et al., *Sorafenib in advanced clear-cell renal-cell carcinoma.* N Engl J Med, 2007. **356**(2): p. 125-34.
182. Fernandez, A., et al., *An anticancer C-Kit kinase inhibitor is reengineered to make it more active and less cardiotoxic.* J Clin Invest, 2007. **117**(12): p. 4044-54.
183. Force, T. and K.L. Kolaja, *Cardiotoxicity of kinase inhibitors: the prediction and translation of preclinical models to clinical outcomes.* Nat Rev Drug Discov, 2011. **10**(2): p. 111-26.
184. Hasinoff, B.B., *The cardiotoxicity and myocyte damage caused by small molecule anticancer tyrosine kinase inhibitors is correlated with lack of target specificity.* Toxicol Appl Pharmacol, 2010. **244**(2): p. 190-5.
185. Minotti, G., E. Salvatorelli, and P. Menna, *Pharmacological foundations of cardio-oncology.* J Pharmacol Exp Ther, 2010. **334**(1): p. 2-8.

186. Kerkela, R., et al., *Sunitinib-induced cardiotoxicity is mediated by off-target inhibition of AMP-activated protein kinase.* Clin Transl Sci, 2009. **2**(1): p. 15-25.
187. Korennykh, A.V., et al., *The unfolded protein response signals through high-order assembly of Ire1.* Nature, 2009. **457**(7230): p. 687-93.
188. Cheng, H. and T. Force, *Molecular mechanisms of cardiovascular toxicity of targeted cancer therapeutics.* Circ Res, 2010. **106**(1): p. 21-34.
189. DeWood, M.A., et al., *Prevalence of total coronary occlusion during the early hours of transmural myocardial infarction.* N Engl J Med, 1980. **303**(16): p. 897-902.
190. Avkiran, M., *Basic biology and pharmacology of the cardiac sarcolemmal sodium/hydrogen exchanger.* J Card Surg, 2003. **18 Suppl 1**: p. 3-12.
191. Ladilov, Y.V., B. Siegmund, and H.M. Piper, *Protection of reoxygenated cardiomyocytes against hypercontracture by inhibition of Na+/H+ exchange.* Am J Physiol, 1995. **268**(4 Pt 2): p. H1531-9.
192. Walls, M.C., et al., *Myocardial edema imaging in acute coronary syndromes.* J Magn Reson Imaging, 2011. **34**(6): p. 1243-50.
193. Ibanez, B., et al., *Evolving therapies for myocardial ischemia/reperfusion injury.* J Am Coll Cardiol, 2015. **65**(14): p. 1454-71.
194. Lassen, T.R., et al., *Effect of paroxetine on left ventricular remodeling in an in vivo rat model of myocardial infarction.* Basic Res Cardiol, 2017. **112**(3): p. 26.
195. Schluter, K.D., et al., *Protection of reoxygenated cardiomyocytes against osmotic fragility by nitric oxide donors.* Am J Physiol, 1996. **271**(2 Pt 2): p. H428-34.
196. Mohazzab, H.K., P.M. Kaminski, and M.S. Wolin, *Lactate and PO2 modulate superoxide anion production in bovine cardiac myocytes: potential role of NADH oxidase.* Circulation, 1997. **96**(2): p. 614-20.
197. Lu, L., M.T. Quinn, and Y. Sun, *Oxidative stress in the infarcted heart: role of de novo angiotensin II production.* Biochem Biophys Res Commun, 2004. **325**(3): p. 943-51.
198. Takimoto, Y., et al., *Differential expression of three types of nitric oxide synthase in both infarcted and non-infarcted left ventricles after myocardial infarction in the rat.* Int J Cardiol, 2000. **76**(2-3): p. 135-45.
199. Kabe, Y., et al., *Redox regulation of NF-kappaB activation: distinct redox regulation between the cytoplasm and the nucleus.* Antioxid Redox Signal, 2005. **7**(3-4): p. 395-403.
200. Lu, L., et al., *Activation of nuclear factor-kappaB and its proinflammatory mediator cascade in the infarcted rat heart.* Biochem Biophys Res Commun, 2004. **321**(4): p. 879-85.
201. Schoonbroodt, S. and J. Piette, *Oxidative stress interference with the nuclear factor-kappa B activation pathways.* Biochem Pharmacol, 2000. **60**(8): p. 1075-83.
202. Ceconi, C., et al., *Tumor necrosis factor in congestive heart failure: a mechanism of disease for the new millennium?* Prog Cardiovasc Dis, 1998. **41**(1 Suppl 1): p. 25-30.
203. Meldrum, D.R., et al., *Hydrogen peroxide induces tumor necrosis factor alpha-mediated cardiac injury by a P38 mitogen-activated protein kinase-dependent mechanism.* Surgery, 1998. **124**(2): p. 291-6; discussion 297.
204. Swirski, F.K. and M. Nahrendorf, *Leukocyte behavior in atherosclerosis, myocardial infarction, and heart failure.* Science, 2013. **339**(6116): p. 161-6.
205. Civitarese, R.A., et al., *Role of integrins in mediating cardiac fibroblast-cardiomyocyte cross talk: a dynamic relationship in cardiac biology and pathophysiology.* Basic Res Cardiol, 2017. **112**(1): p. 6.

206. Frangogiannis, N.G., *The mechanistic basis of infarct healing.* Antioxid Redox Signal, 2006. **8**(11-12): p. 1907-39.
207. van der Laan, A.M., M. Nahrendorf, and J.J. Piek, *Healing and adverse remodelling after acute myocardial infarction: role of the cellular immune response.* Heart, 2012. **98**(18): p. 1384-90.
208. McMurray, J.J. and M.A. Pfeffer, *Heart failure.* Lancet, 2005. **365**(9474): p. 1877-89.
209. Lindsey, M.L., et al., *Guidelines for experimental models of myocardial ischemia and infarction.* Am J Physiol Heart Circ Physiol, 2018. **314**(4): p. H812-H838.
210. Cohn, J.N., R. Ferrari, and N. Sharpe, *Cardiac remodeling--concepts and clinical implications: a consensus paper from an international forum on cardiac remodeling. Behalf of an International Forum on Cardiac Remodeling.* J Am Coll Cardiol, 2000. **35**(3): p. 569-82.
211. Nian, M., et al., *Inflammatory cytokines and postmyocardial infarction remodeling.* Circ Res, 2004. **94**(12): p. 1543-53.
212. Dorn, G.W., 2nd, *The fuzzy logic of physiological cardiac hypertrophy.* Hypertension, 2007. **49**(5): p. 962-70.
213. Opie, L.H., et al., *Controversies in ventricular remodelling.* Lancet, 2006. **367**(9507): p. 356-67.
214. Hill, J.A. and E.N. Olson, *Cardiac plasticity.* N Engl J Med, 2008. **358**(13): p. 1370-80.
215. Burchfield, J.S., M. Xie, and J.A. Hill, *Pathological ventricular remodeling: mechanisms: part 1 of 2.* Circulation, 2013. **128**(4): p. 388-400.
216. Ohtani, T., et al., *Diastolic stiffness as assessed by diastolic wall strain is associated with adverse remodelling and poor outcomes in heart failure with preserved ejection fraction.* Eur Heart J, 2012. **33**(14): p. 1742-9.
217. Schirone, L., et al., *A Review of the Molecular Mechanisms Underlying the Development and Progression of Cardiac Remodeling.* Oxid Med Cell Longev, 2017. **2017**: p. 3920195.
218. Azevedo, P.S., et al., *Cardiac Remodeling: Concepts, Clinical Impact, Pathophysiological Mechanisms and Pharmacologic Treatment.* Arq Bras Cardiol, 2016. **106**(1): p. 62-9.
219. Levine, B. and G. Kroemer, *Autophagy in the pathogenesis of disease.* Cell, 2008. **132**(1): p. 27-42.
220. Harvey, P.A. and L.A. Leinwand, *The cell biology of disease: cellular mechanisms of cardiomyopathy.* J Cell Biol, 2011. **194**(3): p. 355-65.
221. Segura, A.M., O.H. Frazier, and L.M. Buja, *Fibrosis and heart failure.* Heart Fail Rev, 2014. **19**(2): p. 173-85.
222. Prabhu, S.D. and N.G. Frangogiannis, *The Biological Basis for Cardiac Repair After Myocardial Infarction: From Inflammation to Fibrosis.* Circ Res, 2016. **119**(1): p. 91-112.
223. Frangogiannis, N.G., *Regulation of the inflammatory response in cardiac repair.* Circ Res, 2012. **110**(1): p. 159-73.
224. Fujita, S., et al., *Atrial natriuretic peptide exerts protective action against angiotensin II-induced cardiac remodeling by attenuating inflammation via endothelin-1/endothelin receptor A cascade.* Heart Vessels, 2013. **28**(5): p. 646-57.
225. Mortensen, R.M., *Immune cell modulation of cardiac remodeling.* Circulation, 2012. **125**(13): p. 1597-600.

226. Levick, S.P., et al., *Cardiac mast cells mediate left ventricular fibrosis in the hypertensive rat heart.* Hypertension, 2009. **53**(6): p. 1041-7.
227. Salvesen, G.S. and S.J. Riedl, *Caspase mechanisms.* Adv Exp Med Biol, 2008. **615**: p. 13-23.
228. Prokhorova, E.A., et al., *Apoptosis regulation by subcellular relocation of caspases.* Sci Rep, 2018. **8**(1): p. 12199.
229. Schreiber, V., et al., *Poly(ADP-ribose): novel functions for an old molecule.* Nat Rev Mol Cell Biol, 2006. **7**(7): p. 517-28.
230. Decker, P. and S. Muller, *Modulating poly (ADP-ribose) polymerase activity: potential for the prevention and therapy of pathogenic situations involving DNA damage and oxidative stress.* Curr Pharm Biotechnol, 2002. **3**(3): p. 275-83.
231. K, S., et al., *MitoLSDB: a comprehensive resource to study genotype to phenotype correlations in human mitochondrial DNA variations.* PLoS One, 2013. **8**(4): p. e60066.
232. Mellor, H.R., et al., *Cardiotoxicity associated with targeting kinase pathways in cancer.* Toxicol Sci, 2011. **120**(1): p. 14-32.
233. Orphanos, G.S., G.N. Ioannidis, and A.G. Ardavanis, *Cardiotoxicity induced by tyrosine kinase inhibitors.* Acta Oncol, 2009. **48**(7): p. 964-70.
234. Chen, M.H., R. Kerkela, and T. Force, *Mechanisms of cardiac dysfunction associated with tyrosine kinase inhibitor cancer therapeutics.* Circulation, 2008. **118**(1): p. 84-95.
235. Yang, B. and T. Papoian, *Tyrosine kinase inhibitor (TKI)-induced cardiotoxicity: approaches to narrow the gaps between preclinical safety evaluation and clinical outcome.* J Appl Toxicol, 2012. **32**(12): p. 945-51.
236. Zhao, Z.Q., et al., *Reperfusion induces myocardial apoptotic cell death.* Cardiovasc Res, 2000. **45**(3): p. 651-60.
237. Fliss, H. and D. Gattinger, *Apoptosis in ischemic and reperfused rat myocardium.* Circ Res, 1996. **79**(5): p. 949-56.
238. Palojoki, E., et al., *Cardiomyocyte apoptosis and ventricular remodeling after myocardial infarction in rats.* Am J Physiol Heart Circ Physiol, 2001. **280**(6): p. H2726-31.
239. Sam, F., et al., *Progressive left ventricular remodeling and apoptosis late after myocardial infarction in mouse heart.* Am J Physiol Heart Circ Physiol, 2000. **279**(1): p. H422-8.
240. Singh, A.P., et al., *Ponatinib-induced cardiotoxicity: delineating the signalling mechanisms and potential rescue strategies.* Cardiovasc Res, 2019. **115**(5): p. 966-977.
241. Korashy, H.M., et al., *Molecular mechanisms of cardiotoxicity of gefitinib in vivo and in vitro rat cardiomyocyte: Role of apoptosis and oxidative stress.* Toxicol Lett, 2016. **252**: p. 50-61.
242. Abbate, A., et al., *Increased myocardial apoptosis in patients with unfavorable left ventricular remodeling and early symptomatic post-infarction heart failure.* J Am Coll Cardiol, 2003. **41**(5): p. 753-60.
243. Doherty, K.R., et al., *Multi-parameter in vitro toxicity testing of crizotinib, sunitinib, erlotinib, and nilotinib in human cardiomyocytes.* Toxicol Appl Pharmacol, 2013. **272**(1): p. 245-55.
244. Duran, J.M., et al., *Sorafenib cardiotoxicity increases mortality after myocardial infarction.* Circ Res, 2014. **114**(11): p. 1700-1712.

245. Zhao, Y., et al., *Autophagy plays an important role in sunitinib-mediated cell death in H9c2 cardiac muscle cells.* Toxicol Appl Pharmacol, 2010. **248**(1): p. 20-7.
246. Gonzalez-Montero, J., et al., *Myocardial reperfusion injury and oxidative stress: Therapeutic opportunities.* World J Cardiol, 2018. **10**(9): p. 74-86.
247. Chandrashekhar, Y., et al., *Long-term caspase inhibition ameliorates apoptosis, reduces myocardial troponin-I cleavage, protects left ventricular function, and attenuates remodeling in rats with myocardial infarction.* J Am Coll Cardiol, 2004. **43**(2): p. 295-301.
248. Yarbrough, W.M., et al., *Caspase inhibition modulates left ventricular remodeling following myocardial infarction through cellular and extracellular mechanisms.* J Cardiovasc Pharmacol, 2010. **55**(4): p. 408-16.
249. Huang, J.Q., et al., *In vivo myocardial infarct size reduction by a caspase inhibitor administered after the onset of ischemia.* Eur J Pharmacol, 2000. **402**(1-2): p. 139-42.
250. Holly, T.A., et al., *Caspase inhibition reduces myocyte cell death induced by myocardial ischemia and reperfusion in vivo.* J Mol Cell Cardiol, 1999. **31**(9): p. 1709-15.
251. Mocanu, M.M., G.F. Baxter, and D.M. Yellon, *Caspase inhibition and limitation of myocardial infarct size: protection against lethal reperfusion injury.* Br J Pharmacol, 2000. **130**(2): p. 197-200.
252. Kovacs, P., et al., *Non-specific caspase inhibition reduces infarct size and improves post-ischaemic recovery in isolated ischaemic/reperfused rat hearts.* Naunyn Schmiedebergs Arch Pharmacol, 2001. **364**(6): p. 501-7.
253. Cortes, J.E., et al., *Efficacy and Safety of Single-Agent Quizartinib (Q), Potent and SeleEfficacy and Safety of Single-Agent Quizartinib (Q), a Potent and Selective FLT3 Inhibitor (FLT3i), in Patients (pts) with FLT3-Internal Tandem Duplication (FLT3-ITD)-Mutated Relapsed/Refractory (R/R) Acute Myeloid Leukemia (AML) Enrolled in the Global, Phase 3, Randomized Controlled QuANTUM-R Trial.* British Journal of Haematology, 2019. **185**: p. 78-78.
254. Zhao, J., Y. Song, and D. Liu, *Gilteritinib: a novel FLT3 inhibitor for acute myeloid leukemia.* Biomark Res, 2019. **7**: p. 19.
255. Disease, G.B.D., I. Injury, and C. Prevalence, *Global, regional, and national incidence, prevalence, and years lived with disability for 310 diseases and injuries, 1990-2015: a systematic analysis for the Global Burden of Disease Study 2015.* Lancet, 2016. **388**(10053): p. 1545-1602.
256. Cui, B., et al., *Heart Regeneration in Adult Mammals after Myocardial Damage.* Acta Cardiol Sin, 2018. **34**(2): p. 115-123.
257. Tzahor, E. and K.D. Poss, *Cardiac regeneration strategies: Staying young at heart.* Science, 2017. **356**(6342): p. 1035-1039.
258. Gamba, L., M. Harrison, and C.L. Lien, *Cardiac regeneration in model organisms.* Curr Treat Options Cardiovasc Med, 2014. **16**(3): p. 288.
259. Poss, K.D., L.G. Wilson, and M.T. Keating, *Heart regeneration in zebrafish.* Science, 2002. **298**(5601): p. 2188-90.
260. Witman, N., et al., *Recapitulation of developmental cardiogenesis governs the morphological and functional regeneration of adult newt hearts following injury.* Dev Biol, 2011. **354**(1): p. 67-76.
261. Bergmann, O., et al., *Evidence for cardiomyocyte renewal in humans.* Science, 2009. **324**(5923): p. 98-102.

262. Bergmann, O., et al., *Dynamics of Cell Generation and Turnover in the Human Heart.* Cell, 2015. **161**(7): p. 1566-75.
263. Drenckhahn, J.D., et al., *Compensatory growth of healthy cardiac cells in the presence of diseased cells restores tissue homeostasis during heart development.* Dev Cell, 2008. **15**(4): p. 521-33.
264. Porrello, E.R., et al., *Transient regenerative potential of the neonatal mouse heart.* Science, 2011. **331**(6020): p. 1078-80.
265. Porrello, E.R., et al., *Regulation of neonatal and adult mammalian heart regeneration by the miR-15 family.* Proc Natl Acad Sci U S A, 2013. **110**(1): p. 187-92.
266. Haubner, B.J., et al., *Complete cardiac regeneration in a mouse model of myocardial infarction.* Aging (Albany NY), 2012. **4**(12): p. 966-77.
267. Uygur, A. and R.T. Lee, *Mechanisms of Cardiac Regeneration.* Dev Cell, 2016. **36**(4): p. 362-74.
268. Fratz, S., et al., *Long-term myocardial scarring after operation for anomalous left coronary artery from the pulmonary artery.* Ann Thorac Surg, 2011. **92**(5): p. 1761-5.
269. Haubner, B.J., et al., *Functional Recovery of a Human Neonatal Heart After Severe Myocardial Infarction.* Circ Res, 2016. **118**(2): p. 216-21.
270. Engel, F.B., et al., *p38 MAP kinase inhibition enables proliferation of adult mammalian cardiomyocytes.* Genes Dev, 2005. **19**(10): p. 1175-87.
271. Chaudhry, H.W., et al., *Cyclin A2 mediates cardiomyocyte mitosis in the postmitotic myocardium.* J Biol Chem, 2004. **279**(34): p. 35858-66.
272. Pasumarthi, K.B., et al., *Targeted expression of cyclin D2 results in cardiomyocyte DNA synthesis and infarct regression in transgenic mice.* Circ Res, 2005. **96**(1): p. 110-8.
273. Cobrinik, D., *Pocket proteins and cell cycle control.* Oncogene, 2005. **24**(17): p. 2796-809.
274. Sdek, P., et al., *Rb and p130 control cell cycle gene silencing to maintain the postmitotic phenotype in cardiac myocytes.* J Cell Biol, 2011. **194**(3): p. 407-23.
275. Vagnozzi, R.J., J.D. Molkentin, and S.R. Houser, *New Myocyte Formation in the Adult Heart: Endogenous Sources and Therapeutic Implications.* Circ Res, 2018. **123**(2): p. 159-176.
276. Mahmoud, A.I., et al., *Meis1 regulates postnatal cardiomyocyte cell cycle arrest.* Nature, 2013. **497**(7448): p. 249-253.
277. Giacca, M. and S. Zacchigna, *Harnessing the microRNA pathway for cardiac regeneration.* J Mol Cell Cardiol, 2015. **89**(Pt A): p. 68-74.
278. D'Uva, G., et al., *ERBB2 triggers mammalian heart regeneration by promoting cardiomyocyte dedifferentiation and proliferation.* Nat Cell Biol, 2015. **17**(5): p. 627-38.
279. Zhao, L., et al., *Endocardial Notch Signaling Promotes Cardiomyocyte Proliferation in the Regenerating Zebrafish Heart through Wnt Pathway Antagonism.* Cell Rep, 2019. **26**(3): p. 546-554 e5.
280. Meng, Z., T. Moroishi, and K.L. Guan, *Mechanisms of Hippo pathway regulation.* Genes Dev, 2016. **30**(1): p. 1-17.
281. Yu, F.X., B. Zhao, and K.L. Guan, *Hippo Pathway in Organ Size Control, Tissue Homeostasis, and Cancer.* Cell, 2015. **163**(4): p. 811-28.
282. Yu, F.X. and K.L. Guan, *The Hippo pathway: regulators and regulations.* Genes Dev, 2013. **27**(4): p. 355-71.

283. Zhao, B., et al., *Both TEAD-binding and WW domains are required for the growth stimulation and oncogenic transformation activity of yes-associated protein.* Cancer Res, 2009. **69**(3): p. 1089-98.
284. Heallen, T., et al., *Hippo pathway inhibits Wnt signaling to restrain cardiomyocyte proliferation and heart size.* Science, 2011. **332**(6028): p. 458-61.
285. Xin, M., et al., *Regulation of insulin-like growth factor signaling by Yap governs cardiomyocyte proliferation and embryonic heart size.* Sci Signal, 2011. **4**(196): p. ra70.
286. von Gise, A., et al., *YAP1, the nuclear target of Hippo signaling, stimulates heart growth through cardiomyocyte proliferation but not hypertrophy.* Proc Natl Acad Sci U S A, 2012. **109**(7): p. 2394-9.
287. Xin, M., et al., *Hippo pathway effector Yap promotes cardiac regeneration.* Proc Natl Acad Sci U S A, 2013. **110**(34): p. 13839-44.
288. Lin, Z., et al., *Cardiac-specific YAP activation improves cardiac function and survival in an experimental murine MI model.* Circ Res, 2014. **115**(3): p. 354-63.
289. Foglia, M.J. and K.D. Poss, *Building and re-building the heart by cardiomyocyte proliferation.* Development, 2016. **143**(5): p. 729-40.
290. Mochizuki, M., et al., *Polo-Like Kinase 2 is Dynamically Regulated to Coordinate Proliferation and Early Lineage Specification Downstream of Yes-Associated Protein 1 in Cardiac Progenitor Cells.* J Am Heart Assoc, 2017. **6**(10).
291. Simmons, D.L., et al., *Identification of an early-growth-response gene encoding a novel putative protein kinase.* Mol Cell Biol, 1992. **12**(9): p. 4164-9.
292. Liu, X. and R.L. Erikson, *Polo-like kinase 1 in the life and death of cancer cells.* Cell Cycle, 2003. **2**(5): p. 424-5.
293. Lowery, D.M., D. Lim, and M.B. Yaffe, *Structure and function of Polo-like kinases.* Oncogene, 2005. **24**(2): p. 248-59.
294. Kauselmann, G., et al., *The polo-like protein kinases Fnk and Snk associate with a Ca(2+)- and integrin-binding protein and are regulated dynamically with synaptic plasticity.* EMBO J, 1999. **18**(20): p. 5528-39.
295. Lee, K.J., H.S. Hoe, and D.T. Pak, *Plk2 Raps up Ras to subdue synapses.* Small GTPases, 2011. **2**(3): p. 162-166.
296. Duncan, P.I., et al., *Cloning and characterization of Plx2 and Plx3, two additional Polo-like kinases from Xenopus laevis.* Exp Cell Res, 2001. **270**(1): p. 78-87.
297. Zhong, H., et al., *Genetic approach to evaluate specificity of small molecule drug candidates inhibiting PLK1 using zebrafish.* Mol Biosyst, 2010. **6**(8): p. 1463-8.
298. Yang, H., et al., *Polo-like kinase 2 regulates angiogenic sprouting and blood vessel development.* Dev Biol, 2015. **404**(2): p. 49-60.
299. Ma, S., et al., *The serum-inducible protein kinase Snk is a G1 phase polo-like kinase that is inhibited by the calcium- and integrin-binding protein CIB.* Mol Cancer Res, 2003. **1**(5): p. 376-84.
300. Warnke, S., et al., *Polo-like kinase-2 is required for centriole duplication in mammalian cells.* Curr Biol, 2004. **14**(13): p. 1200-7.
301. Ma, S., J. Charron, and R.L. Erikson, *Role of Plk2 (Snk) in mouse development and cell proliferation.* Mol Cell Biol, 2003. **23**(19): p. 6936-43.
302. Burns, T.F., et al., *Silencing of the novel p53 target gene Snk/Plk2 leads to mitotic catastrophe in paclitaxel (taxol)-exposed cells.* Mol Cell Biol, 2003. **23**(16): p. 5556-71.

303. Xie, Y., et al., *Polo-like kinase 2 promotes chemoresistance and predicts limited survival benefit from adjuvant chemotherapy in colorectal cancer.* Int J Oncol, 2018.
304. Georgescu, S.P., et al., *Downregulation of polo-like kinase correlates with loss of proliferative ability of cardiac myocytes.* J Mol Cell Cardiol, 1997. **29**(3): p. 929-37.
305. Coxon, C.H., et al., *Over expression of Plk1 does not induce cell division in rat cardiac myocytes in vitro.* PLoS One, 2009. **4**(8): p. e6752.
306. Zhao, D., et al., *Plk2 Regulated by miR-128 Induces Ischemia-Reperfusion Injury in Cardiac Cells.* Mol Ther Nucleic Acids, 2019. **19**: p. 458-467.
307. Zhou, Q., et al., *The hippo pathway in heart development, regeneration, and diseases.* Circ Res, 2015. **116**(8): p. 1431-47.
308. Anger, M., et al., *Cell cycle dependent expression of Plk1 in synchronized porcine fetal fibroblasts.* Mol Reprod Dev, 2003. **65**(3): p. 245-53.
309. Liby, K., et al., *Identification of the human homologue of the early-growth response gene Snk, encoding a serum-inducible kinase.* DNA Seq, 2001. **11**(6): p. 527-33.
310. Duronio, R.J. and Y. Xiong, *Signaling pathways that control cell proliferation.* Cold Spring Harb Perspect Biol, 2013. **5**(3): p. a008904.
311. Kardami, E., et al., *PKC-dependent phosphorylation may regulate the ability of connexin43 to inhibit DNA synthesis.* Cell Commun Adhes, 2003. **10**(4-6): p. 293-7.
312. Hinrichsen, R., S. Haunso, and P.K. Busk, *Different regulation of p27 and Akt during cardiomyocyte proliferation and hypertrophy.* Growth Factors, 2007. **25**(2): p. 132-40.
313. Doxsey, S., D. McCollum, and W. Theurkauf, *Centrosomes in cellular regulation.* Annu Rev Cell Dev Biol, 2005. **21**: p. 411-34.
314. Cizmecioglu, O., et al., *Plk2 regulated centriole duplication is dependent on its localization to the centrioles and a functional polo-box domain.* Cell Cycle, 2008. **7**(22): p. 3548-55.
315. Mohamed, T.M.A., et al., *Regulation of Cell Cycle to Stimulate Adult Cardiomyocyte Proliferation and Cardiac Regeneration.* Cell, 2018. **173**(1): p. 104-116 e12.
316. Pellegrino, R., et al., *Oncogenic and tumor suppressive roles of polo-like kinases in human hepatocellular carcinoma.* Hepatology, 2010. **51**(3): p. 857-68.
317. Syed, N., et al., *Transcriptional silencing of Polo-like kinase 2 (SNK/PLK2) is a frequent event in B-cell malignancies.* Blood, 2006. **107**(1): p. 250-6.
318. Syed, N., et al., *Polo-like kinase Plk2 is an epigenetic determinant of chemosensitivity and clinical outcomes in ovarian cancer.* Cancer Res, 2011. **71**(9): p. 3317-27.
319. Ou, B., et al., *Plk2 promotes tumor growth and inhibits apoptosis by targeting Fbxw7/Cyclin E in colorectal cancer.* Cancer Lett, 2016. **380**(2): p. 457-66.

Identification of the molecular signature of side population cardiac progenitor cells and of strategies for regenerative potential enhancement

Daria Monogiou Belik, Gabriela Kuster and team

Department of Biomedicine and Division of Cardiology, University Hospital and University of Basel

Universitätsspital Basel

Departement Biomedizin Basel

BACKGROUND

- Restoration of cardiac function after myocardial infarction to prevent or mitigate post-infarct heart failure is a major therapeutic challenge. The intrinsic regenerative capacities of the adult heart are limited and insufficient to rebuild the lost tissue.
- Cell therapy is a promising approach to reduce infarct size and improve cardiac function in patients with myocardial infarction. However, until present cell therapy displays low efficacy due to cell death, low engraftment, as well as limited differentiation capacity of transplanted cells.
- Cardiac progenitor cells can be isolated from murine and human heart and have the potential to differentiate into all major cardiac lineages.

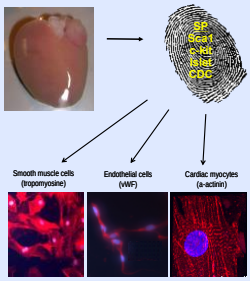

- Properties of progenitor cells are influenced by complex signals from the microenvironment. Cellular quiescence protects from cellular damage and is therefore pivotal for progenitor cell function. However, upon injury the cells are activated to re-enter the cell cycle.

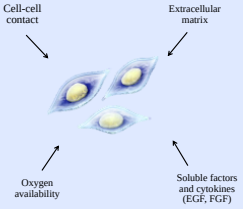

- The side population (SP) phenotype identifies organ-specific progenitor cells in a quiescent state.
- Sca1$^+$/CD31$^-$ cardiac SP (CSP) cells exhibit cardiomyogenic potential as they can differentiate into cardiomyocytes.

AIM

The overall aim of the project is to define the molecular identity of SP-CPCs and to clarify how specific master regulators of CPC fate affect their regenerative potential.

METHODS AND RESULTS

Optimization of culturing

➢ ***Isolation of CSP cells:*** CSP cells are isolated from 12 week-old C57BL/6 mice by FACS using the Hoechst efflux method. The efflux is regulated by the activity of the ATP-binding cassette transporters Mdr1 and Abcg2, which can be blocked by Verapamil. Subpopulations of SP are sorted according to Sca1 and/or CD31 expression.

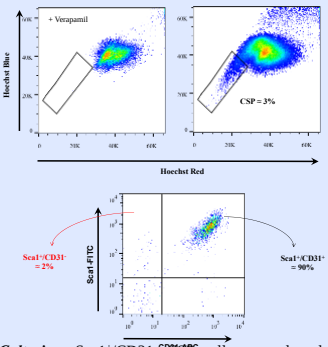

➢ ***Culturing***: Sca1$^+$/CD31$^-$ CSP cells are cultured in 3.5% serum medium complemented with endothelial growth factor (EGF), fibroblast growth factor (FGF) and cardiotrophin 1 (CT-1). Low passages are subjected to differentiation assays to induce expression of endothelial and myogenic markers.

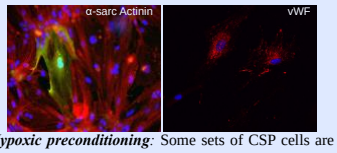

➢ ***Hypoxic preconditioning***: Some sets of CSP cells are exposed to a hypoxic environment of 1.5% oxygen for 24 hours.

Transcriptome analysis

➢ ***RNA sequencing:*** Total RNA is isolated from freshly isolated cardiomyogenic Sca1$^+$/CD31$^-$ and endothelial Sca1$^+$/CD31$^+$ CSP cells as well as from expanded and hypoxic preconditioned CSP and transcriptome is compared between conditions and with cardiomyocytes and embryonic stem cells.

Enhancement of regeneration

➢ ***Genetic modification:*** Upregulation or downregulation of key regulatory genes identified by RNA sequencing using plasmid- and siRNA-based techniques, respectively.

➢ ***Mouse model of myocardial infarction:*** Infarction is induced by left anterior descending coronary artery ligation and cardiac function is assessed by echocardiography.

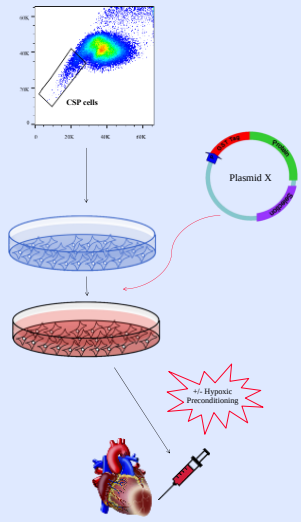

RELEVANCE

The pivotal goal of the project is to develop strategies to enhance the efficacy of cell therapy.

These strategies include the optimization of culturing techniques to preserve cell multipotency and improve cell engrafment and survival, and genetic engineering or small molecule modification to enhance their differentiation capacity.

Results will improve our understanding of how CPC are regulated and contribute to the overall potential of cell therapy for heart disease.

REFERENCES

Pfister *et al.*, CD31$^-$ but Not CD31$^+$ cardiac side population cells exhibit functional cardiomyogenic differentiation, Circulation Research 2005; 97: 52-612005

Noseda *et al.*, PDGFRα demarcates the cardiogenic clonogenic Sca1+ stem/progenitor cell in adult murine myocardium, Nature Communications 2015; 6: 6930

The fms-like tyrosine kinase 3-targeting receptor inhibitor quizartinib (AC220) decreases cardiomyocyte viability *in vitro* and *in vivo*

Daria Monogiou Belik, Giacomo Della Verde, Vera Lorenz, Lifen Xu, Michika Mochizuki, Gabriela Kuster

Laboratory of Myocardial Research, Department of Biomedicine, University of Basel

Background

- Protein phosphorylation is a crucial cellular **regulatory mechanism** taking place in a variety of **cell signaling networks** and modifying the target activities. [1]
- **Tyrosine kinases (TK)** are responsible for cellular transduction signaling for communication and maintenance of homeostasis (cell growth, differentiation, migration, survival) and their hyperactivity, malfunction or overexpression can be found in tumors. [2]
- Targeting TK by **small molecule inhibitors** that interfere with receptor TK signal transmission can serve as a therapeutic method for cancer treatment. [2]

Tyrosine Kinase Inhibitors (TKI)

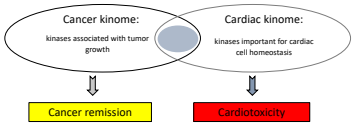

- **Fms-like tyrosine kinase 3 (FLT3)** is a transmembrane receptor TK involved in the proliferation and differentiation of hematopoietic progenitor cells.
- Mutated FLT3 is associated with acute myeloid leukemia (AML). FLT3 is also expressed in non hematopoietic organs (such as the heart).
- The intramyocardial injection of recombinant FLT3 Ligand into the infarct border zone decreased infarct size and ameliorated post-myocardial infarction remodeling and function in mice via a **cytoprotective effect** on cardiomyocytes. [3]

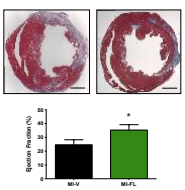

- **Quizartinib** (AC220) is a highly selective FLT3-targeting receptor TK inhibitor and efficient single agent in patients with relapsed/refractory AML. [4]

Aim and Hypothesis

- Given that FLT3 is important for cardiomyocyte survival and that FLT3 inhibitors are used as cancer therapy, we sought to **investigate the effects of pharmacological inhibition of FLT3 in the heart upon injury.**
- We hypothesized that mice treated with quizartinib are more susceptible to ischemic damage.

Methods

In vivo

- Mice were randomly assigned to oral administration of quizartinib (10 mg/kg/day) or vehicle (Captisol) for 4 weeks.
- After 3 weeks of treatment, myocardial infarction (MI) was induced via ligation of the left anterior descending artery (LAD). [5]
- Sham-operated mice (thoracotomy) were used as controls.
- Echocardiography was performed 3 days before drug treatment, 3 days before MI and one week post-MI.
- Mice were sacrificed and hearts were perfused one week post-MI.

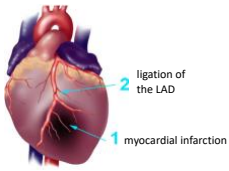

Post-mortem and in vitro

Immunohistochemistry

- Perfused hearts were embedded in paraffin, cut with a microtome into 4µm slices, tissue sections were stained by TUNEL to identify apoptotic cells.

MTT Assay

- H9c2 myoblasts were cultured on 96-well plates. Following over-night serum starvation, cells were pre-treated with 0, 2, 20 and 200nM of AC220 for 2 hours. Then 0, 5, 50 and 100µM H_2O_2 was added into the medium and cells were incubated at 37°C. Cell viability was assessed by MTT assay after 24, 48 and 72h, respectively.

Results

In vivo

1A.

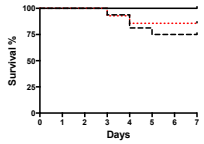

Figure 1A. Survival rate was assessed over 1 week post-MI (n=16 MI-Vehicle, n=14 MI-AC220, n=12 Sham).
Survival rate is not reduced in AC220-treated mice compared to vehicle treated.

1B.

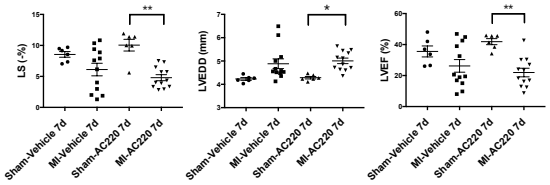

Figure 1B. Longitudinal strain (LS), left-ventricular end-diastolic diameter (LVEDD), left ventricular ejection fraction (LVEF) were assessed by echocardiography 7 days post-MI (n=6 Sham-Vehicle and Sham-AC220, n=12 MI-Vehicle and MI-AC220), **p<0.01, *p<0.05.
Compared to sham-operated mice, infarcted mice show enhanced ventricular dilation and decreased function in terms of EF and global LS. These functional decreases are pronounced in mice treated with quizartinib, although there are no significant differences between quizartinib- and vehicle-treated mice.

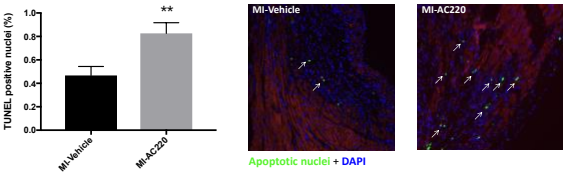

Figure 2. Apoptosis was assessed in the infarct border zone by TUNEL (green) and nuclear counterstaining (DAPI, blue). Representative images are shown. (n=11 MI- Vehicle, n=8 for MI-AC220),**p<0.01.
The number of TUNEL-positive cells is significantly increased in the infarct border zone in mice treated with quizartinib compared to vehicle treated.

In vitro

3A.

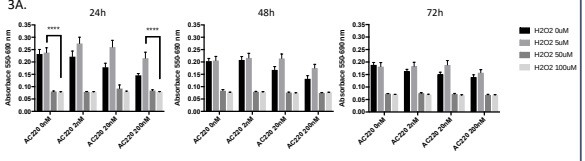

3B.

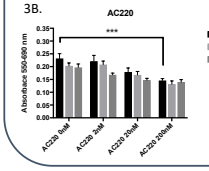

Figure 3. Cell viability was assessed by MTT assay of H9c2 myoblasts under quizartinib (0, 2, 20, 200nM) and H_2O_2 treatment at 24h, 48h and 72h (n=4), ****p<0.0001, ***p<0.001.
A. H_2O_2 decreases cell viability in culture at 50 and 100µM. No additional cytotoxic effect was observed when cells were pre-treated with quizartinib.
B. Quizartinib alone decreases cell viability in a dose- and time dependent manner.

Conclusions

Quizartinib decreases cardiac cell viability *in vitro* and enhances the number of TUNEL-positive cells in the infarct border zone after MI *in vivo*. However, this increase in cardiomyocytes apoptosis was not sufficient to significantly affect the outcome in terms of post-infarct remodeling and function at one week post-MI. Further studies, including longer-term follow-up after MI, are necessary to better understand the effects of quizartinib on post-infarct remodeling and function.

References

[1] *Ardito F, Giuliani M, Perrone D, Troiano G and Muzio L (2017)* The crucial role of protein phosphorylation in cell signaling and its use as targeted therapy. *Int J Mol Med. 40(2): 271–280*
[2] *Gschwind A, Fischer O and Ullrich A (2004)* The discovery of receptor tyrosine kinases: targets for cancer therapy. *Nature reviews 4: 361-370*
[3] *Pfister O et al. (2014)* FLT3 activation improves post-myocardial infarction remodeling involving a cytoprotective effect on cardiomyocytes. *J Am Coll Cardiol. 63(10):1011-9*
[4] *Zarrinkar PP et al. (2009)* AC220 is a uniquely potent and selective inhibitor of FLT3 for the treatment of acute myeloid leukemia (AML). *Blood 114(14):2984-92*
[5] https://www.unil.ch/caf/en/home/menuinst/services/micro-surgery.html

Universitätsspital Basel
University of Basel
Departement Biomedizin Basel
daria.monogioubelik@unibas.ch

DARIA MONOGIOU BELIK, PhD

Biologist passionate about healthcare. Strong team spirit, organized, with well-developed communication and time management skills. Experienced in working within multicultural environment. Always excited to get familiarized with new fields and acquire new knowledge. Responsible, dedicated and energetic professional able to bear work pressure and to handle multiple priorities. Detail-oriented and with aspiration to successfully contribute to development and progress of scientific projects.

Career development

Project Management course, Networking course, Foundations of Business Strategy

Career Program

Selected for annual highly competitive Antelope Program at Novartis, Basel (mentorship, workshops)

Organization

Member of PhD student club (career days, retreats, scientific networking exchange)

Softwares

MS office, FlowJo, ImageJ/Fiji, GraphPad Prism

Languages

Russian (native)
Greek (native)
English (fluent)
German (beginner)

Interests

CrossFit, member of Olympic Weightlifting Club Basel (GHCBB), Psychology, Art, Nutrition

Working Experience

Regulatory Affairs Associate, BeiGene, Basel, Switzerland (2021-present)

Responsibilities:

- Manage the preparation, assembly, review and timely submission of Clinical Trial Applications, amendments, regulatory dossiers for registration of products and new indications
- Support developing and implementing regulatory strategies for the earliest possible approvals/clearance of regulatory submissions associated with assigned projects
- Support and manage the preparation of meeting requests and briefing documents for interactions with EU Health Authorities
- Coordinate the preparation, review and submission of all components of regulatory submissions, including ODD, CTAs, MAAs, annual reports, safety reports etc.

Postdoctoral Fellow, Friedrich Miescher Institute for Biomedical Research, Basel, Switzerland (2020)

Research project: "Engineering chromatin to boost CRISPR-Cas9 gene editing efficiency in human cells"

- Identified novel molecules that change chromatin structure for improvement of gene therapy (gene editing and DNA repair efficiency) using high-throughput methods
- Collaborated and communicated with different line function within the institute and carried out a high-risk project with a further goal of a startup initiation

Doctoral Researcher, University Hospital of Basel, Switzerland (2016-2020)

Dissertation project: "The role of cancer kinome in healthy and injured heart: focus on Flt3 and Plk2". The title of Doctor of Philosophy (PhD) obtained after the successful defense in April 2020

- Investigated the effect of the anti-cancer treatment with quizartinib on the heart function in animal models with myocardial infarction; role of Plk2 in cardiomyocyte proliferation
- Designed, planned and implemented *in vivo* and *in vitro* research experiments
- Collected and analyzed data
- Managed the project independently
- Coordinated and supported other members of the research group and the department
- Acquired project and time management skills
- Prepared and delivered scientific presentations at the conferences

Research Associate, Department of Biomedical Engineering, Khalifa University of Science, Technology and Research, UAE (2014-2015)

Research project: "Establishment of novel 3D atherosclerotic model *in vitro* for mechanistic investigation into dynamic mechanobiology of atherosclerotic plaque formation and the current drug treatment process for personalised medicine"

The realisation of the project included application of variety concepts from different scientific fields

- Assisted Principal Investigators in the laboratory exercises for undergraduate courses
- Mentored graduate and undergraduate students in their research
- Identified materials, chemicals and equipment for procurement
- Overviewed laboratory inventories (chemicals, media, cell lines etc.)
- Managed laboratory independently
- Reviewed pertinent primary literature
- Prepared experimental findings for publication and presentations

Education

University of Basel, Basel, Switzerland (2016-2020)

- **PhD in Cardiovascular Research**

Imperial College London, London, UK (2012-2013)

- **MSc Molecular Medicine (grade: distinction)**

Democritus University of Thrace, Alexandroupolis, Greece (2006-2011)

- **BSc Molecular Biology and Genetics (grade: 7.25/10)**